June 2012

Modeling and Mathematical Analysis of Plant Models in Ecology

Eric A. Eager
University of Nebraska-Lincoln, eeager@uwlax.edu

MODELING AND MATHEMATICAL ANALYSIS OF PLANT MODELS IN
ECOLOGY

by

Eric Alan Eager

A DISSERTATION

Presented to the Faculty of

The Graduate College at the University of Nebraska

In Partial Fulfilment of Requirements

For the Degree of Doctor of Philosophy

Major: Mathematics

Under the Supervision of Professors Richard Rebarber and Brigitte Tenhumberg

Lincoln, Nebraska

August, 2012

MODELING AND MATHEMATICAL ANALYSIS OF PLANT MODELS IN
ECOLOGY

Eric Alan Eager, Ph. D.

University of Nebraska, 2012

Advisers: Richard Rebarber and Brigitte Tenhumberg

Population dynamics tries to explain in a simple mechanistic way the variations of the
size and structure of biological populations. In this dissertation we use mathematical
modeling and analysis to study the various aspects of the dynamics of plant populations
and their seed banks.

In Chapter 2 we investigate the impact of structural model uncertainty by con-
sidering different nonlinear recruitment functions in an integral projection model for
(*Cirsium canescens*). We show that, while having identical equilibrium populations,
these two models can elicit drastically different transient dynamics. We then derive a
formula for the sensitivity of the equilibrium population to changes in kernel elements
and show that these sensitivities can also vary considerably between the two models.

In Chapter 3 we study the global asymptotic stability of a general model for a plant
population with an age-structured seed bank. We show how different assumptions
for density-dependent seed production (contest vs. scramble competition) can change
whether or not the equilibrium population is globally asymptotically stable. Finally,
we consider a more difficult model that does not give rise to a positive system,
complicating the global stability proof.

Finally, in Chapter 4 we develop a stochastic integral projection model for a
disturbance specialist plant and its seed bank. In years without a disturbance,
the population relies solely on its seed bank to persist. Disturbances and a seed's
depth in the soil affect the survival and germination probability of seeds in the seed

bank, which in turn also affect population dynamics. We show that increasing the frequency of disturbances increases the long-term viability of the population but the relationship between the mean depth of disturbance and the long-term viability of the population is not necessarily monotone for all parameter combinations. Specifically, an increase in the probability of disturbance increases the long-term mean of the total seed-bank population and decreases the probability of quasi-extinction. However, if the probability of disturbance is too low, a larger mean depth of disturbance can actually yield a smaller mean total seed-bank population and a larger quasi-extinction probability, a relationship that switches as the probability of disturbance increases.

DEDICATION

I would like to dedicate this dissertation to my wife and best friend, Stephanie Eager, and my parents, Brian and Luann Eager. I have been so blessed to have Stephanie in my life for the last two-and-a-half years, and the last 10 months as my wife. Her love, patience and selflessness blow me away every day.

To my parents: I wouldn't choose a different couple to raise me even if I had the choice. You instilled in me the values that shape my life today. You taught me that disagreement and disrespect are two distinct things, which has made me a much better applied mathematician. Dad, you taught me how to work and work with purpose, which has allowed me to be productive during the times when it would have been easy not to be. Mom, you were always there to place situations I didn't understand into their proper context and shielded me from many things I didn't need to be involved in. Your spiritual and moral guidance has stuck with me through this journey.

ACKNOWLEDGMENTS

I would first like to thank my thesis advisors, Dr. Richard Rebarber and Dr. Brigitte Tenhumberg. I'm very grateful for the time we have spent together the last three years. You have both done a great job mentoring me mathematically, biologically and in general. Thank you for being a great example for me for my next step professionally.

I would also like to thank my committee members, Dr. David Logan, Dr. Glenn Ledder and Dr. Drew Tyre, and fellow members of my research group, Dr. Diana Pilson and Dr. Haridas Chirakkal for their support over the past four years. Special thanks go to Dr. Steve Dunbar for taking his time to discuss the early versions of my stochastic model with me. I am also very grateful for the office staff in the UNL Department of Mathematics, Liz Youroukos, Marilyn Johnson, Lori Mueller and Tom Danaher, for their friendliness and for making my life as a graduate student much, much easier than it had to be.

I would also like to thank the Mathematics Department at my alma mater, MSU-Moorhead, especially Dr. Jim Hatzenbuhler, Dr. Dennis Rhoads and Dr. Ari Wijetunga for motivating and inspiring me to pursue a Ph.D. in mathematics.

I would also like to thank my friends and fellow classmates in the UNL Department of Mathematics, including Mike and Laura Janssen, Zach Roth, Phil Landry, Komla Ahlijah, Drew Wilkerson, Sara Reynolds, Katie Haymaker, Melanie DeVries, Ben Nolting, Ashley Johnson, Molly Williams and certainly many others are not mentioned here. Special thanks go to Jason Hardin for being my go-to guy for a teaching substitute and a ride to/from the airport, as well as a friend to drink coffee and watch football with. Special thanks also goes to Tanner Auch for being my officemate for most of graduate school and my roommate for one year, as well as a great friend who provided much needed distractions from mathematics. I would finally like to thank

Tom Clark for being a great friend and officemate the past few years and for always being available to discuss a mathematics topic with me. I am pretty certain that obtaining my Ph.D. would not have been possible without a great group of friends and classmates.

I would finally like to thank the football teams of Concordia College, Winona State, Concordia-St. Paul, Northern State and Minnesota-Crookston for the five excruciating losses during my senior season at MSU-Moorhead, all by five or fewer points, a needed subliminal message that football was not my optimal career path.

Contents

Chapter 1

Introduction

Population dynamics is the area of science which tries to explain in a simple mechanistic way the time variations of the size and structure of biological populations ([6]). When modelers drop the assumption of homogeneity within the population, a structured population model is needed. Structured population models describe the distribution of individuals throughout different classes, categories or characteristics. For example, the categorization of individuals can be based upon age, measure of body size, life cycle stages, gender or genetic differences ([24]). Structured models have the advantage of being able to create a link between the individual level and the population level, accounting for dynamical behaviors that simple, unstructured models cannot.

When life-cycle events (e.g. seed production) are roughly synchronous, it is common for population biologists to use discrete-time models. Population projection matrix (PPM) models are commonly used for predicting the dynamics of structured populations in discrete time (for a survey of PPMs, see [12]). In many cases, however, the stage used to structure the population is continuous (size, for example). Instead of discretizing the stage variable so that one can use a PPM population modelers, beginning with [31], have started using integral projection models (IPMs), which

consider continuous stages (but still consider time as discrete). Despite the different modeling assumptions, the mathematical properties of PPMs and IPMs are very similar ([53]). If life-cycle events are not synchronous it is usually more appropriate to use a continuous-time model (e.g. an ordinary or partial differential equation) to model the population dynamics. A theoretical comparison of of discrete and continuous time population models can be found in [79].

In this dissertation we will deal with plant and plant-seed bank models. Because the life-cycle events of plants are usually assumed to be synchronous, we will use discrete time models, which can be written as

$$n_{t+1} = Mn_t, \tag{1.1}$$

where the sequence $\{n_t\}_{t=0}^{\infty}$ evolves in a Banach space X (which is often called the population's *state space*) and M is an operator from X to itself. The Banach spaces X we will explicitly consider will be $L^1(\Omega)$ for some continuous set of stages Ω (in the IPM case), $\mathbb{R}^n$ (in the PPM case) or some combination of the two. Provided the operator M is linear (the ecological processes involved are *density independent*), the long-term populations grow (or decline) exponentially at a rate of λ, the leading eigenvalue of M.

Often times the processes governing the population can vary from year-to-year via environmental or demographic stochasticity. In this setting the operator M may be a function of a stochastic process $\{\theta_t\}_{t=0}^{\infty}$, so we can re-write (1.1) as

$$n_{t+1} = M(\theta_t)n_t. \tag{1.2}$$

If $M(\cdot)$ is linear the long-term behavior of (1.2)(which is surveyed in [34]) is analogous

to that of (1.1): The *mean* growth (or decay) rate of the population converges to a constant value λ_s, which is constant with probability one. This is often called *stochastic exponential growth (or decay)*.

Many processes (deterministic and stochastic) in biology are *density dependent*, i.e. the operator M or $M(\cdot)$ is nonlinear. When the operator is nonlinear the population usually does not exhibit exponential or stochastic exponential growth (or decay) as $t \to \infty$. In deterministic, density-dependent models one usually sees the population converge an equilibrium, a cycle, invariant loop or a strange attractor ([13]). In stochastic, density-dependent models the possibilities are more vast, although [41] showed that the probability measure elicited by their model converges to a unique measure, and therefore the population converges to a stationary random sequence.

In this dissertation we will focus on plant and plant-seed bank models. The stage variable for a plant population is often assumed to be some measurement of size ([9], [67], [63], [34]) which, being continuous, is most appropriately modeled as the stage in an IPM rather than a PPM. We will make use of a PPM in Chapter 3, when we structure the population's seed bank with respect to (discrete) age. Thus, a combination of both PPMs and IPMs will be studied in this work.

We assume that density dependence is included in the models in one of two ways: seed recruitment and/or seed production. Both of these processes are in the reproductive stage of the life-cycle. Therefore, if we follow the method of [24], [64] and [76] and break the operator M into two operators $M = A + B$, where A models survival and movement between stages and B models reproduction, then only the operator B is nonlinear. In Chapters 2 and 3 we will use and build upon the results of [64] and [76] for deterministic, density-dependent population models where only B is nonlinear. In those papers they further assumed that the stage of a juvenile is independent of its mother. In the case of a plant-only model, b was the the distribution

of juvenile plants and c^T the functional such that $c^T n$ was the abundance of seeds produced by the population n. The nonlinearity in their model was via a function f, where $f(c^T n)$ was the abundance of juvenile plants that results from $c^T n$ seeds. Thus, $Bn = bf(c^T n)$. With these, one can write (1.1) as

$$n_{t+1} = An_t + bf(c^T n_t). \tag{1.3}$$

It is often convenient to write f as the product of the establishment probability g and the number of seeds, i.e. $f(c^T n) = g(c^T n)c^T n$, where $g \in C(0, \infty)$ and is a decreasing function on $(0, \infty)$. As long as the triple (A, b, c) satisfies realistic ecological assumptions and f is increasing, concave down, with $f(0) = 0$, the long-term dynamics of (1.3) are determined by the *stability radius* of (A, b, c), which we will call p_e. p_e is the smallest positive number p such that the linear operator $A + pbc^T$ has spectral radius equal to 1. It is proved in [43] that

$$p_e = (c^T(I - A)^{-1}b)^{-1}.$$

If we define $g_0 := \sup_{y>0} g(y)$ and $g_\infty := \inf_{y>0} g(y)$, then if $p_e < g_\infty$ the population eventually blows up, if $p_e \in (g_\infty, g_0)$ the population has a globally stable equilibrium vector and if $p_e > g_0$ the population eventually goes extinct. The results can be summarized in the following theorem from [64], a theorem we will use in Chapter 2 and 3 of this dissertation:

Theorem 1.0.1

1) If $p_e > g_0$, then the zero vector is a globally stable equilibrium for (1.3) in the sense

that for every n_0 in the positive cone K of X,

$$\lim_{t\to\infty} n_t = 0.$$

Furthermore, for every $\epsilon > 0$, there exists $\delta > 0$ such that $\|n_0\| \leq \delta$ implies $\|n_t\| \leq \epsilon$ for all $t \in \mathbb{N}$.

2) If $p_e \in (g_\infty, g_0)$ then there exists y^* which satisfies $f(y^*) = p_e y^*$. The vector $n^* \in X$ given by

$$n^* = p_e y^* (I - A)^{-1} b$$

is a globally asymptotically stable equilibrium of (1.3) on $K \setminus \{0\}$, i.e.

$$\lim_{t\to\infty} n_t = n^*,$$

and for every $\epsilon > 0$, there exists $\delta > 0$ such that $\|n_0 - n^*\| \leq \delta$ implies $\|n_t - n^*\| \leq \epsilon$ for all $n \in \mathbb{N}$.

3) If $p_e < g_\infty$, then there exists $n_0 \in K$ such that $\lim_{t\to\infty} \|n_t\| = \infty$.

In Chapter 2 we study the effects of structural model uncertainty of an IPM of the form (1.3) from [67] for Platte thistle (*Cirsium canescens*). For structured population models most research has been focused on analyzing long-term, asymptotic population characteristics, such as a populations asymptotic growth rate or equilibrium population density. However, when a population is forced away from its equilibrium stage distribution by disturbances, such as environmental catastrophes or management actions, the subsequent dynamics of this population can change considerably in the short term, making the analysis of such dynamics extremely relevant ([42]). For example, sudden changes in some vegetative distributions can significantly change the

structure of associated animal communities ([70], [82]). The impacts of such transient events on population dynamics can often not be elucidated with equilibrium analysis (like those summarized in Theorem 1.0.1) alone.

The majority of investigations of transients in discrete-time, structured population models have focused on models that are density independent ([14], [15], [50], [73], [74], [75], [71]). However, as previously stated, many systems are driven by density-dependent mechanisms, but the signal for density dependence in empirical data sets is often weak. A typical example of this is the seedling recruitment data in Fig. 1 of [67] and Figure 1.1: the data are few, very noisy, and collected over a limited range of seed densities. It is challenging to find sensible functions that fit such noisy data well, and commonly used criteria to choose among different candidate functions (such as Akaike information criterion (AIC) or Bayesian information criterion) can only provide a relative ranking of poor fitting functions. Moreover, these statistical criteria do not consider the ability of a function to project dynamics outside the rage of observed data. This is particularly relevant if one is interested in dynamics outside the range of data collection, which is often the case when studying the effect of large perturbations that can cause transient dynamics. When projecting dynamics outside the range of data collected, we might consider functional forms that are derived from first biological principles, but do not rank first based on information criteria, and evaluate the effect of structural model uncertainty on model predictions.

[67] represents density-dependent seedling recruitment with a power function of the form $f(x) = x^\nu$, where x is the density of seeds produced by the population in one time-step, $f(x)$ is the density of seedlings that result from these seeds and the parameter ν is fit to data. If $\nu \in (0, 1)$ (which is essential to describe negative density-dependent dynamics), the power function has mathematical properties which include having an unbounded derivative for low seed densities and being unbounded for

large seed densities. These extreme values of x are outside the range of seed densities considered in the statistical analysis of [67]. When studying transient dynamics, extreme values of x are highly relevant. Therefore, we derived an alternative to the power function for seedling recruitment based on biological principles that takes into account these extreme values and ask the question: How sensitive are the predicted transient dynamics to the choice of the function used to characterize density-dependent seedling recruitment? Our alternative function describes seedling recruitment more realistically for extreme values of x, as recruitment is essentially linear for small seed densities and essentially constant for large seed densities. The resulting function is identical to the classical Michaelis-Menten, Beverton-Holt, or Holling type II functional response functions.

It also follows through an argument in dimensional analysis that if $\nu \in (0, 1)$ the function $f(x) = x^\nu$ cannot be consistent with the rest of model. Whether or not a power function is a valid model for density-dependent recruitment first depends on whether or not it is dimensionally consistent with the rest of the model. Therefore, in Chapter 2 we will add an additional parameter to the power function and use nonlinear regression to fit the additional parameters, obtaining dimensional consistency. This additional analysis was not done in the original publication of this work ([30]).

We show that the predicted transient dynamics can differ considerably depending on which nonlinear function is used for recruitment and, theoretically, this difference does not have a bound. This is even the case when we insist that the equilibrium populations predicted by both models are identical. We illustrate these differences in transient dynamics with ecologically motivated examples.

Once finished with comparing the transient dynamics of the two models, we then turn our attention to the comparing the sensitivity of the equilibrium population n^* to small changes in model parameters. Sensitivity and elasticity analyses have proved
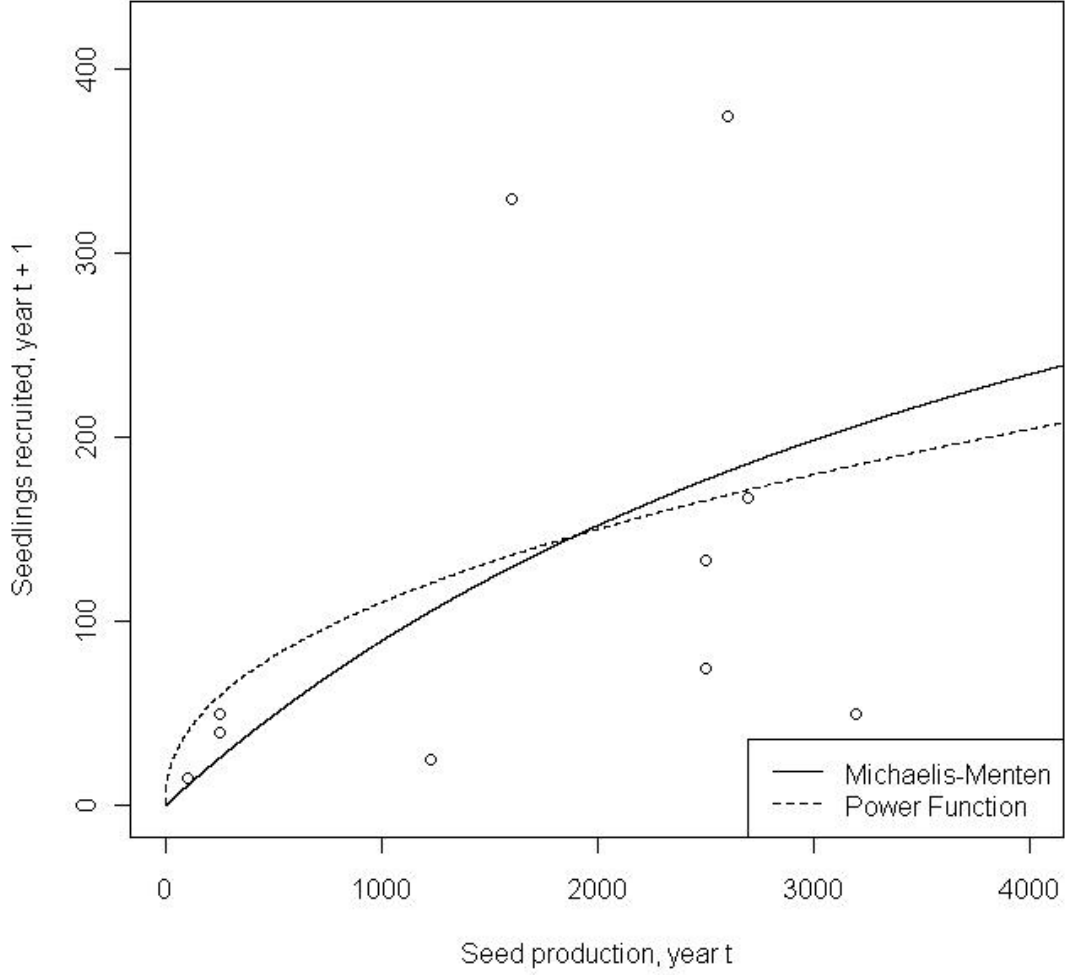
Figure 1.1: The relationship between seedling recruitment in year $t+1$ and estimated seed production in year t. We digitized the data from Fig. 4 in [67] and estimated the parameters for an adjusted, two-parameter power function and Michaelis-Menten function. The dotted curve is the fitted power function $f_1(x) = 5.0899x^{0.4453}$ (AIC = 139.3136) and the solid curve is the fitted Michaelis-Menten function $f_2(x) = \frac{510.0626x}{4706+x}$ (AIC 137.7314). In Appendix A we describe parameter estimation procedure of the Michaelis-Menten function.

to be ubiquitous in the analysis of models in population biology and ecology (see, for example, [11], [12], [27], [28], [23], [66], [45]). As in the case of transient dynamics, sensitivity and elasticity analyses are particularly important in making management decisions about ecosystems. The most common mathematical analysis consists of studying the effect of small changes in model parameters on the long-term population growth rate λ for density-independent (linear) population models. Sensitivity and elasticity of λ in this case is rather straightforward and captures effects of changes in model parameters on population measures such as fitness or the success of population establishment or invasion. However, the model in [67] is density dependent, leading to a population that converges to an equilibrium in lieu of having a long-term growth rate.

There have been some attempts to perform sensitivity and elasticity of density-dependent (nonlinear) population models ([13], [38], [39], [40], [83]). These studies have consisted of analyzing sensitivities and elasticities of λ from a linearized model at an equilibrium point and the sensitivities and elasticities of the equilibrium total population size $N^* := ||n^*||$ itself. However, by studying the population via a single value such as λ or N^*, a modeler may be missing out on important ecological information. One could ask the question: "Do changes in parameter a affect members of the population with characteristic b in the long-run?" By using λ or N^* as a proxy for the population, one cannot sufficiently answer that question.

We derive an exact formula for the sensitivity of n^* to changes in the data (A, b, c). We use these formulas to show, as in the case of transient dynamics, that the sensitivity of n^* can vary considerably depending on which nonlinear function is used for recruitment, even if we insist (again) that the equilibrium populations are identical to begin with. We also show that, since the derived sensitivity function is a function of the stage variable in the model, these differences in sensitivity are larger

for some members of the population than they are for others.

Other theoretical studies have emphasized that, in many circumstances, statistically well-fitting nonlinear functions are not ecologically realistic (see, for instance, [22], [37], [68]). However, Chapter 2 highlights the role that the functional form of the density dependence plays in short-term, transient dynamics and sensitivity of the equilibrium population n^*, which, to our knowledge, has not been addressed.

In Chapter 3 we consider mathematically the abstract plant model (1.3) coupled with an age-structured seed bank in $\mathbb{R}^N$. Many plant populations have persistent seed banks. Seed banks consist of viable seeds that have been produced in previous years. Instead of germinating, the seeds have undergone dormancy and can remain viable in the soil for more than one season. Seed banks buffer plant populations against environmental perturbations like fire or pest outbreaks. Therefore, even if all above ground plant material is destroyed, seeds germinate from the seed bank and, as a consequence, reduce the probability of population extinction. Furthermore, seed banks act as a reservoir for genes and/or gene complexes ([35], [80], [54], [48], [49], [47], [32], [60], [20], [10]). The vital role of seed banks for population viability necessitates incorporating seed banks specifically into demographic models to avoid erroneous model predictions ([48], [49], [25]).

Often the survival and/or germination probabilities decrease with seed age ([48], [2], [17]), in which case it is important to keep track of the age distribution of seeds in the seed bank. We thus characterize the seed bank as an age-structured population (so that it is represented by a vector in $\mathbb{R}^N$), which is coupled with the dynamics of the associated plant species. Furthermore we assume that seed production depends on plant density and seedling establishment depends on the density of germinating seeds. These two density-dependent processes cannot simply be modeled with one nonlinear function, as density-dependent seed production only suppresses the density

of newly created seeds, but density-dependent seedling recruitment depends on the total density of germinating seeds in the population (which is the sum of new and old germinating seeds). We assume that the density dependence in seedling establishment is due to contest competition, and a derivation of this general relationship can be found in Chapter 2. We consider both contest and scramble competition assumptions for the density dependence in seed production, as the per-capita seed production data in [46] suggests that either could be the case.

We prove that, in the case where seed production is modeled with contest competition, there is a globally stable equilibrium vector for the population which is independent of the initial population. In the case where seed production is assumed to be modeled with scramble competition the same global stability results hold for much, but not necessarily all, of parameter space.

Seed banks have infrequently been modeled as structured populations (but see [48], [10], [32], [17]), and we are unaware of any studies of the global asymptotic stability of a density-dependent plant-seed bank model. We apply our analytical results to a model for the annual plant *Sesbania vesicaria* obtained from [46].

We conclude Chapter 3 by exploring mathematically a plant-seed bank model with a scalar seed bank that elicits population data that is not in the positive cone of the population's state space X. Despite this extra difficulty we are able to salvage most of the global stability results obtained in Section 3.2. Finally, we analyze the sensitivity of the equilibrium in a toy plant-seed bank model to changes in the seed survival probability.

In our final chapter, we shift our attention to annual disturbance specialist plants. Many annual plants are disturbance specialists, germinating only in freshly disturbed soil. In these species the frequency, intensity, timing, and spatial extent of disturbance can greatly influence the probability of germination and survival of seeds in the

seed bank ([20], [61], [59]). Disturbances create a more favorable environment for germination by removing more competitive species ([20], [61], [3], [59]). However, disturbance also alters the depth distribution of seeds in the seed bank: burying some seeds deep in the soil where survival is high (and germination rates are low), and relocating other seeds closer to the soil surface where germination rates are high (but survival is low) ([61], [60]).

Most attempts at understanding the dynamics of plant-seed bank populations have ignored the effect of depth. [20] used a stochastic matrix model that considers seed depth as either "shallow" or "deep". In their model a disturbance was determined by a simple Bernoulli random variable with probability of disturbance p, but depth of disturbance is not explicitly or mechanistically considered. Mohler's model [60] included seed depth as a continuous variable, but disturbance was not a stochastic event because plowing, controlled by farmers, was the only type of disturbance considered. The objective of his model was to understand the effect of different plowing regimes on germination probability and seed bank size, but the effect of the seed bank on long-term population dynamics of the plant population was not examined. Neither model considered density-dependent processes a priori, which commonly affect seedling survival and seed production ([54], [46], [61]). If conditions are favorable and the seed bank size is large it is possible that even disturbance specialist plants experience density dependence in some years. Thus, we explicitly include density dependence in the model by assuming that seedling survival decreases with seedling density.

In Chapter 4 we construct a density-dependent stochastic IPM ([31], [33], [34]) for an annual disturbance specialist's population dynamics. In our model seed depth in the soil is a continuous variable, and germination is only possible in the presence of a disturbance. We incorporate the characteristics of a disturbance as a stochastic process. In each time-step there is a probability h that the population will be disturbed

and the distribution of possible disturbance depths is exponentially distributed with mean depth of disturbance ρ (truncated at maximum disturbance depth, D). We further assume that the disturbance in a given time-step uniformly redistributes all seeds between the surface and the disturbance depth r, and that the seeds below r remain in place.

We performed Monte Carlo simulations to study the effect of disturbance probability h and the mean depth of disturbance ρ on the long-term seed bank population's mean, variance, and quasi-extinction probability. Our most interesting result illustrates a tradeoff between depth-dependent germination and survival, which can only be understood by modeling seed depth explicitly. For some values of h the mean depth of disturbance has a non-monotone effect on seed bank population's long-term mean and variance. If recruitment is intermediate to low and the disturbance frequency is low, population mean and variance decreases with increasing mean depth of disturbance because more deeply buried seeds are brought to the surface and germinate. However, if in the following year there is no disturbance most newly produced seeds die, so a high mean depth of disturbance in combination with low disturbance frequency causes a decrease in the seed bank population. As a consequence, the quasi-extinction probability increases with increasing ρ. In contrast, the model predicts the opposite effect of ρ on population mean and variance if disturbance frequency and recruitment are sufficiently high to approach a quasi-extinction probability of zero. These results suggest that incorporating the depth distribution of seeds in the seed bank can be important for evaluating population dynamics and viability of disturbance specialist plants.

Chapter 2

Analyzing Structural Model Uncertainty: Transients and Sensitivity

2.1 Comparison of Transient Dynamics

To create a consistent setting for the comparison of the two models in this chapter, we will first give a detailed account of the physical dimensions of each function used in the IPM. We consider it desirable for a candidate recruitment function to have physical dimensions that are consistent with the rest of the IPM. We will then illustrate the differences in transient dynamics between the IPM using the power function and the Michaelis-Menten function by simulating two ecological events. The first simulation will mimic an ecological catastrophe, like a fire that destroys all above-ground plant biomass, where the initial population will consist entirely of seedlings (recruited from surviving seeds left in the ground). Second, we will simulate an ecological restoration

project where the initial population consists of large, adult plants. We show that both IPMs can yield surprisingly large differences in transient dynamics even though the fit of the Michaelis-Menten function to the empirical data is comparable to the power function (Figure 1.1) and both IPMs predict the same equilibrium population density (see Appendix A). We then derive general mathematical properties of the two models that show why these differences occur.

2.1.1   Model

An IPM can be used to describe how a population with a continuously varying stage structure changes in discrete time ([31]). The use of IPMs in plant ecology has grown tremendously over the last decade ([63]). See [9] for a tutorial on constructing IPMs. The population is characterized by a function, $n(x,t)$, where

$$\int_x^{x+\delta x} n(y,t)\,\mathrm{d}y$$

gives the total density of the population near stage x and time t, with physical dimensions $plants(area)^{-1}$. This function can be thought of as a continuous-stage analog to population vectors $n(t) = [n_1(t)\ n_2(t)\ ...\ n_m(t)]^T$ in population projection matrix models (e.g., [12]). We have chosen to use an IPM because the ability to capture the transient dynamics is often linked to the number of life history stages assumed in the model ([73], [71]). In a general IPM, the population $n(x,t)$ satisfies the integrodifference equation,

$$n(x,t+1) = \int_L^U K(x,y)n(y,t)\,\mathrm{d}y,$$

where $K(x, y)$ is called the kernel of the IPM and L and U are the smallest and largest observed value for the stage, respectively. We decompose the kernel into two parts ([24]):

$$K(x, y) = p_1(x, y) + p_2(x, y)$$

where $p_1(x, y)$ describes survival and growth, which models the probability of movement from stage y to stage x in one time-step. The fecundity portion of the kernel, $p_2(x, y)$, models the density of stage x individuals that are produced by stage y individuals.

We use a version of the model of [67] that ignores the effect of seed predation ([9]); this modification does not affect the way density dependence is implemented in the model. The natural logarithm of the plants root crown diameter is used as an indicator of plant size (the stage variable); the time-step is 1 year. We start by mentioning the physical dimensions of each of the model components to contrast the two seedling recruitment functions (power function and Michaelis-Menten function) on the basis of dimensional analysis. The Platte thistle populations distribution, $n(\cdot, \cdot)$, has the dimension of $plants(size)^{-1}(area)^{-1}$.

Plants that do not flower in a given time-step have to grow and survive to make it to the next time-step. Let $s(\cdot)$ and $f_p(\cdot)$ be the survival and flowering probabilities, respectively, of members of the population with size y, which are both assumed dimensionless. We will call the growth function $g(\cdot, \cdot)$ where

$$\int_x^{x+\delta x} g(z, y) \, dz \tag{2.1}$$

is the probability of a size y plant growing to a size near x in one time-step (which is a probability distribution for each fixed y). $g(\cdot, \cdot)$ has the dimension of $(size)^{-1}$(with $\int_x^{x+\delta x} g(z, y) \, dz$ being dimensionless).

The probability of not flowering, $1 - f_p(\cdot)$, is incorporated into the survival part of

the kernel because Platte thistle is a monocarpic plant and, as a consequence, flowering is fatal. The model assumes that survival, flowering, and growth are statistically independent events. Therefore, the survival/growth portion of the kernel is

$$p_1(x, y) = s(y)(1 - f_p(y))g(x, y). \tag{2.2}$$

In order to produce juvenile plants (seedlings), existing plants must survive and flower. The seeds produced by these flowering plants then need to establish. Seedling size is assumed to be independent of the size of the mother plant (a low maternal effect on seedling size has also been reported for other plant species ([81], [69]). Therefore, the fecundity portion of the kernel is

$$p_2(x, y) = p_e(t)s(y)f_p(y)S_d(y)J(x),$$

where $S_d(y)$ is the number of seeds produced by members of the population with size y (with dimension of $(seeds)(plant)^{-1}$), and $J(\cdot)$ is the probability distribution of the size of seedlings, with dimension of $(size)^{-1}$. The term $p_e(t)$ is the probability of a seed establishing to become a seedling by the next time-step, that is, the probability that a seed germinates and survives until the next population census. The density of seeds produced at time t, which we will call $\gamma(t)$, can be computed via the integral

$$\gamma(t) = \int_L^U s(y)f_p(y)S_d(y)n(y, t)\, \mathrm{d}y.$$

The dimension of $\gamma(\cdot)$ is $seeds(area)^{-1}$.

Seed establishment probability for Platte thistle is assumed to be density dependent in ([67]). Therefore, for each t, the term $p_e(t)$ is a function of $\gamma(t)$, the total density of seeds produced at time t. We will call the function modeling seedling recruitment

$f(\cdot)$, which will be the product of seed establishment probability and the total density of seeds in the population at time t, i.e.

$$f(\gamma(t)) = p_e(\gamma(t))\gamma(t). \tag{2.3}$$

We will assume for the remainder of this chapter that $s(\cdot), f_p(\cdot), S_d(\cdot), J(\cdot)$ and $g(\cdot, \cdot)$ are positive and continuous, with $s(\cdot), f_p(\cdot) < 1$. The full density-dependent IPM can therefore be expressed as

$$n(x, t+1) = \int_L^U p_1(x, y)n(y, t)\, \mathrm{d}y + \int_L^U p_e(\gamma(t))J(x)s(y)f_p(y)S(y)n(y, t)\, \mathrm{d}y,$$

where $p_1(\cdot, \cdot)$ is as defined in (2.2). More concisely,

$$n(x, t+1) = \int_L^U p_1(x, y)n(y, t)\, \mathrm{d}y + J(x)f(\gamma(t)). \tag{2.4}$$

Notice that the model in (2.4) is the sum of a density-independent growth and survival and density-dependent seedling recruitment. For the connection between (2.4) and (1.3) see Section 2.2.1. We must note that some authors have used the term "recruitment" to mean the same as "establishment probability" (see, for instance, [68]). In this chapter, these terms are used to describe two distinct, albeit related, concepts, as seedling recruitment is the product of seed establishment and seed density.

The seed establishment probability in [67] is given by

$$p_e(\gamma(t)) = \gamma(t)^{\nu-1}, \tag{2.5}$$

where the estimated value for ν in [67] is 0.67. When $p_e(\gamma(t))$ is as in (2.5), we have that $f(\gamma(t)) = \gamma(t)^{\nu} = p_e(\gamma(t))\gamma(t)$. In general, a seedling recruitment function,

$f(\gamma(t))$, needs to have the dimension of $plants(area)^{-1}$ for (2.4) to be dimensionally consistent. Hence, $p_e(\gamma(t))$ needs to have the dimensions of $plants(seed)^{-1}$. Since $\nu \in (0,1)$, the function $p_e(\gamma(t)) = \gamma(t)^{\nu-1}$ does not have these dimensions for any choice of $\nu \in (0,1)$, which is unacceptable. To remedy this situation we will use the parameters κ_1 and κ_2 to define a more appropriate function for seed establishment probability in the power function case as

$$p_e(\gamma(t)) = \kappa_1(\kappa_2\gamma(t))^{\nu-1}. \tag{2.6}$$

If κ_2 has dimension $(area)(seeds)^{-1}$ (which makes the product $\kappa_2\gamma(t)$ dimensionless) and κ_1 has dimension $plants(seed)^{-1}$, then $p_e(\gamma(t)) = \kappa_1(\kappa_2\gamma(t))^{\nu-1} := \kappa(\gamma(t))^{\nu-1}$ is dimensionally consistent with the rest of the model. For the remainder of this chapter we will use this redefined version of the power function, with $\kappa = 5.0899$ and $\nu = 0.4453$, which were found via nonlinear regression ([62]) on the data from Figure 1 in [67] (Figure 1.1).

While the introduction of κ has remedied the fact that the power function in [67] is not dimensionally consistent with the remainder of the model, we still lack a clear biological interpretation for the parameters κ and ν. Furthermore, the power function still has mathematically pathological properties (e.g. having an unbounded derivative at the origin and being unbounded for large seed densities). In the next section, we derive a different seedling recruitment function from first principles so that every parameter has a clear biological interpretation from the dimensional analysis point of view and the aforementioned mathematical pathologies are not present.

2.1.2 Derivation of Seedling Recruitment Function

To mechanistically derive the seedling recruitment function, $f(\gamma(t))$, we follow in the spirit of the derivation of the Holling type II functional response in classical predation theory ([44]). We envision seeds participating in "predation of space", with the analogy of "handing time" by Holling in classical predation theory becoming "handling space" in our derivation. In this model, we only consider *intraspecific* competition.

Let $N(t)$ be the density of seedlings that are recruited between time t and $t+1$, i.e., the density of seeds produced that survive to become a seedling within one time-step. First, we make the assumption that the number of seedlings between time t and $t+1$ increases with the space available for seeds to establish, $S(t)$, which has the dimension of *area*. Also, assume that $N(t)$ increases (as a function of $\gamma(t)$) with the establishing efficiency rate a, where a has the dimension $plants(seed)^{-1}(area)^{-1}$. A first attempt at a relationship between $N(t)$ and $\gamma(t)$ yields

$$N(t) = aS(t)\gamma(t). \tag{2.7}$$

To obtain a more realistic relationship between $N(t)$ and $\gamma(t)$, it is reasonable to assume that the space available to establish will decrease with the number of seedlings, so $S(t)$ is decreasing with respect to $N(t)$. We envision a seed addition experiment where only seeds compete among themselves for the available microsite area. If we define the constant S_e to be the space taken up (as a proportion of the total space available) by one seed that establishes and becomes a seedling, where S_e has dimension $area(plant)^{-1}$, we can re-write $S(t)$ as follows:

$$S(t) = S_{\text{tot}} - S_{\text{tot}}S_eN(t) = S_{\text{tot}}(1 - S_eN(t)), \tag{2.8}$$

Where S_{tot} is a fixed characteristic of the population's environment and is the total area of the space available for the plant population's seeds to establish. Substituting (2.8) into (2.7) and solving for $N(t)$ yields:

$$N(t) = \frac{aS_{\text{tot}}\gamma(t)}{1 + aS_{\text{tot}}S_eS_{\text{tot}}}. \tag{2.9}$$

Or, more concisely,

$$N(t) = \frac{\alpha\gamma(t)}{\beta + \gamma(t)}, \tag{2.10}$$

where

$$\alpha = (S_e)^{-1}, \ \beta = (aS_{\text{tot}}S_e)^{-1}. \tag{2.11}$$

The dimensions of α and β are $plants(area)^{-1}$ and $seeds(area)^{-1}$, respectively. (2.10) is the Michaelis-Menten function. Notice that, if we let $N(t) = f(\gamma(t))$, we can write

$$f(\gamma(t)) = \left(\frac{\alpha}{\beta + \gamma(t)}\right)\gamma(t) = p_e(\gamma(t))\gamma(t). \tag{2.12}$$

Using the Michaelis-Menten function for seedling recruitment, we can clearly interpret the parameters and their dimensions in a way that is consistent with the rest of the IPM. For example, the function $p_e(\gamma(t))$ has dimension $plants(seeds)^{-1}$ and decreases to zero as the number of seeds grows to infinity, as one should expect in the dynamics of negative density-dependent seed establishment. Also, when $\gamma(t)$ is small, we see that $p_e(\gamma(t))$ is roughly the constant $\alpha(\beta)^{-1} = aS_{\text{tot}}$, which describes the probability of a seed establishing in the total absence of density dependence. β is an analog for the familiar half-saturation constant in classical predation theory ([77]) and is here the seed production needed to attain half of the maximum total seedling recruitment, α.

The Michaelis-Menten function is a limiting case of the derivation of a general

seedling recruitment function of [29], which considers safe sites for seeds to establish and makes assumptions about the distribution of seeds after flowering and dispersal. The derivation in this chapter is considerably simpler and, given that we are not modeling space explicitly as a variable in the population, perhaps more appropriate for this setting.

For the remainder of this chapter, we call the IPM that uses the power function for seedling production the power function model, and we call the IPM that uses the Michaelis-Menten function the mechanistic model. Note that the survival, growth, seed production, and distribution of seedlings components remain identical in the two models, and therefore these names are simply to distinguish the way the seedling recruitment is implemented in the IPMs.

2.1.3 Results

To compare the two Platte thistle IPMs fairly, we initially calibrated the parameters of the Michaelis-Menten function to obtain the same equilibrium population density as the power function model (see Appendix A). Therefore, the subsequent comparisons of the transient dynamics in Example 1 and 2 are of two IPMs having identical equilibrium population densities and size distributions. The fit (AIC value) of the calibrated Michaelis-Menten to the empirical recruitment data was comparable to the fit of the power function used in [67], while the fit of the power function with the additional parameter κ was slightly worse (see Figure 1.1).

We define the transient function $T(t, \rho)$ to be the per-capita difference in the total population density from time $t - 1$ to time t, dependent on the initial population

distribution, $\rho(\cdot)$. Mathematically

$$T(t, \rho) := \frac{||n(\cdot, t)|| - ||n(\cdot, t-1)||}{||n(\cdot, t-1)||}, \tag{2.13}$$

for $t = 1, 2, ...$ Here, $|| \cdot ||$ refers to the L^1 norm defined by

$$||\phi(\cdot, t)|| := \int_L^U |\phi(x, t)| \, \mathrm{d}x, \tag{2.14}$$

which equals the total density of the population $\phi(x, t)$, with dimension $plants(area)^{-1}$. This transient function definition is similar to the GR metric in [50] for matrix models and is a function of t and $\rho(\cdot)$ alone, as $n(x, t)$ implicitly depends on the initial population, $\rho(\cdot)$. The "$\cdot$" symbol indicates that the stage variable, x, is integrated away. This measurement of transients compares the populations current total density with its total density in the previous time-step. We say that the population experiences a *transient attenuation* at time t_0 if $T(t_0, \rho) < 0$ and a *transient amplification* if $T(t_0, \rho) > 0$. Note that we can rewrite the transient function as the per-capita growth rate minus unity. This makes clear our intention to have the cutoff between transient attenuation and amplification at zero. Therefore, using our definition, if a population has a transient attenuation (amplification), it has a smaller (larger) density than it had one time-step ago.

We have made certain to explicitly write that the transient function depends on the initial population distribution because the transient dynamics of a single-species, structured population tend to depend on the population structure that is remaining after the ecological disturbance (corresponding to $t = 0$). For examples of this phenomenon in density-independent matrix models, see [74] and [50]. Next, we illustrate that the stage structure of the initial population is the key determinant of the

transient dynamics predicted by the Platte thistle IPMs and provide a mathematical proof.

Theorem 2.1.1 *For a non-zero population $n(x,t)$, which solves the density-dependent IPM*

$$n(x, t+1) = \int_L^U p_1(x, y) n(y, t)\, \mathrm{d}y + f(\gamma(t)) J(x), \quad n(x, 0) = \rho(x), \qquad (2.15)$$

the value of the transient function at time $t_0 + 1$ can be re-written as

$$T(t_0 + 1, \rho) = E_{n(\cdot, t_0)}((1 - f_p(x)) s(x)) - 1 + \frac{f(\|n(\cdot, t_0)\| E_{n(\cdot, t_0)}(c(x)))}{\|n(\cdot, t_0)\|}, \qquad (2.16)$$

where $c(x) := s(x) f_p(x) S(x)$ and $E_{n(\cdot, t_0)}(z)$ is the expected value of z subject to the probability density function defined by the normalized population structure $P(x, t_0) := n(x, t_0)(\|n(\cdot, t_0)\|)^{-1}$. More specifically, the initial value of the transient function is

$$T(1, \rho) = E_{\rho(\cdot)}((1 - f_p(x)) s(x)) - 1 + \frac{f(\|\rho(\cdot)\| E_{\rho(\cdot)}(c(x)))}{\|\rho(\cdot)\|}. \qquad (2.17)$$

Proof:

The transient function can be explicitly written as

$$T(t_0 + 1, \rho) = \frac{\|\int_L^U p_1(\cdot, y) n(y, t_0)\, \mathrm{d}y + f(\gamma(t_0)) J(\cdot)\| - \|n(\cdot, t_0)\|}{\|n(\cdot, t_0)\|},$$

which, if we define $P(y, t_0) := n(y, t_0)(\|n(\cdot, t_0)\|)^{-1}$, $T(t_0 + 1, \rho)$ becomes

$$= \int_L^U \int_L^U s(y)(1 - f_p(y)) g(x, y) P(y, t_0)\, \mathrm{d}y\, \mathrm{d}x + \frac{f(\gamma(t_0))}{\|n(\cdot, t_0)\|} \int_L^U J(x)\, \mathrm{d}x - 1$$

$$= \int_L^U \int_L^U s(y)(1 - f_p(y)) g(x, y) P(y, t_0)\, \mathrm{d}y\, \mathrm{d}x + \frac{f(\gamma(t_0))}{\|n(\cdot, t_0)\|} - 1,$$

since $J(\cdot)$ is a probability density function. Because we are assuming that the functions in the kernel $p_1(\cdot,\cdot)$ are all positive and sufficiently smooth functions, with $f_p(y) < 1$ for every $y \in [L, U]$, we can use the Fubini-Tonelli Theorem ([36]) to change the order of the remaining integral. Therefore,

$$\int_L^U \int_L^U s(y)(1 - f_p(y))g(x,y)P(y,t_0)\,\mathrm{d}y\,\mathrm{d}x$$

can be rearranged to become

$$\begin{aligned}
&= \int_L^U \int_L^U s(y)(1 - f_p(y))g(x,y)P(y,t_0)\,\mathrm{d}x\,\mathrm{d}y \\
&= \int_L^U s(y)(1 - f_p(y))P(y,t_0) \int_L^U g(x,y)\,\mathrm{d}x\,\mathrm{d}y \\
&= \int_L^U s(y)(1 - f_p(y))P(y,t_0)\,\mathrm{d}y,
\end{aligned}$$

as $g(\cdot, y)$ is a probability distribution for each fixed y. By the definition of $P(y, t_0)$, we see that

$$\int_L^U s(y)(1 - f_p(y))P(y,t_0)\,\mathrm{d}y = E_{n(\cdot,t_0)}(s(x)(1 - f_p(x))).$$

Finally, note that for every t, $\gamma(t)$ has the property that

$$\gamma(t) = \int_L^U c(y)n(y,t)\,\mathrm{d}y = ||n(\cdot, t)||E_{n(\cdot,t_0)}(c(x)),$$

which completes the proof.

$\square$

Theorem 2.1.1 states that the transient function is the sum of expected probability of death (due to flowering and mortality) and expected per-capita seedling production.

At equilibrium, the transient function is roughly zero, and therefore, per-capita seedling production offsets mortality. However, when a population is not at equilibrium, we can expect that the right-hand side of (2.16) will not be zero.

Note that the presence of the expected values in (2.16) and (2.17) strengthens what is widely believed about the size distributions impact on single-species transient dynamics. For example, in a plant population where the smallest plants have the lowest survival probability and produce the fewest seeds, one should expect that the largest transient attenuations would occur with an initial population largely consisting of small plants. This is due to the fact that the expected survival probability, seed production, and subsequent seedling recruitment for small plants will be small. This will result in the first term of the transient function plus the per-capita seedling recruitment being small relative to unity, resulting in negative transient function values.

A surprising result in this chapter is that the total population *density* alone can explain why the predicted transient dynamics differ between the two models. For instance, if the population density in the power function model becomes sufficiently low (as in transient attenuation), the mathematical properties of the power function force the transient function to have extremely high values. Notice that, in the power function model, the transient function can be re-written as:

$$T(t_0 + 1, \rho) = E_{n(\cdot, t_0)}((1 - f_p(x))s(x)) - 1 + \frac{\kappa E_{n(\cdot, t_0)}(c(x)^\nu)}{||n(\cdot, t_0)||^{1-\nu}}. \qquad (2.18)$$

Assume that the initial population distribution is a predetermined density, M, of seedlings, i.e., $\rho(x) = MJ(x)$. In subsequent time-steps, the only new members of the population are seedlings, distributed according to $J(\cdot)$. Because not all seedlings survive to their second year (for example, $E_{J(\cdot)}((1 - f_p(x))s(x)) = 0.502$ in [67]) and

grow to a much larger size, the stage distribution stays roughly the same for small t (see (2.4)). Let us assume that the total population density changes in the right-hand side of (2.18) without changing the stage distribution at time t_0. This implies that the expected values in (2.18) are also unaffected. When $\nu \in (0, 1)$ the right-hand side of (2.18), viewed as a function of $||n(\cdot, t_0)||$, is *unbounded* as $||n(\cdot, t_0)||$ approaches zero. This is due to the fact that the derivative of the power function $f'(x) = \kappa \nu x^{\nu-1}$, goes to infinity as x approaches zero. Thus, for every positive real number N, there exists a total population density $||n(\cdot, t_0)|| = M_N$ such that for all total population densities *smaller* than M_N, we have

$$T(t_0 + 1, \rho) > N. \tag{2.19}$$

The conclusion in (2.19) states that, given a fixed stage distribution for the population, the power function model predicts that there exists a population density that ensures the beginning of a recovery (i.e., the population density starts rapidly increasing towards the equilibrium), once the total population density dips *below* this value. For instance, in the power function model, it is possible that a population of largely non-reproducing plants (seedlings) starts to grow once the population density drops below a particular threshold. We will illustrate this idea in Example 1.

The previous mathematical artifact is not present in the mechanistic model, whose transient function can be written as

$$T(t_0 + 1, \rho) = E_{n(\cdot, t_0)}((1 - f_p(x))s(x)) - 1 + \frac{\alpha E_{n(\cdot, t_0)}(c(x))}{\beta + ||n(\cdot, t_0)||E_{n(\cdot, t_0)}(c(x))}. \tag{2.20}$$

When viewed as a function of $||n(\cdot, t_0)||$ (2.20) is a bounded function. Therefore, no threshold population density exists below which a population is guaranteed to increase. For instance, a population of seedlings cannot grow until some of the plants grow sufficiently large to reproduce.

When transient amplification occurs, the differences in the predictions of the two models stem from the properties of the two seedling recruitment functions when the seed production is greater than the equilibrium seed production $\gamma^* = \int_L^U s(y) f_p(y) S_d(y) n^*(y) \, dy$ (here $n^*(\cdot)$ is the equilibrium population). Because the power function $f(x) = \kappa x^\nu$ goes to infinity as x goes to infinity, in theory, the power function will eventually predict much larger seedling recruitment than the Michaelis-Menten function, and thus, everything else being equal, the power function model will have larger densities than the mechanistic model when seed production is large. In Example 1 and 2, we chose model parameters so that equilibrium populations of the power function model and the mechanistic model are the same (see Appendix A), thus

$$(\gamma^*)^\nu = \frac{\alpha \gamma^*}{\beta + \gamma^*}. \tag{2.21}$$

Assume that γ^* in (2.21) is the largest seed production such that the two seedling recruitment functions intersect (as it is the Example 1 and 2, see Figure A.1). In a way that is analogous to the argument for transient attenuation, for any initial population $\rho(\cdot)$ and specified difference N between total population densities in the two models, there exists a seed production γ_N that elicits (at least) this difference at time $t = 1$. To see this, let $n_1(\cdot, t)$ and $n_2(\cdot, t)$ and solve (2.15) with the same initial condition $\rho(\cdot)$, but with different seedling recruitment functions $f_1(\cdot)$ and $f_2(\cdot)$. Then, since the survival and growth portions of the kernel are the same for both models, one has

$$\|n_1(\cdot, 1)\| - \|n_2(\cdot, 1)\| = (f_1(\gamma(0)) - f_2(\gamma(0))) \int_L^U J(x) \, dx,$$

which reduces to

$$\|n_1(\cdot, 1)\| - \|n_2(\cdot, 1)\| = f_1(\gamma(0)) - f_2(\gamma(0)),$$

as $J(\cdot)$ is a probability distribution and the $f_i's$ are independent of x. If $f_1(\cdot)$ is the power function, we have that $\gamma(0) \to \infty$ implies that $f_1(\gamma(0)) \to \infty$. In contrast, if $f_2(\cdot)$ is the Michaelis-Menten function, $\gamma(0) \to \infty$ implies that $f_2(\gamma(0)) \to \alpha$, which confirms the claim of the existence of a γ_N that elicits a difference of at least N between the two models. Furthermore, because

$$\gamma(0) = ||\rho(\cdot)|| E_{\rho(\cdot)}(c(x)),$$

it follows that, given an initial probability density function for the population, one can find $||\rho(\cdot)||_N$ such that for $||\rho(\cdot)|| > ||\rho(\cdot)||_N$, we have

$$||n_1(\cdot, 1)|| - ||n_2(\cdot, 1)|| > N. \tag{2.22}$$

In Example 2, we will assume a homogeneous initial population and display this result by showing how increasing $||\rho(\cdot)||$ increases the difference between the predicted populations after only one time-step.

2.1.3.1   Example 1: Transient Attenuation

To illustrate the consequences of the preceding mathematical discussions for predicted transient dynamics, we first envision a brief ecological disturbance, like a fire, that wipes out the entire population of plants, with the exception of seeds in the soil that germinate to become seedlings in the following year, but does not significantly alter the long-term environmental conditions. While this is clearly an oversimplification, the goal of this example is to merely evaluate if the way we implement density dependence influences predicted transient dynamics.

To simulate this event, we will let $\rho(x) = MJ(x)$ be the initial population,

which consists entirely of seedlings, so $\rho(\cdot)$ is the population distribution of M $seedlings(area)^{-1}$. Very small plants do not reproduce, and seed production increases with plant size (see [67]), but plants of all sizes can die. Thus, we expect that a population consisting entirely of seedlings will decrease initially, before rising back to its equilibrium population density. Accordingly, for small t both IPMs predict transient attenuation because $c(\cdot)$ is increasing and survival and the probability of not flowering are always below unity. The main difference in transient dynamics between the two models is how quickly the population increases to its equilibrium density following the disturbance event. We began our simulations with M values equal to $10, 15, 25,$ and 50 $seedlings(area)^{-1}$ using identical initial size distributions of the seedlings, $J(\cdot)$ in each simulation. As expected, in both IPMs the population density values decline initially (see $t = 1$ in Figure 2.1). However, the power function model predicts a faster recovery than the mechanistic model and the smaller the M value the larger the difference between the predicted recovery patterns For example, if $M = 10$ and $t = 10$, the power function model predicts a population that is roughly twice as large as that of the mechanistic model. This is in accordance with the mathematical observation in (2.19). Initially, the total population densities and size distributions of the populations are very similar for both models. However, when the population density becomes small enough, the transient function of the power function model has large positive values (relative to the mechanistic model), and faster recovery begins (see $t = 1$ years in Figure 2.2).

2.1.3.2 Example 2: Transient Amplification

We expect transient amplification when the initial size distribution is skewed toward larger plants with higher reproductive value relative to the stable size distribution

because the function $c(\cdot)$ is increasing. We envision a restoration scenario where plants are grown in a greenhouse, until they reach a large target size and then transplanted into the field. In this case, the initial population consists entirely of large plants. To simulate this hypothetical situation, we used an approximation to the Dirac-Delta distribution (an explanation of the Dirac-Delta distribution can be found [52]), centered at nine tenths of U, the largest root crown diameter in the population. Thus, $\rho(x) = M\delta(x - 0.9U)$, with initial population densities, M, of $10, 15, 25$, and 50. As Figure 2.3 illustrates, the power function model predicts transient amplifications that are much larger relative to the mechanistic model, and this difference is more extreme for large initial population densities. If recruitment is modeled by the power function, the large seed densities produced by a population of large plants correspond to larger seedling densities compared to recruitment being modeled by the Michaelis-Menten function. This difference grows with the initial density because, naturally, large initial populations of seed-producing plants correspond to large seed production values, and thus, when large seed production values are the input for an unbounded power function, the model subsequently predicts larger seedling densities than that if we used the (bounded) Michaelis-Menten function. For example, in our simulation, a density of 50 large $plants(area)^{-1}$ produces $1,021,754\ seeds$. This is much larger than the equilibrium seed production of $\gamma^* = 18,904.6\ seeds$ (see Appendix A for this calculation), and thus, we would expect from (2.22) that the differences in recruitment would be quite large. In fact, the power function allows 1.07% of these seeds to become seedlings while the Michaelis-Menten function allows only 0.05% of these seeds to become seedlings. This difference in seed establishment probability corresponds to an order-of-magnitude difference in transient amplification between the two models.
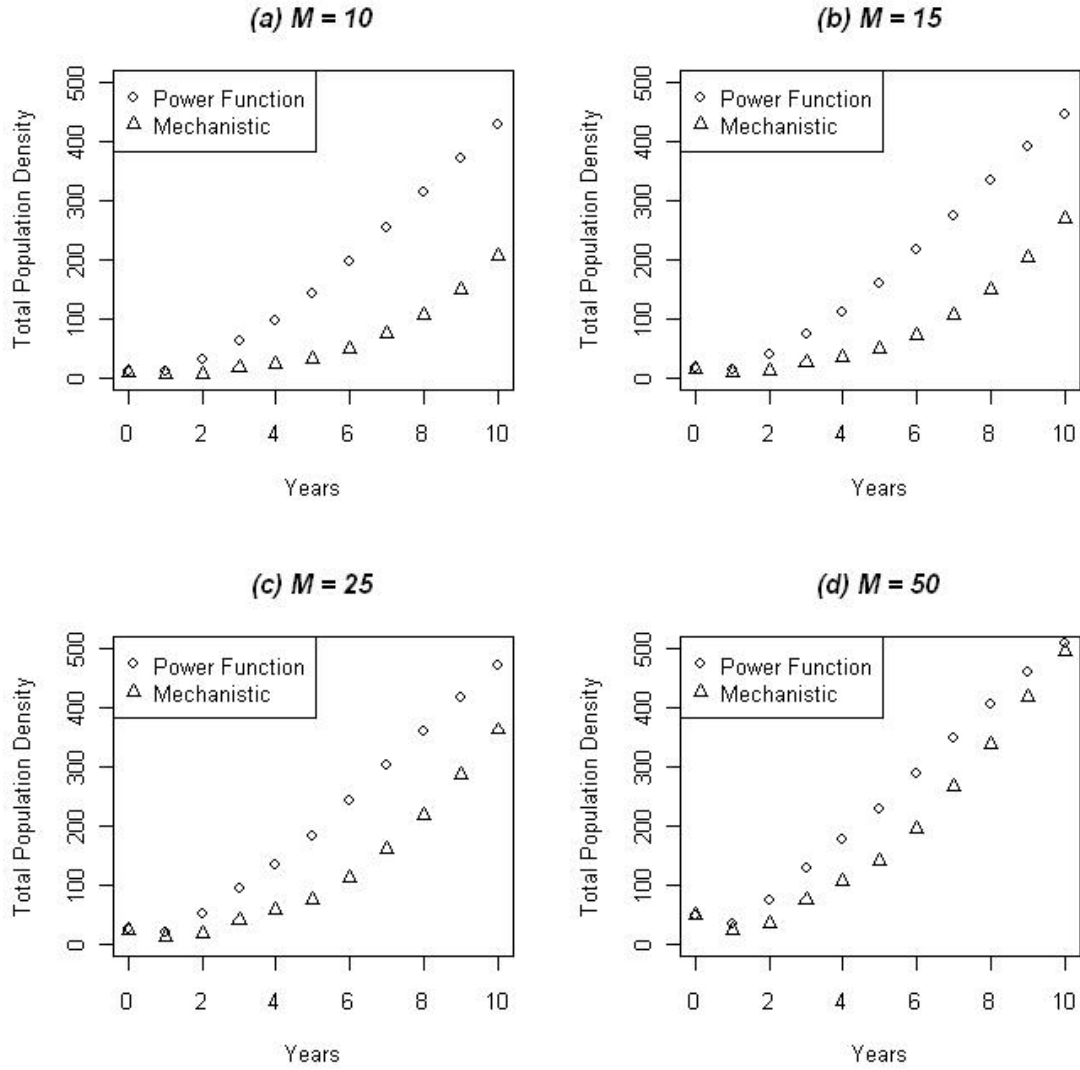
Figure 2.1: Predicted transient population dynamics for the two Platte thistle models resulting from simulating the ecological event in Example 1. The initial densities, M, are (a) 10, (b) 15, (c) 25, and (d) 50 $seedlings(area)^{-1}$; in each simulation, the size distribution of the seedlings was identical to that reported in [67].
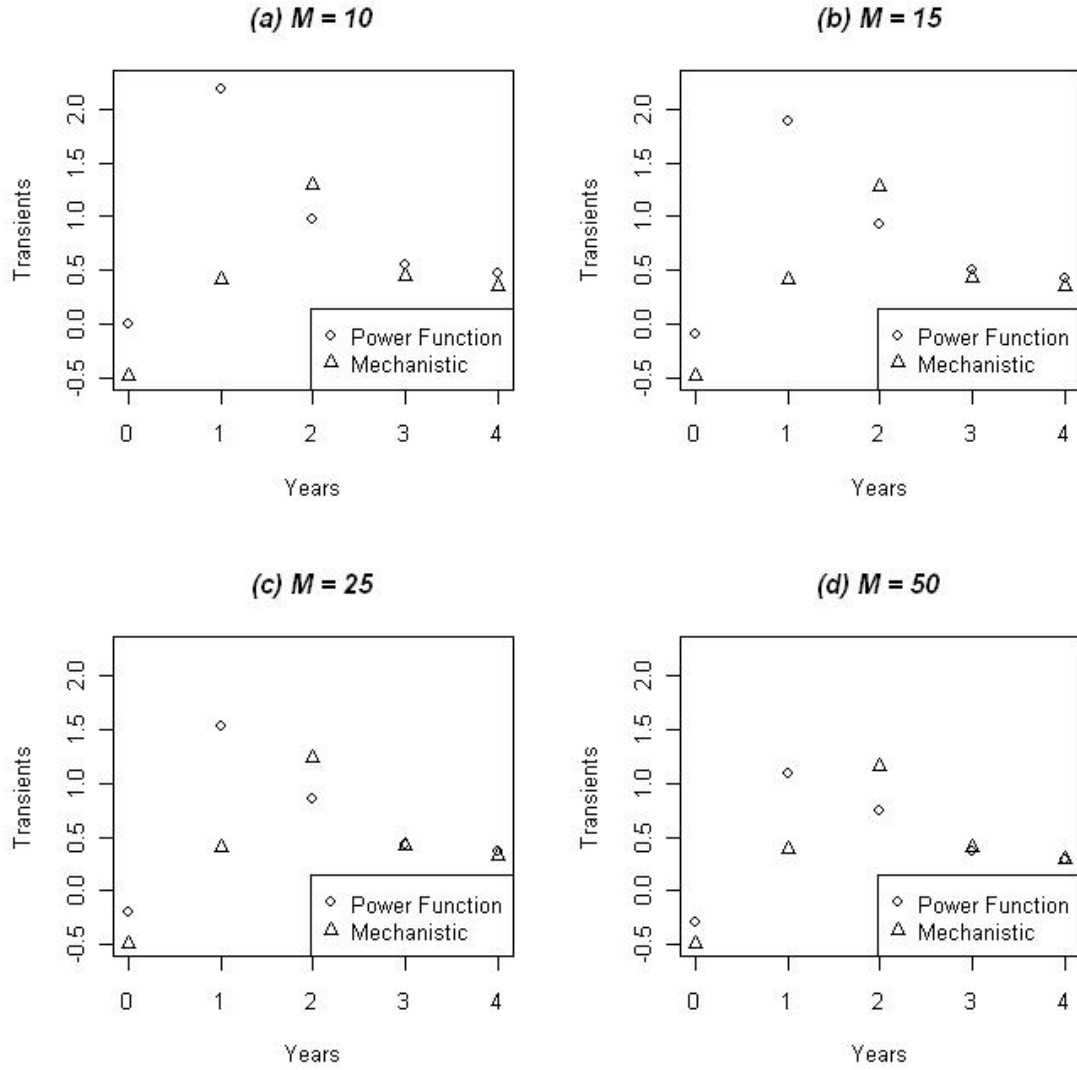
Figure 2.2: Predicted transient function values for the two Platte thistle models resulting from simulating the ecological event in Example 1. The initial densities, M, are (a) 10 (b) 15 (c) 25 and (d) 50 $seedlings(area)^{-1}$; in each simulation, the size distribution of the seedlings was identical to that reported in [67].
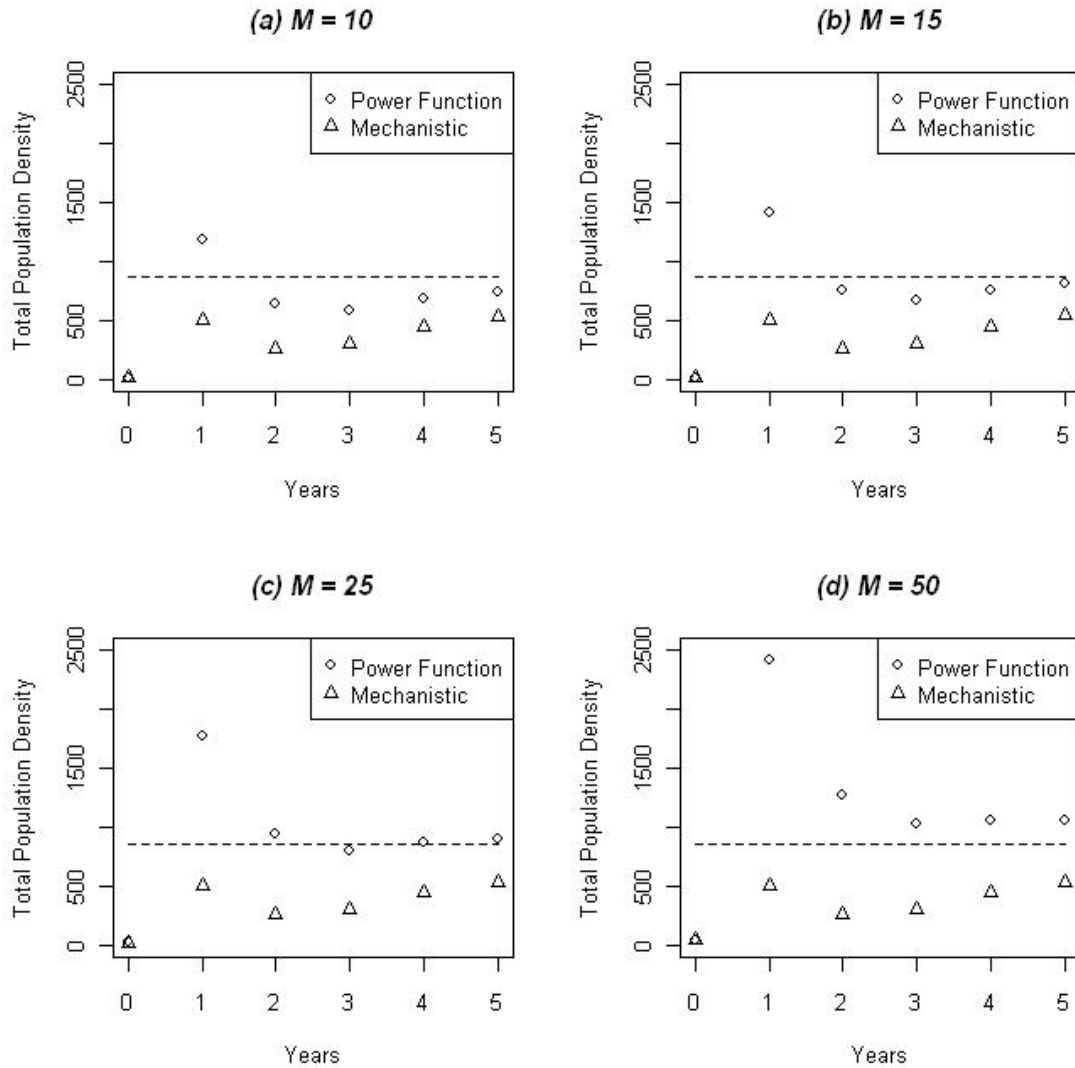
Figure 2.3: Predicted total population densities for the two Platte thistle models resulting from simulating the ecological event in Example 2. The initial densities, M, are (a) 10, (b) 15, (c) 25, and (d) 50; in each simulation, M was distributed according to the Dirac-Delta distribution centered at nine-tenths of the largest observable plants size. The dashed line illustrates the equilibrium population density (862.29 $seedlings(area)^{-1}$).

2.2 Comparison of Sensitivities

In this section we will derive exact sensitivities for the general nonlinear population model analyzed rigorously in [64] and [76] and reviewed in Chapter 1. This sensitivity is a structured sensitivity, i.e. it is a function of the stage variable in the model, as opposed to being one value (like λ or $N^* = ||n^*||$). We will then provide formulas for the sensitivities for the mechanistic and power function models from [67] used in the previous section. We will use these formulas to highlight further differences between the using a power function and a Michaelis-Menten function for seedling recruitment. We will also show that these differences are a function of the root crown diameter (the stage in the model) because the sensitivities of the equilibrium are also a function of the root crown diameter, showing the extra information one can obtain via structured sensitivities.

2.2.1 Derivation of Sensitivities

To derive the sensitives of the equilibrium population n^* we will consider the model (2.4) in the abstract form (from 1.3)

$$n_{t+1} = An_t + bf(c^T n_t). \tag{2.23}$$

We will consider the sensitivity of n^* to small changes in the data (A, b, c). In the model (2.4) A is the survival and movement operator defined by the integral kernel

$$Au = \int_L^U p_1(x, y)u(y)\, \mathrm{d}y,$$

for $u \in L^1[L, U]$. A small change $\epsilon \Delta A$ to the (x_0, y_0) element of A would be the limit of smooth functions approximating ϵ multiplied by the 2-dimensional Dirac-Delta

distribution $\delta(x - x_0, y - y_0)$.

The vector of newborns b from (2.4) is simply the probability distribution $J(\cdot) \in L^1[L, U]$ and the fecundity functional c is defined by

$$c^T u = \int_L^U c(y)u(y)\,\mathrm{d}y,$$

where a small change in b or c at the point x_0 would analogously be ϵ multiplied by the limit of smooth functions approximating the 1-dimensional Dirac-Delta distribution $\delta(x - x_0)$. For notational purposes we'll use δ to denote the Dirac-Delta distribution used for each perturbation. The actual Dirac-Delta distribution used will be clear according to context.

We will consider the case where n^* is positive for any non-zero initial population n_0 (i.e. the stability radius $p_e < \sup_{y>0} g(y) := g_0$). From Chapter 1,

$$n^* = p_e y^*(I - A)^{-1}b,$$

where y^* is the unique nonzero solution of the equation $f(y^*) = p_e y^*$. Because there is a simple formula for the equilibrium population n^* we can find exact sensitivities of this equilibrium to changes in the data (A, b, c).

We will first look at a small change in the operator A defined by the integral kernel in (2.2.1). Let $\Delta A := \epsilon \delta$ be a small perturbation to the (x_0, y_0) element of the integral kernel A, small enough so that the spectral radius of $A + \Delta A$ is still smaller than unity. The subsequent change in n^* is then

$$\Delta n^* = \Delta(p_e y^*)(I - A)^{-1}b + p_e y^* \Delta((I - A)^{-1}b).$$

For the models compared in this chapter one can express $p_e y^*$ as a function of p_e, which

we'll denote $p_e y^* := \psi(p_e)$. For example, if f is the power function $f(x) = \kappa x^\nu$, then $\psi(p_e) = \kappa^{\frac{1}{1-\nu}} p_e^{\frac{\nu}{\nu-1}}$ and if f is the Michaelis-Menten function, then $\psi(p_e) = \alpha - \beta p_e$. Since we write $p_e y^* := \psi(p_e)$ we can therefore write

$$\Delta(p_e y^*) = \Delta(\psi(p_e))\Delta(p_e).$$

Since $p_e = (c^T(I - A)^{-1}b)^{-1}$ we can calculate $\Delta(p_e)$ as follows:

$$\begin{aligned}
\Delta(p_e) &= \frac{1}{c^T(I - (A + \Delta A))^{-1}b} - \frac{1}{c^T(I - A)^{-1}b} \\
&= \frac{-c^T(I - (A + \Delta A))^{-1}\Delta A(I - A)^{-1}b}{c^T(I - (A + \Delta A))^{-1}bc^T(I - A)^{-1}b}.
\end{aligned}$$

Dividing by ϵ and taking the limit as $\epsilon \to 0$, we have

$$\frac{dp_e}{dA} = \frac{-c^T(I - A)^{-1}\delta(I - A)^{-1}b}{(c^T(I - A)^{-1}b)^2} := -(p_e)^2 w^T \delta v,$$

where $w := c^T(I - A)^{-1}$ and $v := (I - A)^{-1}b$ are the left and right eigenvectors, respectively, of the operator $A + p_e bc^T$, with eigenvalue $\lambda = 1$. Using a similar calculation we have that

$$\frac{d((I - A)^{-1}b)}{dA} = (I - A)^{-1}\delta v,$$

Therefore, the sensitivity of n^* to changes in the (x_0, y_0) element of A is

$$\frac{dn^*}{dA} = \frac{d\psi(p_e)}{dp_e}(-(p_e)^2 w^T \delta v)v + \psi(p_e)(I - A)^{-1}\delta v. \tag{2.24}$$

Notice that the sensitivity of the equilibrium population n^* to a change in A is the sum of the change due to changes in equilibrium reproduction $(\psi(p_e))$ and the

change due to changes in equilibrium population structure ($v = (I - A)^{-1}b$).

Employing a similar calculation one can show that the sensitivity of the equilibrium population n^* to a change $\Delta c := \epsilon\delta$ in c obeys the following equation

$$\frac{dn^*}{dc} = \frac{d\psi(p_e)}{dp_e}(-(p_e)^2\delta^T v)v.$$

Notice that, since the equilibrium population structure $v = (I - A)^{-1}b$ does not depend on c, the sensitivity $\frac{dn^*}{dc}$ comes only from changes in equilibrium reproduction.

Because b is usually a probability vector, if one makes a perturbation to an element in b a compensatory perturbation must also be made to another (or a series of other) elements in b. The biological realism of these perturbations notwithstanding, let's assume for now that one is perturbing b by removing ϵ from the x_0 element and adding ϵ to the x_1 element, using $\Delta b := \epsilon\delta$ to denote such a perturbation. By an analogous calculation to that of $\frac{dn^*}{dA}$ we have that

$$\frac{dn^*}{db} = \frac{d\psi(p_e)}{dp_e}(-(p_e)^2 w^T\delta)v + \psi(p_e)(I - A)^{-1}\delta. \qquad (2.25)$$

2.2.2 Results

We will now compare the sensitivity of n^* in the power function model (from [67]) to that of the sensitivity of n^* mechanistic model. To do this it is advantageous of us to write the abstract equations (2.24), (2.2.1), (2.25) using the terms in the integral projection model. In this setting the population is a function of the root crown diameter, x, and thus $n^* = n^*(x)$. Define $w(\cdot)$ and $v(\cdot)$ to be the left and right

eigenfunctions, respectively, of the integral operator $A + p_e bc^T$ defined by

$$(A + p_e bc^T)u := \int_L^U (p_1(x, y) + p_e J(x)c(y))u(y)\,\mathrm{d}y,$$

for all $u \in L^1[L, U]$, with eigenvalue 1. Also, let $K(\cdot, \cdot)$ denote the kernel function such that, for all $u \in L^1[L, U]$

$$(I - A)^{-1}u := \int_L^U K(x, y)u(y)\,\mathrm{d}y. \tag{2.26}$$

Using (2.26), the sensitivity of $n^*(\cdot)$ to changes in the (x_0, y_0) element of $p_1(\cdot, \cdot)$ becomes

$$\frac{dn^*(x)}{dp_1(x_0, y_0)} = \frac{d\psi(p_e)}{dp_e}(-(p_e)^2 w(x_0)v(y_0))v(x) + (\psi(p_e)v(y_0))K(x_0, x). \tag{2.27}$$

The sensitivity of $n^*(\cdot)$ to changes in the x_0 element of $c(\cdot)$ becomes

$$\frac{dn^*(x)}{dc(x_0)} = \frac{d\psi(p_e)}{dp_e}(-(p_e)^2 v(x_0))v(x). \tag{2.28}$$

Finally, the sensitivity of $n^*(\cdot)$ to a small decrease in the x_0 element of $J(\cdot)$ with a compensatory small increase in the x_1 element of $J(\cdot)$ becomes

$$\frac{dn^*(x)}{db(x_0, x_1)} = \frac{d\psi(p_e)}{dp_e}(-(p_e)^2(w(x_1) - w(x_0)))v + \psi(p_e)(K(x_1, x) - K(x_0, x)). \tag{2.29}$$

To compare the power function and mechanistic models' sensitivities we will only consider the situation where the models have identical equilibrium populations. It is important to note that, if the equilibrium populations are the same, the second terms of (2.27) and (2.29) will both be the same. Therefore, any differences between

the two models will come from differences in the term $\frac{d\psi(p_e)}{dp_e}$. For the power function model $\frac{d\psi(p_e)}{dp_e} = \kappa^{\frac{1}{1-\nu}} \frac{\nu}{\nu-1} p_e^{\frac{1}{\nu-1}}$, which is roughly equal to -15178. For the mechanistic model $\frac{d\psi(p_e)}{dp_e} = -\beta$, which is equal to -4706. This is an order of magnitude difference. Therefore (2.28) and the first terms of (2.27) and (2.29) will differ by an order of magnitude.

The presence of structure in the sensitivity functions (2.27), (2.28), (2.29) yields interesting results for the differences between the power function model and the mechanistic model. For example, Figure 2.4 shows that the sensitivity functions are essentially the same for $x < -0.25$ and $x > 3$, but can differ greatly in the interval $[0, 2.5]$ (the spike is due to the second term in (2.27)). This structure in sensitivity is even more apparent when exploring these differences in the sensitivities (2.29) and (2.28) (Figures 2.5 and 2.6, respectively). The lack of a spike in Figure 2.6 is due to the lack of a second term in (2.28).

Overall, the power functional model's equilibrium population is more sensitive than that of the mechanistic model, although this sensitivity is not generally distributed equally throughout the population. The change in a particular element in the kernel can elicit a spike in the sensitivity function (due to the second term in (2.27) and (2.29)), but there is also proportional change in the long-term population structure $v(\cdot)$ that is from the term $\frac{d\psi(p_e)}{dp_e}$ (which we've shown is very different depending on the nonlinearity used). Because the population is weighted heavily towards members with stage variable $x \in [0, 2.5]$ (see Figure 2.7), a proportional change in population structure $v(\cdot)$ is going to more drastically change members of the population whose stage variable falls into this interval in the long term.

An interesting result is that the differences in the fecundity sensitivity (2.28) between the power function model and the mechanistic model are smaller than the differences in the survival and movement sensitives (2.27) and the sensitivities to

changes in the newborn vector (2.29). This may be due to the fact that the function $c(\cdot)$ contains the largest terms in the model, so a small change in $c(\cdot)$ may not be noticeable when eventually calculating the new stability radius p_e. It may also be due to the fact that $c(\cdot)$ has no bearing on the long-term population structure, $v(\cdot)$, leaving (2.28) with only one term.
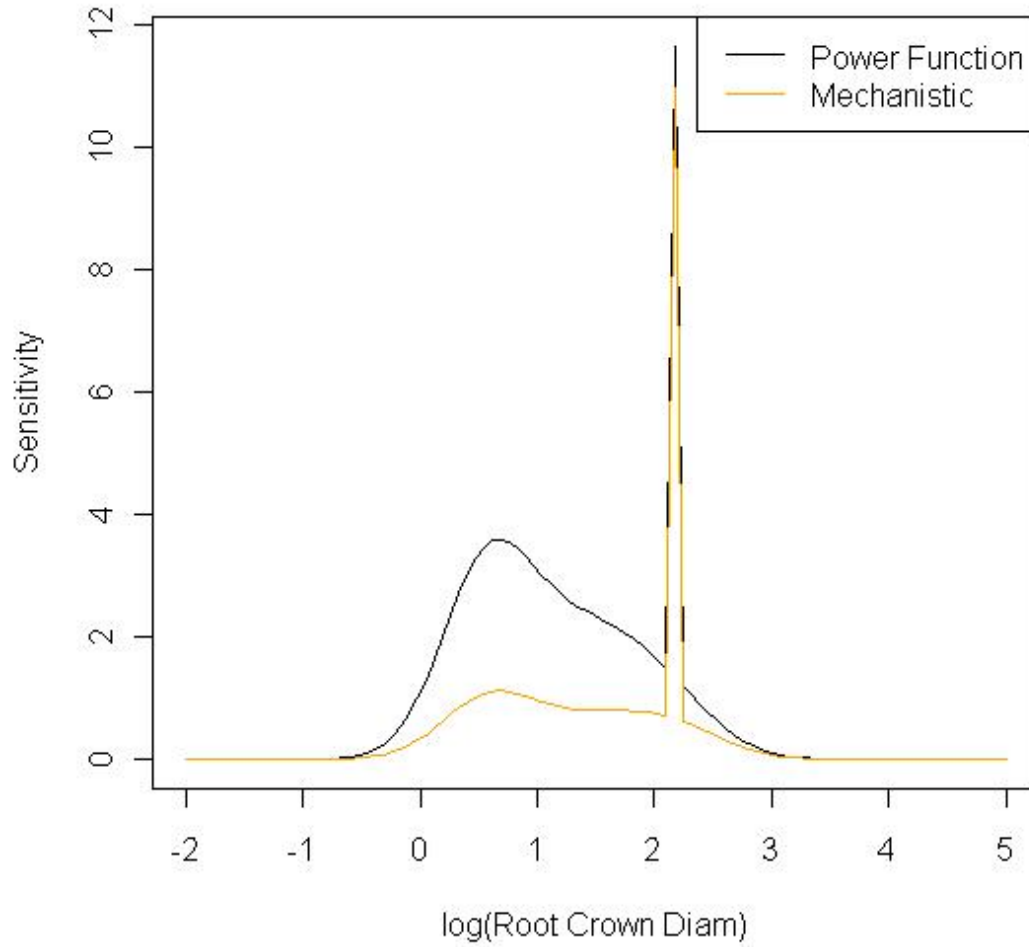
Figure 2.4: The sensitivity of the power function model (black lines) and the mechanistic model (orange lines) to a small change in the $(x_0, y_0) = (2.46, 2.46)$ term of the kernel $p_1(\cdot, \cdot)$.

2.3 Discussion

Using the model for Platte thistle in [67] as a case study, we have shown that the predicted transient dynamics and sensitivities of the predicted equilibrium population can
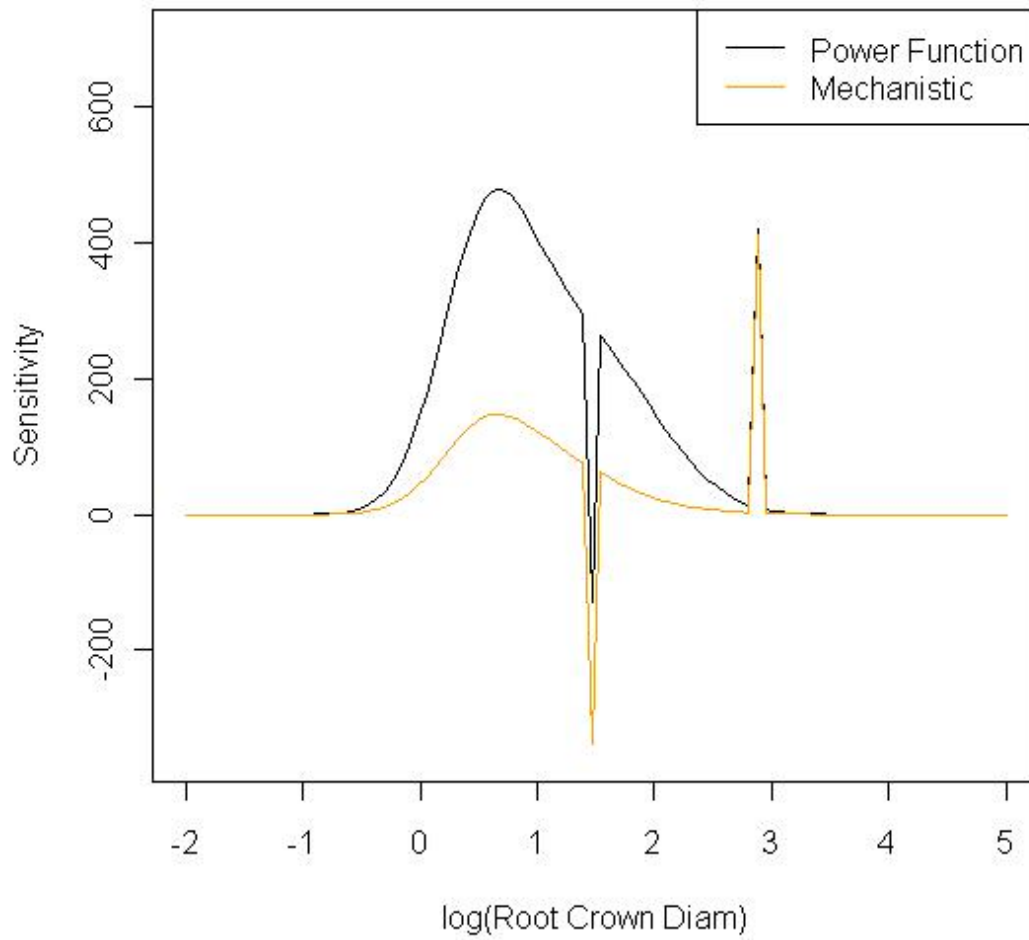
Figure 2.5: The sensitivity of the power function model (black lines) and the mechanistic model (orange lines) to a small decrease in the $x_0 = 1.71$ term and a compensatory increase in the $x_1 = 3.21$ term of the function $J(\cdot)$.
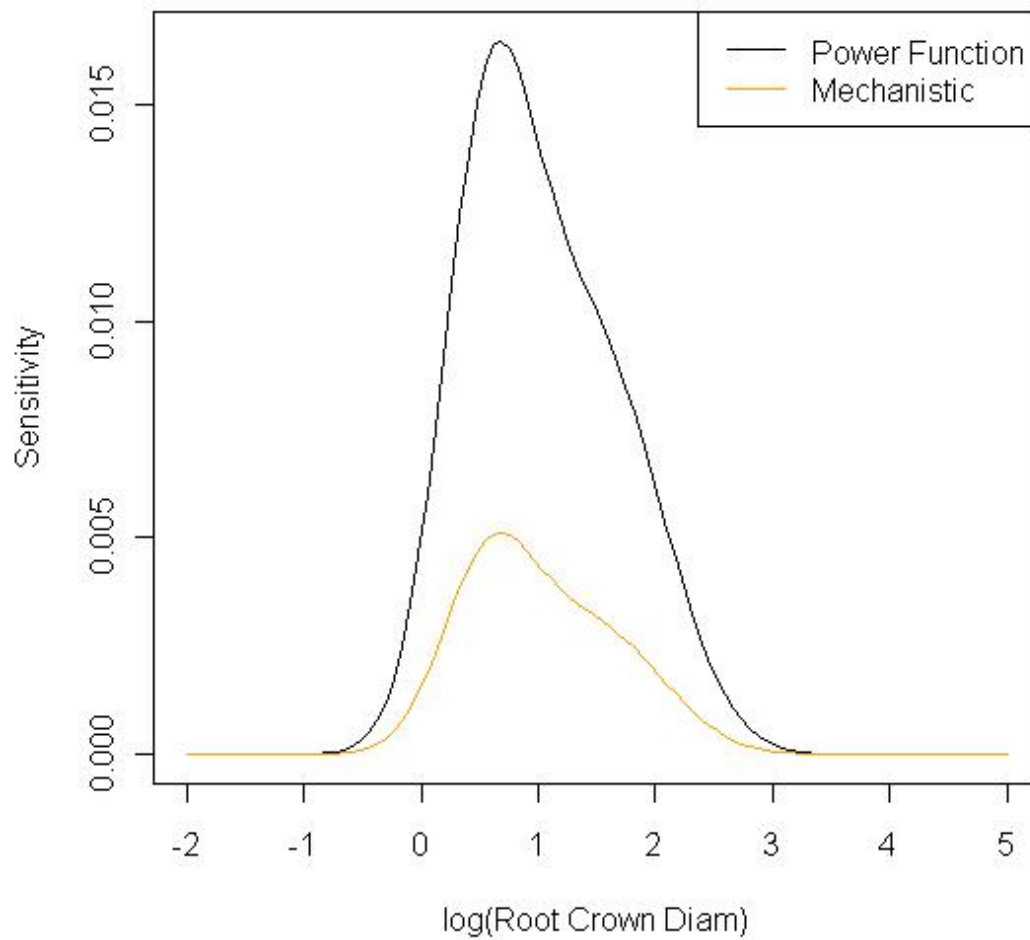
Figure 2.6: The sensitivity of the power function model (black lines) and the mechanistic model (orange lines) to a small change in the $x_0 = 2.46$ term of the function $c(\cdot)$.
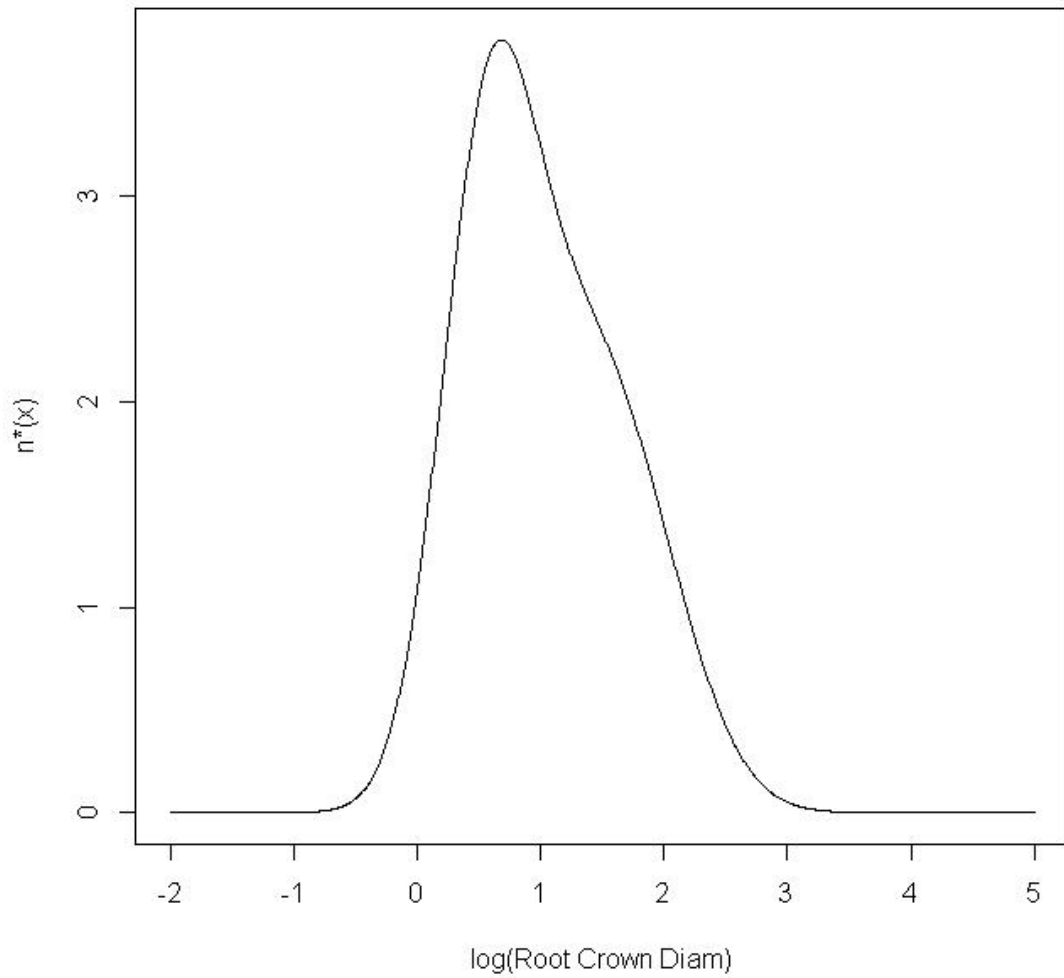
Figure 2.7: The equilibrium population $n^*(\cdot)$ of the model in [67] with the adjusted power function. Note that this function is proportional to the right eigenfunction $v(\cdot)$ of the integral operator $\int_L^U (p_1(\cdot, y) + p_e J(\cdot)c(y))(\cdot)\,\mathrm{d}y$ with eigenvalue 1.

vary considerably depending on how we implement density dependence in recruitment, even if the equilibrium dynamics are the same. Through mathematical arguments we verify that the differences in transient dynamics between these two models are due to the differences in functional form, and not simply a product of parameter uncertainty, as the results in (2.19) and (2.22) are for general power functions and general Michaelis-Menten functions. So while some parameter values may display these differences more drastically than others, the results in this chapter suggest that for some ecological outcomes the predicted transient dynamics will differ, regardless of parameter values used, and these differences do not have a bound.

It is interesting to note that when the parameters in the Michaelis - Menten function were fit independently in [30], the resulting equilibrium population density $(||n^*|| = 429 \ plants(area)^{-1})$ was similar to the beginning population size reported in Fig. 1a in [67] prior to the invasion by *Rhinocyllus*. This would appear to build on the suggestion made in this chapter that mechanistic modeling, followed by standard methods of parameter estimation, offers the ideal prospect for obtaining a useful model when the data are poor.

The differences in the sensitivities of n^* between the two models should not be surprising: The differences in sensitivity stem from differences in the derivative of $\psi(p_e)$, which is implicity tied to the functional form for f used. It is an observed phenomenon in approximation theory that the derivative of the function that best fits a particular set of data often bears no resemblance to the derivative of the "true" function being approximated (see, for example, Example 6.3 in [72]). Thus, it is very possible that two models can have very distinct derivatives $\frac{d\psi(p_e)}{dp_e}$ while having very similar $\psi(p_e)$ functions, which is what is seen in Section 2.2.2.

The importance of choosing the most appropriate functional form for density-dependent recruitment has been recognized in other contexts. For example, [68]

has shown that the functional form used for recruitment can influence the optimal harvesting strategy for duck populations in a nontrivial way. They argue that the differences between these functions often lie outside the range of observed, or even anticipated, data, and therefore, statistical methods are limited in determining what functional relationships in vital rates are most appropriate. To address the effect of the resulting structural uncertainty on model predictions, the authors advocate for active probing of models that vary in their implementation of vital rates, which means exploring model predictions outside the realm of data collection. The benefit of this active scrutiny is often overlooked because model validation typically focuses on replicating previously observed phenomena ([55]). In the study by [67], there were no empirical recruitment data for very low or very high seed densities available and the two alternative recruitment functions differ mainly in the unobserved data range (Figure 1.1), and in the way they elicit $\frac{d\psi(p_e)}{dp_e}$. The differences in the predicted transient dynamics and in the sensitivities to the predicted equilibrium population to the choice of the recruitment function highlights the value of active probing of model components.

Density dependence occurs due to the regulatory nature of limited resources in a system. The strength of density dependence should be highest at some carrying capacity, and population growth should not be limited at low population density, resulting in essentially linear dynamics. The Michaelis-Menten function is essentially linear for small seed densities (provided that β is sufficiently large). This implies that the density dependence does not influence population dynamics until the seed density is sufficiently high, which is what we expect to see. In contrast, when using the power function, seedling recruitment is never linear for low seed densities. Thus, the power function may poorly predict the dynamics at low density levels. In other words, while the population might not be experiencing the biological effects of density

dependence, we are still predicting its dynamics subject to the *mathematical* effects of density dependence ([42]). In Example 1, we discovered that the power function models transient function can become arbitrarily large when the populations density becomes sufficiently small (see (2.19)). This is due to the fact that the power functions derivative is unbounded for seed production densities close to zero, which causes seed establishment probability to be greater than unity for small seed densities. For example, if $\gamma(\cdot) = 3$, then

$$\kappa\gamma(\cdot)^{\nu} = 5.0899(3)^{0.4453} = 8.301782$$

which implies that $p_e(\cdot) = 2.777$, which is clearly false, as seed establishment probability needs to be bounded above by a number smaller than unity to make sense. The largest seed establishment value for the Michaelis-Menten function is much smaller than unity, as $p_e(\cdot) \leq \alpha(\beta)^{-1} = 0.108$.

In the case where the total seed production is much larger than the available number of microsites, a constant number of seedlings are recruited for each time-step. No such limiting value will be obtained in the power function because it is unbounded for large seed values, and the number of seedlings always increases with the number of seeds produced. Even though models using the power function to represent density-dependent recruitment predict equilibrium population densities, the lack of an upper bound for recruitment may still lead to poor predictions of annual seedling recruitment if populations are skewed toward individuals with high reproductive value. The result is an overestimation of the potential magnitude of transient amplification (see (2.22) and Figure 2.3). In contrast, the Michaelis-Menten function is more realistic in this situation because, as the number of seeds produced goes to infinity, the density of recruited seedlings approaches the constant α. This constant is determined by the

number of available microsites.

We have shown that the choice of the functional forms, such as density-dependent recruitment, can have profound effects on predicted transient dynamics and the sensitivity of the equilibrium population to changes in model parameters. This suggests that more emphasis should be placed on functional relationships that are derived based on mechanistic ecological principles.

Chapter 3

Global Stability of Plant-Seed Bank Models with Age-Structured Seeds

3.1 Plant-Seed Bank Model

In this chapter we will analyze the global stability of a general plant population with an age-structured seed bank. Seed banks have been modeled as structured populations in only a few references (e.g. [48], [10], [32], [17]). We are unaware of any studies of *global* asymptotic dynamics of a general density-dependent plant-seed bank model with an age-structured seed bank.

Plant Population

The plant population at time t is described by a vector n_t, which is assumed to be in the cone of non-negative vectors in a Banach Space X_1 for $t = 0, 1, \ldots$. In a PPM ([12]) X_1 is a finite dimensional space $\mathbb{R}^m$ (so n_t is a population vector), and in an

IPM ([33]) X_1 is often the space $L^1[L,U]$ of integrable functions on the interval of stages $[L,U]$ (so $n_t(x)$ is a function of a continuous variable x). In the absence of a seed bank, the plant population is governed by the abstract, nonlinear population projection model

$$n_{t+1} = An_t + bf(h(c^T n_t)), \tag{3.1}$$

which is similar to (1.3) with $f(\cdot) = f(h(\cdot))$. In this model, however, there are two nonlinearities representing density dependence; one for seed production (h) and one for recruitment from seedlings to plants (f). In the absence of a seed bank one could simply compose these functions into one nonlinearity. However, when modeling the seed bank this distinction, as we will see in later sections, is important.

The terms in (3.1) are as follows: The population projection operator A is in $\mathcal{L}(X_1)$, the space of bounded, linear operators from X_1 to itself. An example of A is the kernel

$$An = \int_L^U p_1(x,y)n(y)\,\mathrm{d}y,$$

from Chapter 2. In this example $n \in X_1 = L^1[L,U]$. The operator A models the two ecological processes of survival and movement from one stage to another. Since this process cannot create new members of the population, $r(A) < 1$ (where $r(A)$ is the spectral radius of A). The vector $b \in X_1$ models the stage distribution of new plants (which is assumed to be independent of mother plant, [33]), and c^T is a bounded linear functional on X_1, where $c^T n_t$ gives the abundance of available seeds produced by the population at time t in a completely density-independent environment. The notation c^T is used instead of c in order to distinguish a functional on X_1 from a vector in X_1, much like a row vector is distinguished from a column vector. An example of b is the

probability distribution $J(\cdot)$ from Chapter 2, and an example of the functional c is

$$c^T n = \int_L^U c(y) n(y) \, \mathrm{d}y$$

from Chapter 2, for $n \in X_1$, which again in this example is $L^1[L, U]$.

3.1.1 Density Dependence

Consider the following feedback between plants, seeds and seedlings, which is assumed to occur in one time-step:

$$\text{mature plants} \xrightarrow{\text{seed production}} \text{seeds} \xrightarrow{\text{germination}} \text{seedlings} \xrightarrow{\text{establishment}} \text{juvenile plants.}$$

We will assume that the *seed production* and *establishment* processes can be density dependent. The seed production density dependence will be modeled with the function h and the establishment density dependence with the function f.

In many models the density of seeds produced (the *seed production* step) by the plants in the population is assumed to be density independent (for example the model studied in Chapter 2 from [67]). In the model studied in Section 3.2.1 we assume such a density-independent relationship by letting $h(y) = y$, so the number of new seeds produced in the population during time t will simply be $c^T n_t$.

However, some plant populations experience a density-dependent relationship between the abundance of plants and seeds produced (see, for example, [46]). Therefore, we will assume in Sections 3.2.2, 3.2.3, 3.2.3.1 and 3.2.3.2 that the abundance of new seeds produced at time t is $h(c^T n_t)$, where h is a nonlinear function (which we'll assume has a maximum of $c^T n_t$, the seed production in the complete absence of

density dependence).

The *establishment* density dependence will be modeled as follows: The scalar quantity $f(y)$ represents the number of new plants generated by y available germinating seeds, which we will assume is the sum of newly created seeds that germinate at time t and the sum of all older seeds that germinate. We assume that seeds become seedlings (via germination) in a density-independent way. This process is implicit in the function f; as one could assume that $f(y) = \tilde{f}(g_p y)$, where g_p is the (constant) germination probability for the y available seeds and $\tilde{f}(\cdot)$ is the function such that $f(y) = \tilde{f}(g_p y)$ for all $y \in [0, \infty)$, but we will suppress this subtlety. The diminishing amount of available microsites then causes a density-dependent relationship between the abundance of germinating seeds and the subsequent abundance of new plants in the population.

It is natural to view $f(y)$ as the product of the number of germinating seeds y available and the probability $g(y)$ that a germinating seed eventually becomes a new plant in that time-step. Thus

$$f(y) = g(y)y. \tag{3.2}$$

We will call the function g the *establishment probability*.

We consider the following conditions on f and g:

(D1) $g \in C(0, \infty)$, g is a decreasing function on $(0, \infty)$, $f(0) = 0$, and f is strictly increasing and concave down.

These are the same as the conditions on g and f assumed in [64] and [76]. Some ecologically motivated functions that satisfy these assumptions are power functions of the form

$$f(y) = \kappa y^\nu \qquad \text{with } \nu \in (0, 1) \text{ and } \kappa > 0, \tag{3.3}$$

and Michaelis-Menten type functions of the form

$$f(y) = \frac{\alpha y}{\beta + y} \qquad \text{with } \alpha \in (0,1) \text{ and } \beta > 0. \qquad (3.4)$$

See Chapter 2 for a derivation of the Michaelis-Menten function for seed-to-plant density dependence in a general plant population.

In Section 3.2.1 we assume $h(y) = y$, and the global asymptotic stability of the plant-seed bank population is a corollary of the work in [64].

When h models either *contest competition* or *scramble competition* the two non-linearities f and h will require more than one stability radius, which will force us to obtain more conditions for these stability radii to satisfy. The analysis of global stability in Sections 3.2.2 and 3.2.3 will therefore require a substantial modification of the results in [64] and [76], surveyed in Chapter 1, which is the main mathematical novelty in this chapter.

3.1.2 Age-Structured Seed Bank Model

We assume that the seed bank is structured with respect to the age of the seeds, in the sense that the survival of the seeds in the seed bank is a function of age. There is evidence that this is true in general ([2], [48], [54]). We assume that each seed, while potentially surviving at different rates, has the same probability of germinating. We further assume there is an age after which a dormant seed in the seed bank is either no longer viable or is placed in a final class of "old" seeds.

We will use the following notation: the seed bank at time t has N discrete *age* stages, $s_{1,t}, s_{2,t}, \ldots s_{N,t}$, where $s_{j,t}$ are seeds that are j time steps old at time t. Then $s_t = [s_{1,t}, s_{2,t}, \ldots s_{N,t}]^T$ is the seed population vector at time t. As previously stated,

the number of available seeds $\tilde{y}_t$ at time t is the sum of newly created seeds and available old seeds at time t. Written mathematically,

$$\tilde{y}_t := h(c^T n_t) + s_{1,t} + s_{2,t} + \dots + s_{N,t}.$$

We define the values $\gamma_j \in (0,1)$ to be the product of the probability of not germinating and survival (assumed statistically independent) in one time step from the $(j-1)$th age class to the jth age class, for $j = 1, 2, \dots, N$. The number γ_{N+1} is the product of not germinating and survival in one time step from the Nth age class to all later ages. If g_p is the germination probability of seeds in the seed bank, then it follows that $g_p + \gamma_j < 1$, as seeds cannot *directly* create new seeds.

The seed population vector at time $t+1$ is obtained from the seed population vector at time t by the following: $s_{1,t+1}$ consists of the density of seeds produced by plants which survive and do not germinate in the current year. Later seed classes $s_{j,t+1}$ consists of seeds that do not germinate and survive from seed class $s_{j-1,t}$, for $j = 2, \dots N - 1$. $s_{N,t}$ contains all ages N or higher, so $s_{N,t+1}$ also contains seeds that do not germinate and survive from $s_{N-1,t}$ and $s_{N,t}$.

Hence the seed bank population $\{s_t\}_{t=0}^{\infty}$ evolves in $\mathbb{R}^N$ for some integer N which represents the oldest seed class. The resulting plant-seed bank model can be written

as

$$
\begin{aligned}
n_{t+1} &= An_t + bf(\tilde{y}_t), \quad \tilde{y}_t = h(c^T n_t) + ||s_t||_1 \\
s_{1,t+1} &= \gamma_1 h(c^T n_t) \\
s_{2,t+1} &= \gamma_2 s_{1,t} \\
&\vdots \\
s_{N-1,t+1} &= \gamma_{N-1} s_{N-2,t} \\
s_{N,t+1} &= \gamma_N s_{N-1,t} + \gamma_{N+1} s_{N,t}.
\end{aligned}
\tag{3.5}
$$

3.1.3 Abstract Formulation

We will write (3.5) as an abstract first-order system, in order to prove the desired global stability results. Let the norm on the Banach space X_1 be denoted by $\|\cdot\|_{X_1}$, and let X_2 be $\mathbb{R}^N$ with associated 1-norm

$$
\|[x_1, x_2, \ldots x_N]^T\|_1 = \sum_{j=1}^{N} |x_j|.
$$

We wish to work with nonnegative vectors in, and nonnegative operators on, X_1 and X_2. Let K_1 and K_2 be reproducing cones for X_1 and X_2, respectively, with the partial ordering $\geq$ (see [51] for a general theory). We will call vectors in K_1 and K_2 non-negative vectors. An example of a reproducing cone in $\mathbb{R}^N$ is $\{[x_1, x_2, ..., x_n]^T | x_j \geq 0$ for $j = 1, 2, ..., N\}$. An example of a reproducing cone in $L^1[L, U]$ is $\{f \in L^1[L, U] | f(x) \geq 0 \ a.e\}$. In both of these examples the idea of a non-negative vector is consistent with intuition.

For $i = 1, 2$ we will call an operator on X_i that maps non-negative vectors to

non-negative vectors a *non-negative operator*. An example of such an operator is an $N \times N$ matrix A with all non-negative entries.

The following hypotheses are natural in the study of plant-seed bank dynamics. First, we state the conditions on the data for the plant population, (A, b, c).

(E1) $A \in \mathcal{L}(X_1)$ is a non-negative operator with spectral radius $r(A) < 1$;

(E2) b is a non-negative vector in X_1;

(E3) $c^T : X_1 \to \mathbb{R}$ is a strictly positive linear functional, i.e. there exits $c_{\min} > 0$ such that

$$c^T n \geq c_{\min} \|n\|, \qquad \text{for all } n \geq 0; \tag{3.6}$$

(E4) The coefficients $\gamma_j \in (0, 1)$ for all $j = 1, 2, ...N$ and $\gamma_{N+1} \in [0, 1)$.

Conditions (E1) and (E2) are not restrictive for most plant population models. Condition (E3) is not restrictive for when (A, b, c) is an integral projection model (see Section 4 of [64]), but can be restrictive when (A, b, c) is a matrix projection model. However, the following results can be replicated if we assume primitivity of the matrices used to model the plant population (see Section 3.4).

We can describe the coupled system (3.5) by a first-order system. The state of this system is

$$\tilde{n}_t := [n_t \ s_t]^T \subset X := X_1 \otimes X_2.$$

All convergence discussed in this chapter is in the Banach Space norm defined on X by $\|\cdot\| = \|\cdot\|_{X_1} + \|\cdot\|_1$.

Let

$$\tilde{A} := \begin{bmatrix} A & \emptyset \\ \Gamma & S \end{bmatrix}, \qquad \tilde{b} := \begin{bmatrix} b \\ 0 \\ \vdots \\ 0 \end{bmatrix}, \qquad \tilde{c}^T := \begin{bmatrix} h(c^T \cdot) & 1 & \dots & 1 \end{bmatrix}.$$

Here $\emptyset := [0 \; 0 \dots 0] \in \mathcal{L}(X_2, X_1)$ where 0 represents the zero vector in X_1,

$$\Gamma := [\gamma_1 h(c^T \cdot) \; 0^T \; \dots \; 0^T]^T \in \mathcal{L}(X_1, X_2),$$

where 0^T is the zero functional on X_1, and $S \in \mathcal{L}(X_2)$ is the $N \times N$ substochastic shift matrix

$$S = \begin{bmatrix} 0 & 0 & \dots & 0 \\ \gamma_2 & 0 & \dots & 0 \\ 0 & \gamma_3 & \dots & 0 \\ \vdots & \vdots & \vdots & \vdots \\ 0 & \dots & \gamma_N & \gamma_{N+1} \end{bmatrix}.$$

Using the amended system data, we can write the coupled system (3.5) as

$$\tilde{n}_{t+1} = \tilde{A}\tilde{n}_t + \tilde{b}f(\tilde{y}_t), \qquad \tilde{y}_t = \tilde{c}^T \tilde{n}_t. \tag{3.7}$$

Notice that, unless h is linear, Γ is a nonlinear operator, which makes $\tilde{A}$ a nonlinear operator. This nonlinearity is the substantial difference between the model in this chapter and that in [64] and [76].

3.2 Global Stability Results

3.2.1 Density-Independent Seed Production

In the case of density-independent seed production we have $h(y) = y$ for all y. We will obtain global asymptotic stability results for (3.7), and hence for (3.5) by applying the results in [64]. To do this we will need to recall the concept of the stability radius of the linear system

$$\tilde{n}_{t+1} = \tilde{A}\tilde{n}_t + p\tilde{b}\tilde{c}^T\tilde{n}_t,$$

where p is a scalar and $f(y)$ is replaced with $f(y) = py$. From Chapter 1 the stability radius $\tilde{p}_e$ is the smallest positive number p such that $r(\tilde{A} + p\tilde{b}\tilde{c}^T) = 1$. From [43] $\tilde{p}_e$ is equal to $(\tilde{c}^T(\tilde{I} - \tilde{A})^{-1}\tilde{b})^{-1}$.

As also reviewed in Chapter 1 the asymptotic behavior of (3.7) and (3.5) depends upon the relationship between the function g (see (3.2)) and the stability radius $\tilde{p}_e$. Roughly speaking, the nonlinear establishment probability function g needs to able to achieve the value $\tilde{p}_e$ for there to be a non-zero equilibrium. In particular, if $g(y) < \tilde{p}_e$ for all $y \geq 0$, then the population dies out. Furthermore, g needs to be able to eventually fall below $\tilde{p}_e$ for the population to settle down, i.e. if $g(y) > \tilde{p}_e$ for all $y \geq 0$ the population can grow without bound. If $\tilde{p}_e$ is between these two thresholds the population has a globally asymptotically stable, strictly positive equilibrium vector. Define

$$g_\infty := \lim_{y \to \infty} g(y), \quad g_0 := \lim_{y \searrow 0} g(y). \tag{3.8}$$

Theorem 3.2.1 *Let $h(y) = y$ and suppose that (D1), (E1), (E2), (E3) and (E4) hold.*

1) If $\tilde{p}_e > g_0$, then the zero vector is a globally stable equilibrium for (3.7) in the

sense that for every non-negative $\tilde{n}_0 \in X_1 \otimes X_2$,

$$\lim_{t \to \infty} \tilde{n}_t = 0.$$

Furthermore, for every $\epsilon > 0$, there exists $\delta > 0$ such that $\|\tilde{n}_t\| < \epsilon$ for all $t \in \mathbb{N}$ whenever $\|\tilde{n}_0\| < \delta$.

2) *If $\tilde{p}_e < g_\infty$, then there exists a non-negative initial vector $\tilde{n}_0 \in X_1 \otimes X_2$ such that*

$$\lim_{t \to \infty} \|\tilde{n}_t\| = \infty.$$

3) *If $\tilde{p}_e \in (g_\infty, g_0)$ then there exists y^* such that $f(y^*) = \tilde{p}_e y^*$. The vector $\tilde{n}^*$ given by*

$$\tilde{n}^* = \tilde{p}_e y^* (\tilde{I} - \tilde{A})^{-1} \tilde{b}$$

is a strictly positive globally asymptotically stable equilibrium of the system (3.7) in the sense that for every positive $\tilde{n}_0 \in X_1 \otimes X_2$,

$$\lim_{t \to \infty} \tilde{n}_t = \tilde{n}^*.$$

Furthermore, for every $\epsilon > 0$, there exists $\delta > 0$ such that $\|\tilde{n}_t - \tilde{n}^*\| < \epsilon$ for all $t \in \mathbb{N}$ whenever $\|\tilde{n}_0 - \tilde{n}^*\| < \delta$.

Proof: We need to show that when (E1), (E2) and (E3) are satisfied then (3.7) will satisfy conditions (A1), (A2) and (A3') in [64], and we will be able to apply Theorems 3.1, 3.2 and 3.3 in that paper to obtain 1), 2) and 3) of Theorem 3.2.1, with p_e replaced

by $\tilde{p}_e$. Since $b \geq 0$ in X_1, it immediately follows that $\tilde{b} \geq 0$ in $X = X_1 \otimes X_2$, showing that (E2) is satisfied for $\tilde{b}$.

For every $\tilde{n} \in X_1 \otimes X_2$:

$$\tilde{c}^T \tilde{n} = c^T n + \|s\|_1 \geq c_{\min} \|n\|_{X_1} + \|s\|_1$$

Thus $\tilde{c}^T \tilde{n} \geq \tilde{c}_{\min} \|\tilde{n}\|$, where $\tilde{c}_{\min} := \min\{1, c_{\min}\}$, verifying (E3) for $\tilde{c}$.

Since $r(A) < 1$ and $\gamma_{N+1} \in [0, 1)$,

$$r(\tilde{A}) = \max\{r(A), \gamma_{N+1}\} < 1,$$

verifying (E1) for $\tilde{A}$.

$\square$

3.2.2 Density-Dependent Seed Production - Contest Competition

We now assume that seed production is limited by overcrowding. In this section we will further assume that $h \in C[0, \infty)$ is increasing and concave down into $[0, \infty)$, with $h(0) = 0$. This nonlinearity models *contest competition* ([4]), which assumes that, when there are many competitors, some competitors obtain all the resources they need for seed production, while the rest obtain insufficient resources. We also assume that $h(y) \leq y$ for every $y \geq 0$, so the maximum density-dependent seed production is no greater than the density-independent seed production. For the remainder of this chapter we will assume that $g_\infty := \lim_{y \to \infty} g(y) = 0$, i.e. the establishment probability goes to zero as the number of available seeds goes to infinity.

We will motivate what we expect for the equilibrium vector. Since there are two nonlinearities f and h in this model, it is reasonable that our results should depend upon *two* stability radii, as $\tilde{A}$ is a nonlinear operator. The presence of the second stability radius actually gives us an extra degree of freedom to obtain a nonzero equilibrium vector. To see this, assume for the moment that $h(c^T n_t) = p_2 c^T n_t$ for some fixed $p_2 \in (0,1)$. p_2 is what we envision as the equilibrium proportion of maximum seed production $c^T n_t$ that are actually produced, which would indeed be a constant if the population was at an equilibrium. Consider the system (3.5), with $h(c^T n_t)$ replaced by $p_2 c^T n_t$. This modified system is equivalent to

$$\tilde{n}_{t+1} = \tilde{A}_{p_2} \tilde{n}_t + \tilde{b} f(\tilde{y}_t), \qquad \tilde{y}_t = \tilde{c}_{p_2}^T \tilde{n}_t, \tag{3.9}$$

with

$$\tilde{A}_{p_2} := \begin{bmatrix} A & \varnothing \\ \Gamma_{p_2} & S \end{bmatrix}, \qquad \tilde{c}_{p_2}^T := [\; p_2 c^T \quad 1 \quad ... \quad 1], \qquad \Gamma_{p_2} := [p_2 \gamma_1 c^T \; 0^T \; ... \; 0^T]^T \; .$$

$\tilde{A}_{p_2}$ is now a linear operator. It follows similarly from Theorem 3.2.1 that if g_0 is greater than the stability radius $p_1 := (\tilde{c}_{p_2}^T (\tilde{I} - \tilde{A}_{p_2})^{-1} \tilde{b})^{-1}$ the adjusted system has a globally stable equilibrium vector

$$\tilde{n}^* = p_1 y^* (\tilde{I} - \tilde{A}_{p_2})^{-1} \tilde{b}, \tag{3.10}$$

where y^* is the positive solution of

$$f(y^*) = p_1 y^*. \tag{3.11}$$

It also follows from Theorem 3.2.1 that, if the stability radius p_1 is larger than g_0 for all p_2 then the adjusted system's equilibrium is the zero vector.

Since the *linear* data ($\tilde{A}_{p_2}$, $\tilde{b}$ and $\tilde{c}_{p_2}$) are non-negative, p_1 is the only positive number p such that $r(\tilde{A}_{p_2} + p\tilde{b}\tilde{c}_{p_2}^T) = 1$. When we allow $h \in C[0, \infty)$ be increasing and concave down into $[0, \infty)$, with $h(0) = 0$, instead of $h(y) = p_2 y$, the upcoming theorem says that the equilibrium vector (3.10) is indeed globally stable.

What makes the upcoming results useful is that we can determine (p_1, p_2, y^*) easily through a system of three equations and three unknowns, in terms of the original system data. Let $\tilde{M}$ be the first column of $(I - S)^{-1}$. Then

$$(\tilde{I} - \tilde{A}_{p_2})^{-1} = \begin{bmatrix} (I - A)^{-1} & \varnothing \\ \tilde{M}\gamma_1 p_2 c^T (I - A)^{-1} & (I - S)^{-1} \end{bmatrix},$$

Hence, by simple computation,

$$p_1^{-1} = (\tilde{c}_{p_2}^T \tilde{I} - \tilde{A}_{p_2})^{-1}\tilde{b} = \frac{p_2(1 + \gamma_1 \|\tilde{M}\|_1)}{p_e}. \tag{3.12}$$

where $p_e := (c^T(I - A)^{-1}b)^{-1}$ is the stability of the plant-only system. Furthermore,

$$\tilde{n}^* = p_1 y^* (\tilde{I} - \tilde{A}_{p_2})^{-1}\tilde{b} = [n^* \ s^*]^T = p_1 y^* [(I - A)^{-1}b \ \frac{p_2 \gamma_1 \tilde{M}}{p_e}]^T. \tag{3.13}$$

and, since $c^T n^* = \frac{p_1 y^*}{p_e}$,

$$h(c^T n^*) = p_2 c^T n^* = \frac{p_2 p_1 y^*}{p_e}. \tag{3.14}$$

We can think of equations (3.11), (3.12) and (3.14) as the following three (slightly

rewritten) equations in the three unknowns p_1, p_2 and y^*:

$$f(y^*) = p_1 y^*$$

$$p_1 p_2 = \frac{p_e}{(1 + \gamma_1 \|\tilde{M}\|_1)} \tag{3.15}$$

$$h\left(\frac{p_1 y^*}{p_e}\right) = \frac{p_2 p_1 y^*}{p_e}.$$

From the above discussion and component-wise calculation on (3.13) we see that if p_1, p_2 and y^* satisfy (3.15) then $\tilde{n}^*$ is a non-zero equilibrium for (3.9).

Since $g(y) \leq g_0$ for all $y \in (0, \infty)$ we have that $f(y) \leq g_0 y$ for all $y \in [0, \infty)$. We also assumed that $h(y) \leq y$, which means that if (3.15) were to be true we would need $p_1 \in [0, g_0]$ and $p_2 \in [0, 1]$. By the second equation in (3.15) $p_1 > 0$ and $p_2 > 0$. If $p_1 = g_0$ then the suppositions on f imply that $y^* = 0$, which implies that $p_2 = 1$. Similarity, if $p_2 = 1$ then $y^* = 0$, would imply that $p_1 = g_0$ Thus, if (3.15) has a solution it is either the point $(g_0, 1, 0)$ or it's in $(0, g_0) \times (0, 1) \times (0, \infty)$.

As stated, if $(p_1, p_2, y^*) \in (0, g_0) \times (0, 1) \times (0, \infty)$ one can obtain the triple (p_1, p_2, y^*) easily via (3.15) and compute the equilibrium $\tilde{n}^* = p_1 y^* (\tilde{I} - \tilde{A}_{p_2})^{-1} \tilde{b}$, whose global asymptotic stability is the subject of the next theorem.

Theorem 3.2.2 *Suppose that $(E1), (E2), (E3), (E4)$ and $(D1)$ hold, and the function $h(y)$ is continuous, strictly increasing, and concave down on $[0, \infty)$ with $h(0) = 0$. Further assume that $h(y) \leq y$ on $[0, \infty)$.*

1) *If $\frac{p_e}{(1+\gamma_1 \|\tilde{M}\|_1)} = (\tilde{c}_1^T (\tilde{I} - \tilde{A}_1)^{-1} \tilde{b})^{-1} > g_0$, then the zero vector is a globally stable equilibrium for the system (3.7) in the sense that for every non-negative $\tilde{n}_0 \in X_1 \otimes X_2$,*

$$\lim_{t \to \infty} \tilde{n}_t = 0.$$

Furthermore, for every $\epsilon > 0$, there exists $\delta > 0$ such that $\|\tilde{n}_t\| < \epsilon$ for all $t \in \mathbb{N}$ whenever $\|\tilde{n}_0\| < \delta$.

2) *If there exists a solution (p_1, p_2, y^*) of (3.15) in $(0, g_0) \times (0, 1) \times (0, \infty)$, then the vector $\tilde{n}^*$ given by*

$$\tilde{n}^* = p_1 y^* (\tilde{I} - \tilde{A}_{p_2})^{-1} \tilde{b}$$

is a strictly positive globally asymptotically stable equilibrium of the system (3.7) in the sense that for every positive $\tilde{n}_0 \in X_1 \otimes X_2$

$$\lim_{t \to \infty} \tilde{n}_t = \tilde{n}^*.$$

Furthermore, for every $\epsilon > 0$, there exists $\delta > 0$ such that $\|\tilde{n}_t - \tilde{n}^*\| < \epsilon$ for all $t \in \mathbb{N}$ whenever $\|\tilde{n}_0 - \tilde{n}^*\| < \delta$.

Proof: For (1), since $(\tilde{c}_1^T (\tilde{I} - \tilde{A}_1)^{-1} \tilde{b})^{-1} > g_0 = \sup_{y > 0} g(y)$ and $h(y) \leq y$,

$$\tilde{n}_{t+1} \leq \tilde{A}_1 \tilde{n}_t + \tilde{b} g(\tilde{c}_1^T \tilde{n}_t) \tilde{c}_1^T \tilde{n}_t \leq \tilde{A}_1 \tilde{n}_t + m \tilde{b} \tilde{c}_1^T \tilde{n}_t,$$

for some $m < p_1$. By induction

$$\tilde{n}_t \leq (\tilde{A}_1 + m \tilde{b} \tilde{c}_1^T)^t \tilde{n}_0, \qquad t \in \mathbb{N}$$

Since $p_1 = (\tilde{c}_1^T (\tilde{I} - \tilde{A}_1)^{-1} \tilde{b})^{-1}$ is the stability radius of $(\tilde{A}_1, \tilde{b}, \tilde{c}_1^T)$, we have that $r(\tilde{A}_1 + m \tilde{b} \tilde{c}_1^T) < 1$. Thus

$$\lim_{t \to \infty} \tilde{n}_t = 0.$$

The (ϵ, δ) conclusion follows from the boundedness of $\tilde{A}_1 + m \tilde{b} \tilde{c}_1^T$.

For (2), Without loss of generality we can assume that $n_0 \in K_1 \setminus 0$, as if it were not then $s_{i,0} > 0$ for some $i = 1, 2, .., N$, which would imply that $n_1 \in K_1 \setminus 0$ (using

(3.5) and (E4)).

With the triple $(p_1, p_2, y^*) \in (0, g_0) \times (0, 1) \times (0, \infty)$ satisfying (3.15) define the functional

$$\tilde{w}_{p_2}^T := \tilde{c}_{p_2}^T (\tilde{I} - \tilde{A}_{p_2})^{-1}. \tag{3.16}$$

It is straightforward to verify that $\tilde{w}_{p_2}^T$ is a left eigenvector for the operator $\tilde{A}_{p_2} + p_1 \tilde{b} \tilde{c}_{p_2}^T$ with eigenvalue 1, i.e.

$$\tilde{w}_{p_2}^T (\tilde{A}_{p_2} + p_1 \tilde{b} \tilde{c}_{p_2}^T) = \tilde{w}_{p_2}^T. \tag{3.17}$$

Applying $\tilde{w}_{p_2}^T$ to (3.7),

$$\tilde{w}_{p_2}^T \tilde{n}_{t+1} = \tilde{w}_{p_2}^T \tilde{A} \tilde{n}_t + \tilde{w}_{p_2}^T \tilde{b} f(\tilde{y}_t). \tag{3.18}$$

If $\tilde{y}_t \leq y^*$ and $c^T n_t \leq c^T n^*$, then $f(\tilde{y}_t) \geq p_1 y_t$ and $h(c^T n_t) \geq p_2 c^T n_t$, so (3.18) implies that

$$\tilde{w}_{p_2}^T \tilde{n}_{t+1} \geq \tilde{w}_{p_2}^T (\tilde{A}_{p_2} + p_1 \tilde{b} \tilde{c}_{p_2}^T) \tilde{n}_t = \tilde{w}_{p_2}^T \tilde{n}_t. \tag{3.19}$$

If $\tilde{y}_t \leq y^*$ and $c^T n_t \geq c^T n^*$, then $f(\tilde{y}_t) \geq p_1 \tilde{y}_t$ and $h(c^T n_t) \geq p_2 c^T n^*$, so (3.18) implies that

$$\tilde{w}_{p_2}^T \tilde{n}_{t+1} \geq \tilde{w}_{p_2}^T \tilde{A} \tilde{n}_t + \tilde{w}_{p_2}^T p_1 \tilde{b} (h(c^T n_t) + \|s_t\|_1) \geq \tilde{w}_{p_2}^T p_2 p_1 \tilde{b} c^T n^*. \tag{3.20}$$

If $\tilde{y}_t \geq y^*$, then $f(\tilde{y}_t) \geq p_1 y^*$, so (3.18) implies that

$$\tilde{w}_{p_2}^T \tilde{n}_{t+1} \geq \tilde{w}_{p_2}^T \tilde{A} \tilde{n}_t + \tilde{w}_{p_2}^T p_1 \tilde{b} y^* \geq \tilde{w}_{p_2}^T p_1 \tilde{b} y^*. \tag{3.21}$$

Hence (3.19), (3.20) and (3.21) imply that

$$\tilde{w}_{p_2}^T \tilde{n}_t \geq \min\{\tilde{w}_{p_2}^T \tilde{n}_0, \ p_2 p_1 \tilde{w}_{p_2}^T \tilde{b} c^T n^*, \ \tilde{w}_{p_2}^T \tilde{b} p_1 y^*\}. \tag{3.22}$$

By Holder's inequality

$$\tilde{w}_{p_2}^T \tilde{n}_t \leq \|\tilde{w}_{p_2}\| \|\tilde{n}_t\|, \qquad so \qquad \|\tilde{n}_t\| \geq \frac{1}{\|\tilde{w}_{p_2}\|} \tilde{w}_{p_2}^T \tilde{n}_t. \tag{3.23}$$

Using again that either $h(c^T n_t) \geq p_2 c^T n_t$ or $h(c^T n_t) \geq p_2 c^T n^*$, it follows from (3.23) that

$$\tilde{y}_t = h(c^T n_t) + \|s_t\|_1 \geq h(c^T n_t) \geq \min\{\frac{\alpha_1 p_1 p_2 y^*}{p_e}, \ \frac{\min\{p_2 c_{\min}, \alpha_{\min}\}}{\|\tilde{w}_{p_2}^T\|} \tilde{w}_{p_2}^T \tilde{n}_t\}.$$

Finally, since $\tilde{n}_0$ is a positive vector in $X_1 \otimes X_2$

$$(\tilde{I} - \tilde{A}_{p_2})^{-1} \tilde{n}_0 = \tilde{n}_0 + \sum_{j=1}^{\infty} \tilde{A}_{p_2}^j \tilde{n}_0 \geq \tilde{n}_0. \tag{3.24}$$

Thus,

$$\tilde{w}_{p_2}^T \tilde{n}_0 = \tilde{c}_{p_2}^T (\tilde{I} - \tilde{A}_{p_2})^{-1} \tilde{n}_0 > \min\{p_2 c_{\min}, 1\} \|\tilde{n}_0\| > 0. \tag{3.25}$$

Similarly, $p_2 p_1 \tilde{w}_{p_2}^T \tilde{b} c^T n^*$ and $\tilde{w}_{p_2}^T \tilde{b} p_1 y^*$ are positive, so $\tilde{y}_t$ is bounded away from zero for all $t > 0$. Also, using condition (E3) and the fact that n_0 is a positive vector in X_1, $c^T n_t$ is bounded away from zero for all $t > 0$, by a similar argument. Thus, since f and h are increasing and concave down (see Figure 3.1), the secant slopes have the property that

$$\frac{|f(\tilde{y}_t) - f(y^*)|}{|\tilde{y}_t - y^*|} < p_1 \qquad \frac{|h(c^T n_t) - h(c^T n^*)|}{|c^T n_t - c^T n^*|} < p_2 \tag{3.26}$$

Therefore there exist $m_1 < p_1$ and $m_2 < p_2$ such that for all $t \geq 0$,

$$|f(\tilde{y}_t) - f(y^*)| \leq m_1|\tilde{y}_t - y^*| \qquad |h(c^T n_t) - h(c^T n^*)| \leq m_2|c^T n_t - c^T n^*|. \quad (3.27)$$

Also, since f is increasing, h is increasing and concave down, and $\tilde{y}_t > 0$ for all $t > 0$, for any $\mu > 0$,

$$|h(\mu f(\tilde{y}_t)) - h(\mu f(y^*))| \leq m_2|\mu f(\tilde{y}_t) - \mu f(y^*)| \qquad \forall t \geq 0. \quad (3.28)$$

We can easily verify from (3.13) that $\tilde{n}^* = \tilde{A}_{p_2}\tilde{n}^* + p_1\tilde{b}\tilde{c}_{p_2}^T\tilde{n}^* = \tilde{A}\tilde{n}^* + \tilde{b}f(y^*)$ by construction. Thus

$$\tilde{n}_{t+1} - \tilde{n}^* = \tilde{A}\tilde{n}_t - \tilde{A}\tilde{n}^* + \tilde{b}f(\tilde{y}_t) - \tilde{b}f(y^*).$$

By the variation of parameters formula

$$\tilde{n}_t - \tilde{n}^* = \tilde{A}^t\tilde{n}_0 - \tilde{A}^t\tilde{n}^* + \sum_{j=0}^{t-1}\tilde{A}^{t-j-1}\tilde{b}f(\tilde{y}_j) - \tilde{A}^{t-j-1}\tilde{b}f(y^*). \quad (3.29)$$

We will now multiply on the right by the functional $\tilde{c}_{p_2}^T$ and analyze each component individually. To do so, notice that

$$\tilde{A}^t = \begin{bmatrix} A^t & \varnothing \\ \sum_{i=0}^{t-1} S^i\Gamma A^{t-1-i} & S^t \end{bmatrix}. \quad (3.30)$$

Taking the first component of (3.29) multiplied on the left by $\tilde{c}_{p_2}^T$

$$p_2c^T(n_t - n^*) = \tilde{c}_{p_2}^T(\tilde{A}^t\tilde{n}_0 - \tilde{A}^t\tilde{n}^*)|_{X_1} + p_2\sum_{j=0}^{t-1}c^TA^{t-j-1}b(f(\tilde{y}_j) - f(y^*)), \quad (3.31)$$
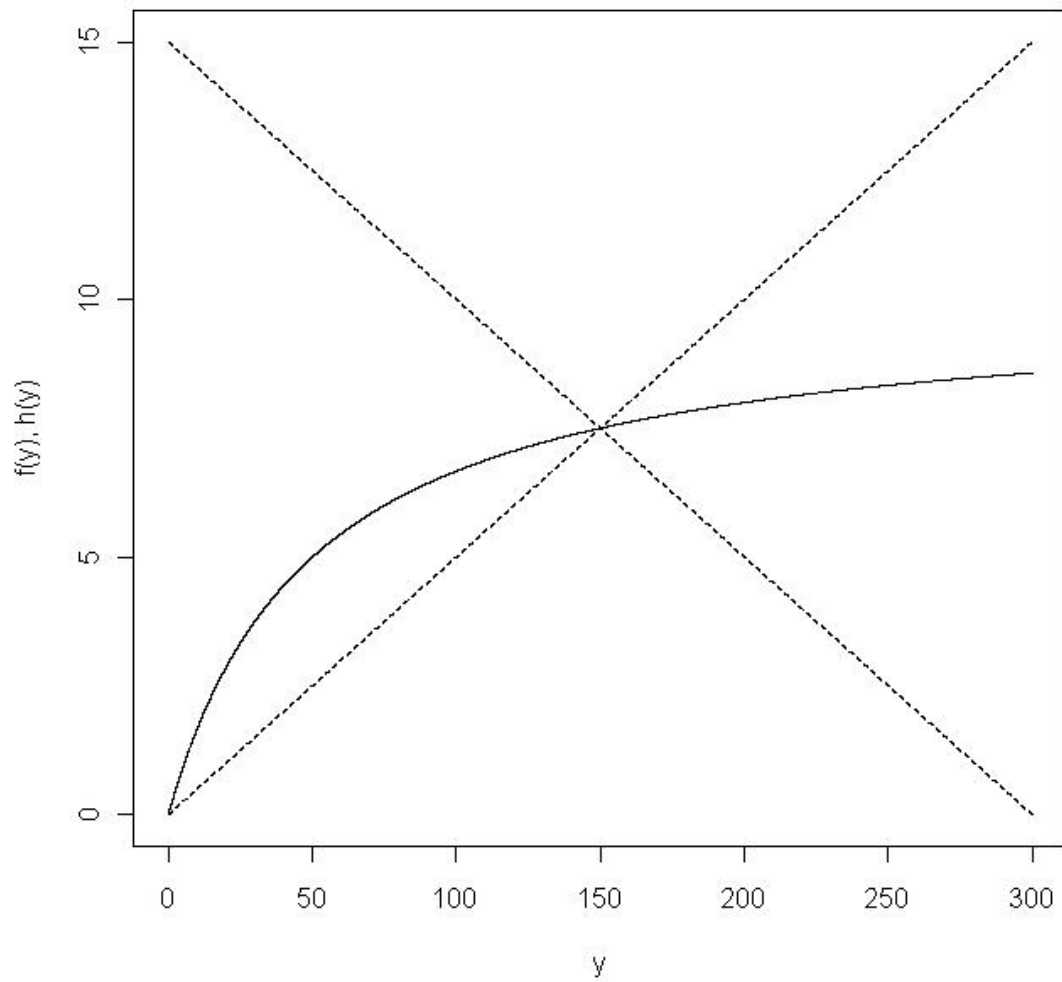
Figure 3.1: Typical nonlinearities f or h which satisfy (D1) and sectors defined by lines with slopes $\pm p_1$ or $\pm p_2$ (dotted), showing how (3.26) holds.

where $(\tilde{A}^t \tilde{n}_0 - \tilde{A}^t \tilde{n}^*)|_{X_1}$ is the X_1 component of the vector $\tilde{A}^t \tilde{n}_0 - \tilde{A}^t \tilde{n}^*$. Taking

absolute values and using positivity implies that

$$|p_2 c^T (n_t - n^*)| \le |\tilde{c}_{p_2}^T (\tilde{A}^t \tilde{n}_0 - \tilde{A}^t \tilde{n}^*)|_{X_1}| + p_2 \sum_{j=0}^{t-1} c^T A^{t-j-1} b |(f(\tilde{y}_j) - f(y^*))|. \quad (3.32)$$

Using (3.26),

$$
\begin{aligned}
|p_2 c^T (n_t - n^*)| &\le |\tilde{c}_{p_2}^T (\tilde{A}^t \tilde{n}_0 - \tilde{A}^t \tilde{n}^*)|_{X_1}| \\
&+ p_2 m_1 \sum_{j=0}^{t-1} c^T A^{t-j-1} b(|h(c^T n_j) - h(c^T n^*)| + \|s_j - s^*\|_1) \\
&\le |\tilde{c}_{p_2}^T (\tilde{A}^t \tilde{n}_0 - \tilde{A}^t \tilde{n}^*)|_{X_1}| \\
&+ p_2 m_1 \sum_{j=0}^{t-1} c^T A^{t-j-1} b(m_2 |c^T n_j - c^T n^*| + \|s_j - s^*\|_1).
\end{aligned}
$$

Summing from $t = 0$ to M, where M is large, we have

$$
\sum_{t=0}^{M} |p_2 c^T (n_t - n^*)| \le \sum_{t=0}^{M} |\tilde{c}_{p_2}^T (\tilde{A}^t \tilde{n}_0 - \tilde{A}^t \tilde{n}^*)|_{X_1}| +
$$

$$(3.33)$$

$$
p_2 m_1 \sum_{t=0}^{M} \sum_{j=0}^{t-1} c^T A^{t-j-1} b(m_2 |c^T n_j - c^T n^*| + \|s_j - s^*\|_1).
$$

The nonlinear operator $\tilde{A}$ is bounded above by the linear operator $\tilde{A}_1$ in the

sense that $\tilde{A}x \le \tilde{A}_1 x$ for all x in the positive cone $K_1 \otimes K_2$. Since $r(\tilde{A}_1) = \max\{r(A), \gamma_{N+1}\} < 1$, the first term in (3.33) converges as $M \to \infty$. If we rear-

range the second sum and use the fact that the system is positive, we have that

$$\sum_{t=0}^{M} |p_2 c^T (n_t - n^*)| \leq \sum_{t=0}^{\infty} |\tilde{c}_{p_2}^T (\tilde{A}^t \tilde{n}_0 - \tilde{A}^t \tilde{n}^*)|_{X_1}| +$$

$$p_2 m_1 \sum_{j=0}^{M-1} (m_2 |c^T n_j - c^T n^*| + \|s_j - s^*\|_1) \sum_{t=j+1}^{M} c^T A^{t-j-1} b.$$

Adding more terms (so that some of the sums are infinite) and changing indices

$$\sum_{t=0}^{M} |p_2 c^T (n_t - n^*)| \leq \sum_{t=0}^{\infty} |\tilde{c}_{p_2}^T (\tilde{A}^t \tilde{n}_0 - \tilde{A}^t \tilde{n}^*)|_{X_1}| +$$

$$p_2 m_1 \sum_{j=0}^{M-1} (m_2 |c^T n_j - c^T n^*| + \|s_j - s^*\|_1) \sum_{t=0}^{\infty} c^T A^{t-j-1} b \quad (3.34)$$

$$\leq \sum_{t=0}^{\infty} |\tilde{c}_{p_2}^T (\tilde{A}^t \tilde{n}_0 - \tilde{A}^t \tilde{n}^*)|_{X_1}| + \frac{p_2 m_1}{p_e} \sum_{t=0}^{M} (m_2 |c^T n_t - c^T n^*| + \|s_t - s^*\|_1).$$

Using (3.30), the ith component of s_t satisfies

$$(s_t - s^*)_i = \tilde{c}_{p_2}^T (\tilde{A}^t \tilde{n}_0 - \tilde{A}^t \tilde{n}^*)|_{X_2})_i +$$

$$\sum_{j=0}^{t-1} \sum_{k=0}^{t-j-2} (S_{i,1}^k)(\Gamma A^{t-j-k-2} b f(\tilde{y}_j) - \Gamma A^{t-j-k-2} b f(y^*)),$$

where $S_{i,1}^k$ is the $(i, 1)$ entry of S_k. By the definition of Γ,

$$(s_t - s^*)_i = \tilde{c}_{p_2}^T (\tilde{A}^t \tilde{n}_0 - \tilde{A}^t \tilde{n}^*)|_{X_2})_i + \quad (3.35)$$

$$\sum_{j=0}^{t-1} \sum_{k=0}^{t-j-2} \gamma_1 S_{i,1}^k (h(c^T A^{t-j-k-2} b(f(\tilde{y}_j)) - h(c^T A^{t-j-k-2} b f(y^*)).$$

Using (3.28) with $\mu = c^T A^{t-j-k-2} b > 0$

$$|(s_t - s^*)_i| \leq |\tilde{c}_{p_2}^T (\tilde{A}^t \tilde{n}_0 - \tilde{A}^t \tilde{n}^*)|_{X_2})_i| +$$
$$m_2 \sum_{j=0}^{t-1} \sum_{k=0}^{t-j-2} \gamma_1 S_{i,1}^k c^T A^{t-j-k-2} b |(f(\tilde{y}_j)) - f(y^*)|.$$

Using (3.26) again, we have that

$$|(s_t - s^*)_i| \leq |\tilde{c}_{p_2}^T (\tilde{A}^t \tilde{n}_0 - \tilde{A}^t \tilde{n}^*)|_{X_2})_i| +$$
$$m_2 m_1 \sum_{j=0}^{t-1} \sum_{k=0}^{t-j-2} \gamma_1 S_{i,j}^k c^T A^{t-j-k-2} b (m_2 |c^T n_j - c^T n^*| + \|s_j - s^*\|_1).$$

Summing from $t = 0$ to M and rearranging we have

$$\sum_{t=0}^{M} |(s_t - s^*)_i| \leq \sum_{t=0}^{M} |\tilde{c}_{p_2}^T (\tilde{A}^t \tilde{n}_0 - \tilde{A}^t \tilde{n}^*)|_{X_2})_i| +$$
$$m_2 m_1 \sum_{t=0}^{M} \sum_{j=0}^{t-1} \sum_{k=0}^{t-j-2} \gamma_1 S_{i,j}^k c^T A^{t-j-k-2} b (m_2 |c^T n_j - c^T n^*| + \|s_j - s^*\|_1)$$
$$= \sum_{t=0}^{M} |\tilde{c}_{p_2}^T (\tilde{A}^t \tilde{n}_0 - \tilde{A}^t \tilde{n}^*)|_{X_2})_i| +$$
$$m_2 m_1 \sum_{j=0}^{M-1} \sum_{t=j+1}^{M} \sum_{k=0}^{t-j-2} \gamma_1 S_{i,j}^k c^T A^{t-j-k-2} b (m_2 |c^T n_j - c^T n^*| + \|s_j - s^*\|_1).$$

Since $\tilde{A}x \leq \tilde{A}_1 x$ for all x in the positive cone $K_1 \otimes K_2$. the first term converges as

$M \to \infty$. Adding more terms, and again letting $\tilde{M}$ be the first column of $(I - S)^{-1}$

$$\sum_{t=0}^{M} |(s_t - s^*)_i| \leq \sum_{t=0}^{\infty} |\tilde{c}_{p_2}^T(\tilde{A}^t \tilde{n}_0 - \tilde{A}^t \tilde{n}^*)|_{X_2})_i| +$$

$$m_2 m_1 \sum_{j=0}^{M-1} (m_2 |c^T n_j - c^T n^*| + \|s_j - s^*\|_1) \sum_{t=j+1}^{M} \sum_{k=0}^{t-j-2} \gamma_1 S_{i,1}^k c^T A^{t-j-k-2} b$$

$$\leq \sum_{t=0}^{\infty} |\tilde{c}_{p_2}^T(\tilde{A}^t \tilde{n}_0 - \tilde{A}^t \tilde{n}^*)|_{X_2})_i| +$$

$$\frac{m_2 m_1 \gamma_1 (\tilde{M})_i}{p_e} \sum_{t=0}^{M} (m_2 |c^T n_t - c^T n^*| + \|s_t - s^*\|_1).$$

The last inequality follows from using (3.12). Collecting all of the terms, by the triangle inequality we have

$$\sum_{t=0}^{M} (|p_2 c^T(n_t - n^*)| + \|s_t - s^*\|_1) \leq \sum_{t=0}^{\infty} |\tilde{c}_{p_2}^T(\tilde{A}^t \tilde{n}_0 - \tilde{A}^t \tilde{n}^*)| +$$

$$\frac{p_2 m_1 + m_2 m_1 \gamma_1 \|\tilde{M}\|_1}{p_e} \sum_{t=0}^{M} (m_2 |c^T n_t - c^T n^*| + \|s_t - s^*\|_1).$$

Since $m_1 < p_1$ and $m_2 < p_2$, and using (3.12) there exists an $m < 1$ such that

$$\frac{p_2 m_1 + m_2 m_1 \gamma_1 \|\tilde{M}\|_1}{p_e} \leq p_2 m_1 \frac{1 + \gamma_1 \|\tilde{M}\|_1}{p_e} \leq \frac{p2 m_1}{p_1 p_2} \leq m < 1.$$

Hence

$$\sum_{t=0}^{M} (|p_2 c^T(n_t - n^*)| + \|s_t - s^*\|_1) \leq \sum_{t=0}^{\infty} |\tilde{c}_{p_2}^T(\tilde{A}^t \tilde{n}_0 - \tilde{A}^t \tilde{n}^*)| +$$

$$m \sum_{t=0}^{M} (m_2 |c^T n_t - c^T n^*| + \|s_t - s^*\|_1),$$

which implies that

$$\sum_{t=0}^{M}(|(p_2 - m_2)c^T(n_t - n^*)| + \|s_t - s^*\|_1) \le (1 - m)^{-1}\sum_{t=0}^{\infty}|\tilde{c}_{p_2}^T(\tilde{A}^t\tilde{n}_0 - \tilde{A}^t\tilde{n}^*)|. \quad (3.36)$$

This bound is independent of M. Therefore the sequence

$$\{(p_2 - m_2)c^T(n_t - n^*)| + \|s_t - s^*\|_1)\}_{t=0}^{\infty} \in \ell_1(\mathbb{N}),$$

so

$$\lim_{t\to\infty}|c^T(n_t - n^*)| + \|s_t - s^*\|_1) = 0. \quad (3.37)$$

By supposition (E3) this implies that

$$\lim_{t\to\infty}\tilde{n}_t = \tilde{n}^*, \quad (3.38)$$

as sought. The (ϵ, δ) conclusion follows from the fact that $\tilde{A}x \le \tilde{A}_1 x$ for all $x \in K_1$, $r(\tilde{A}_1) < 1$ and Holder's inequality.

$\square$

3.2.3 Density-Dependent Seed Production - Scramble Competition

In the case where the function h models *scramble competition* ([4]) the global stability is not as straightforward. Scramble competition assumes that, when there are many competitors, the available resources are insufficient for any one competitor. In this case we no longer require h to be increasing and concave down, since for large y it is possible that the density of seeds produced decreases, possibly to zero.

The key in the proof of Theorem 3.2.1 is the fact that h is *sector bounded*, i.e.

$$|h(c^T n_t) - h(c^T n^*)| \leq m_2 |c^T n_t - c^T n^*|,$$

$$(3.39)$$

$$|h(\mu f(\tilde{y}_t)) - h(\mu f(y^*))| \leq m_2 |\mu f(\tilde{y}_t) - \mu f(y^*)|$$

for some $m_2 < p_2$ and all $\mu \geq 0$. It's clear that h does not need to be strictly increasing for this to occur. For instance, consider the Ricker function proposed in [46]

$$h_R(y) = y \exp(-y/c_m),$$ $$(3.40)$$

where c_m elicits the maximum seed production for the population $c_m \exp(-1)$ (see Figure 3.2). We will show that some of Theorem 3.2.2 holds for $h = h_R$.

Theorem 3.2.3 *Suppose that* $(E1), (E2), (E3), (E4)$ *and* $(D1)$ *hold and* $h = h_R$.

1) *If* $(\tilde{c}_1^T (\tilde{I} - \tilde{A}_1)^{-1} \tilde{b})^{-1} > g_0$, *then the conclusions in part (1) of Theorem 3.2.2 hold.*

2) *If there exists a solution* (p_1, p_2, y^*) *of (3.15) in* $(0, g_0) \times (\exp(-2), 1) \times (0, \infty)$ *then the conclusions in part (2) of Theorem 3.2.2 hold.*

3) *If there exists a solution* (p_1, p_2, y^*) *of (3.15) in* $(0, g_0) \times (0, \exp(-2)) \times (0, \infty)$ *and* f *is further assumed to be* $C^1[0, \infty)$, *with*

$$r(\tilde{A}_{(1+\ln(p_2))p_2} + f'(y^*)\tilde{b}\tilde{c}_{(1+\ln(p_2))p_2}^T) < 1,$$

then $\tilde{n}^*$ *asymptotically stable.*

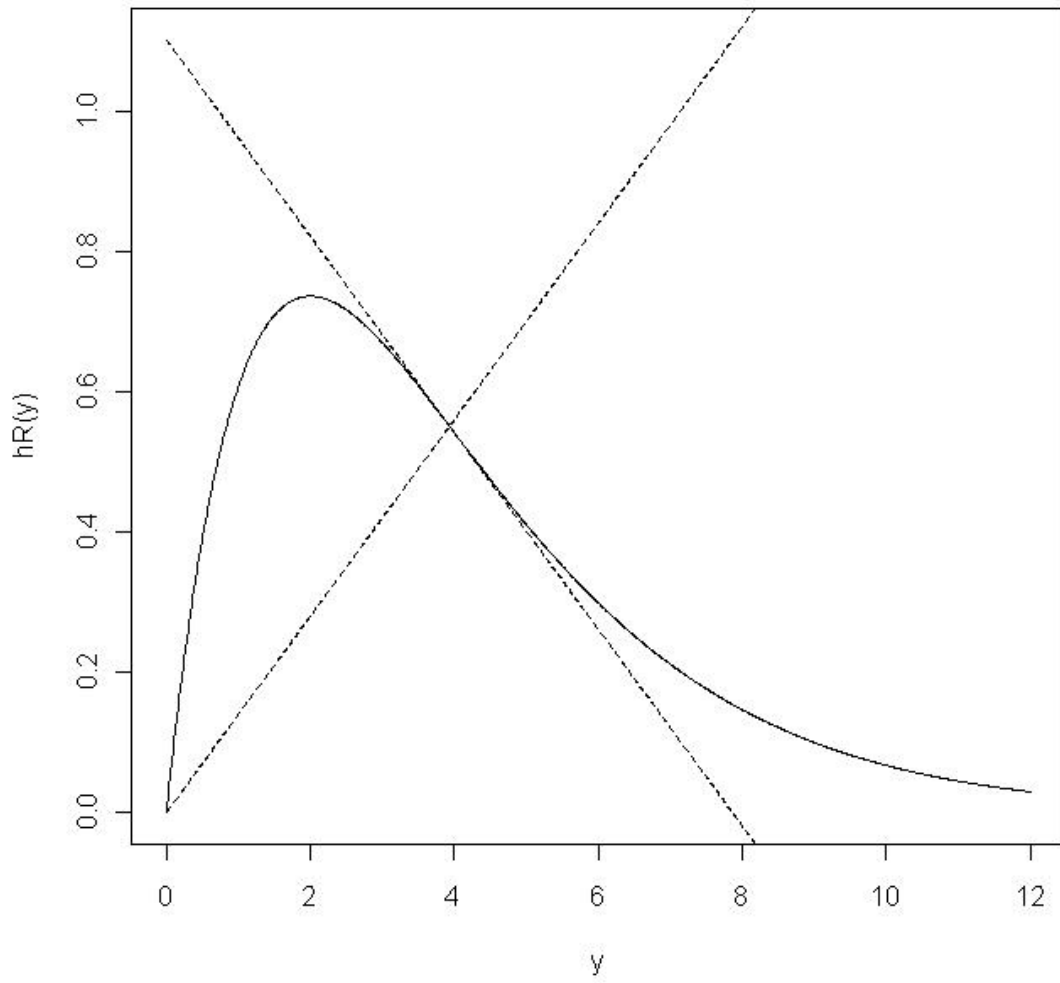**Proof:** The proof of (1) is identical to the proof of (1) in Theorem 3.2.2.

Figure 3.2: A typical Ricker function h_R and sectors defined by lines with slopes $\pm p_2$ (dotted), with $p_2 \in (\exp(-2), 1)$.

For (2) note that if there exists a solution (p_1, p_2, y^*) of (3.15) in $(0, g_0) \times$ $(\exp(-2), 1) \times (0, \infty)$ and $m > 0$ such that $\tilde{y}_t > m$ and $c^T n_t > m$ for all $t \in \mathbb{N}$, then h_R is sector bounded as in (3.39) (Fig. 2). This follows from the fact that

$$h'_R(y) = (1 - \frac{y}{c_m})\exp(-y/c_m), \quad h''_R(y) = \frac{1}{c_m}(\frac{y}{c_m} - 2)\exp(-y/c_m).$$

Thus h_R has $\exp(-2)$ as its maximum negative slope. Thus, if $\tilde{y}_t, c^T n_t > m$, h_R satisfies (3.39) for some $m_2 < p_2$ and all $\mu \geq 0$. To see that there exists $m > 0$ such that $\tilde{y}_t > m$ and $c^T n_t > m$ for all $t \in \mathbb{N}$, we note that if $\tilde{y}_t \leq y^*$ and $c^T n_t \leq c^T n^*$ or $\tilde{y}_t \geq y^*$ the lower bound follows as in Theorem 3.2.2. If $\tilde{y}_t \leq y^*$ and $c^T n_t \geq c^T n^*$ we need to show that the solution $\{\tilde{y}_t\}_{t=0}^{\infty}$ is bounded above. Noting that $f(y) \leq f(y^*) + m_1 y$ for some $m_1 < p_1$ and $y \geq 0$ and $h_R(y) \leq c_m \exp(-1)$ for all $y \geq 0$ it follows that

$$\tilde{c}_1^T \tilde{n}_t \leq \tilde{c}_1^T \hat{A} \tilde{n}_{t-1} + c^T b f(y^*) + (mc^T b + \gamma_1)c_m \exp(-1) := \tilde{c}_1^T \hat{A} \tilde{n}_{t-1} + K,$$

where

$$\hat{A} := \begin{bmatrix} A & B_{m_1} \\ \Gamma_0 & S \end{bmatrix}, \quad B_{m_1} := \begin{bmatrix} m_1 b & m_1 b & \ldots & m_1 b \end{bmatrix},$$

and $r(\hat{A}) < 1$. Thus $\tilde{c}_1^T \tilde{n}_t \leq M$ for some $M < \infty$. Thus, if $\tilde{y}_t \leq y^*$ and $c^T n_t \geq c^T n^*$ we have that $f(\tilde{y}_t) \geq f(y^*)$ and $h_R(c^T n_t) > \min\{h_R(c^T n^*), h_R(M)\} > 0$. Letting $\tilde{w}_{p_2}^T$ be defined as in Theorem 3.2.2,

$$\tilde{w}_{p_2}^T \tilde{n}_t \geq \min\{\tilde{w}_{p_2}^T \tilde{n}_0, \ p_2 p_1 \tilde{w}_{p_2}^T \tilde{b} c^T n^*, \ \tilde{w}_{p_2}^T \tilde{b} p_1 h_R(M)\}, \tag{3.41}$$

and similarly for $c^T n_t$. Therefore $\tilde{y}_t$ and $c^T n_t$ are bounded from below. The remainder of the proof for (2) is the same as in Theorem 3.2.2.

For part (3) note that, for $p_2 \in (0, \exp(-2))$,

$$h'_R(c^T n^*) = p_2(1 + \ln(p_2)) < -p_2, \tag{3.42}$$

so we cannot sector-bound h_R as we did in (2) of this theorem. The linearization about $\tilde{n}^*$ yields

$$\tilde{n}_{t+1} = \tilde{A}_{h'_R(c^T n^*)}\tilde{n}_t + f'(y^*)(h'_R(c^T n^*)c^T n_t + \|s_t\|_1)$$
$$= (\tilde{A}_{(1+\ln(p_2))p_2} + f'(y^*)\tilde{b}\tilde{c}^T_{(1+\ln(p_2))p_2})\tilde{n}_t.$$

Thus if $r(\tilde{A}_{(1+\ln(p_2))p_2} + f'(y^*)\tilde{b}\tilde{c}^T_{(1+\ln(p_2))p_2}) < 1$ then $\tilde{n}^*$ is asymptotically stable, as sought. $\qquad\square$

3.2.3.1 Relaxing Assumption (E3)

As previously alluded to in Section 3.1.3, one may argue that the assumption (E3) is too restrictive when the plant population is modeled with a vector in $\mathbb{R}^m$. For example, in some populations only the very largest members reproduce, so c may be the (vector) functional

$$c^T := [0 \ \ 0 \ \ ... \ \ 0 \ \ M]$$

for some $M > 0$, which violates (E3). However, using the methods developed in this chapter, along with the techniques in [76] we can recover the results summarized Theorems 3.2.1, 3.2.2 and 3.2.3 for $X_1 = \mathbb{R}^m$.

Theorem 3.2.4 *Let $X_1 = \mathbb{R}^m$ and assume that $(E1), (E2), (E4)$ and $(D1)$ hold. Assume further that the plant-only system $A + pbc^T$ is primitive for every $p > 0$. Then the results summarized in Theorems 3.2.1, 3.2.2 and 3.2.3 hold.*

Proof: The proof when the zero vector is the globally stable equilibrium vector is exactly the same as in Theorems 3.2.1, 3.2.2 and 3.2.3.

If h is the identity function the proof of Theorem 3.2.1 is identical to the proof of Theorem 2.1 (3) in [76], as $X_1 \otimes X_2 = \mathbb{R}^{m+N}$ and the primitivity of the plant-only matrix $A + pbc^T$ for all $p > 0$ implies the primitivity of whole matrix $\tilde{A} + p\tilde{b}\tilde{c}^T$ for all $p > 0$.

Assume now that h is not the identity function. To prove that $\tilde{n}^* = p_1 y^* (\tilde{I} - \tilde{A}_{p_2})^{-1} \tilde{b}$ is globally stable as in Theorems 3.2.2 and 3.2.3 it suffices to show that there exists a k such that $\tilde{y}_t$ is bounded from above and away from zero for all $t \geq k$, as the rest of the proof follows from the techniques above and [76].

The proof of $\tilde{y}_t$ being bounded above follows from the fact that $\tilde{A}$ is bounded above by $\tilde{A}_1$ with $r(\tilde{A}_1) < 1$ and

$$f(\tilde{y}_t) \leq f(y^*) + m_1 \tilde{y}_t \quad \text{and} \quad h(c^T n_t) \leq h(c^T n^*) + m_2 c^T n_t$$

for $m_1 < p_1, m_2 < p_2$ and all $t \in \mathbb{N}$ (in the contest competition case) or

$$f(\tilde{y}_t) \leq f(y^*) + m_1 \tilde{y}_t \quad \text{and} \quad h_R(c^T n_t) \leq c_m \exp(-1)$$

for $m_1 < p_1$ and all $t \in \mathbb{N}$ (in the scramble competition case).

As stated, the assumed primitivity of the plant-only matrix $A + pbc^T$ for any $p > 0$ implies the primitivity of the of the whole matrix $\tilde{A}_{p_2} + p\tilde{b}\tilde{c}_{p_2}^T$ for any $p_2 > 0$. The Perron-Frobenius theorem implies the existence of a strictly positive left eigenvector (which we know to be $\tilde{w}_{p_2}^T := \tilde{c}_{p_2}^T (\tilde{I} - \tilde{A}_{p_2})^{-1}$). Using the exact same argument as Theorem 3.2.2 we have

$$\tilde{w}_{p_2}^T \tilde{n}_t \geq \min\{\tilde{w}_{p_2}^T \tilde{n}_0, p_2 p_1 \tilde{w}_{p_2}^T \tilde{b} c^T n^*, p_1 \tilde{w}_{p_2}^T \tilde{b} y^*, p_1 \tilde{w}_{p_2}^T \tilde{b} h_R(M)\},$$

which by Holder's inequality implies that $||\tilde{n}_t||$ is bounded away from zero for all $t \in \mathbb{N}$.

Since $\tilde{y}_t$ is bounded above, there exists $g_{\min} > 0$ and $h_{\min} > 0$ such that, for all $t \in \mathbb{N}$,

$$f(\tilde{y}_t) = g(\tilde{y}_t)\tilde{y}_t \geq g_{\min}\tilde{y}_t \quad \text{and} \quad h(c^T n_t) \geq h_{\min} c^T n_t$$

in the contest competition case, or

$$f(\tilde{y}_t) = g(\tilde{y}_t)\tilde{y}_t \geq g_{\min}\tilde{y}_t \quad \text{and} \quad h_R(c^T n_t) \geq h_{\min} c^T n_t$$

in the scramble competition case. Since $\tilde{A}_{p_2} + p\tilde{b}\tilde{c}_{p_2}^T$ is primitive for any $p, p_2 > 0$ there exists a k such that $(\tilde{A}_{h_{\min}} + g_{\min}\tilde{b}\tilde{c}_{h_{\min}}^T)^k$ consists of strictly positive elements. So, for $t \geq k$

$$\tilde{n}_t \geq (\tilde{A}_{h_{\min}} + g_{\min}\tilde{b}\tilde{c}_{h_{\min}}^T)\tilde{n}_{t-1} \geq ... \geq (\tilde{A}_{h_{\min}} + g_{\min}\tilde{b}\tilde{c}_{h_{\min}}^T)^k\tilde{n}_{t-k}.$$

Since $\tilde{c}^T$ is non-negative and $||\tilde{n}_t||$ is bounded away from zero we have that

$$\tilde{y}_t = \tilde{c}^T\tilde{n}_t \geq \tilde{c}^T(\tilde{A}_{h_{\min}} + g_{\min}\tilde{b}\tilde{c}_{h_{\min}}^T)^k\tilde{n}_{t-k}$$

is bounded away from zero for all $t \geq k$. The rest of the proof follows from the techniques of Theorem 3.2.2 and [76]. $\qquad\square$

3.2.3.2 Density Dependence in Seed Production Only

Up until now we have assumed in this chapter that the recruitment from seeds to plants has been density dependent and have considered the effect of assuming whether or not seed production was density dependent as well. It is reasonable to ask if the previous results in this chapter hold if seed production was density dependent but the

recruitment from seeds to plants was *density independent.* In this case the plant-seed bank model would be

$$
\begin{aligned}
n_{t+1} &= An_t + p_s b(h(c^T n_t) + ||s_t||_1) \\
s_{1,t+1} &= \gamma_1 h(c^T n_t) \\
s_{2,t+1} &= \gamma_2 s_{1,t} \\
&\vdots \\
s_{N-1,t+1} &= \gamma_{N-1} s_{N-2,t} \\
s_{N,t+1} &= \gamma_N s_{N-1,t} + \gamma_{N+1} s_{N,t},
\end{aligned}
\tag{3.43}
$$

where p_s is the (constant) establishment probability. Notice that the model (3.43) has only one nonlinearity, h. As in (3.7) from Section 3.1.3 we can still write this model concisely as

$$
\tilde{n}_{t+1} = \tilde{A}\tilde{n}_t + \tilde{b}h(\tilde{c}^T \tilde{n}_t).
\tag{3.44}
$$

However, the collection $(\tilde{A}, \tilde{b}, \tilde{c})$ now takes the form

$$
\tilde{A} := \begin{bmatrix} A & B \\ \varnothing & S \end{bmatrix}, \qquad
\tilde{b} := \begin{bmatrix} b \\ \gamma_1 \\ 0 \\ \vdots \\ 0 \end{bmatrix}, \qquad
\tilde{c}^T := \begin{bmatrix} c^T & 0 & \dots & 0 \end{bmatrix},
$$

where $\varnothing := [0^T \ 0^T ... \ 0^T]^T \in \mathcal{L}(X_1, X_2)$ is a collection of N zero functionals from X_1 to $\mathbb{R}$ and $B := [p_s b \ p_s b... \ p_s b] \in \mathcal{L}(X_2, X_1)$ is a collection of N vectors in X_1.

Notice that, much like the issue faced in Theorem 3.2.4, $\tilde{c}^T$ is not a strictly positive functional. Furthermore, since X_1 is not assumed to be $\mathbb{R}^m$, Theorems 3.2.1 and 3.2.4

do not apply. However, as with Theorem 3.2.4, the issues associated with $\tilde{c}^T$ not being strictly positive can be dealt with.

Theorem 3.2.5 *Assume that* $(E1), (E2), (E3), (E4)$ *and* $(D1)$ *hold. Then the results summarized in Theorem 3.2.1 hold for the model (3.44).*

Proof:

As with Theorem 3.2.4 it suffices to show that there exists a k such that $\tilde{y}_t$ is from above and below for all $t \geq k$. The boundedness of $\tilde{y}_t$ from above follows again from the fact that $r(\tilde{A}) < 1$ and

$$h(c^T n_t) \leq h(c^T n^*) + m_2 c^T n_t$$

for $m_2 < p_2$ and all $t \in \mathbb{N}$ (in the contest competition case) or

$$h_R(c^T n_t) \leq c_m \exp(-1)$$

for all $t \in \mathbb{N}$ (in the scramble competition case).

To prove the $\tilde{y}_t$ is bounded from below, notice that the functional

$$\tilde{w}^T := \tilde{c}^T (I - \tilde{A})^{-1} = \left[\begin{array}{cccc} c^T (I - A)^{-1} & \frac{||M_1||p_s}{p_e} & \cdots & \frac{||M_N||p_s}{p_e} \end{array} \right],$$

where M_j is the jth column of the matrix $(I - S)^{-1}$. From this, it follows from the boundedness of $\tilde{y}_t$, by a constant M_0, that

$$\tilde{w}^T \tilde{n}_t \geq \min\{\tilde{w}^T \tilde{n}_0, \tilde{w}^T \tilde{b} m_0\},$$

where m_0 is either $\tilde{p}_e y^*$ in the contest competition case or $h(M_0)$ in the scramble

competition case. Since $\tilde{w}^T\tilde{b} = \frac{1+\gamma_1||M_1||_1 p_s}{p_e} > 0$ and $\tilde{w}^T\tilde{n}_0 > 0$ for any non-zero $\tilde{n}_0$ it follows that $||\tilde{n}_t||$ is bounded below from zero by Holder's inequality for all t.

Finally, since $\tilde{y}_t = \tilde{c}^T\tilde{n}$ is bounded above by M_0, $c^T n_t$ is bounded above by M_0. Thus, there exists an $h_{\min} = \frac{h(M_0)}{M_0}$ such that $h(c^T n_t) \geq h_{\min} c^T n_t$ for all $t \in \mathbb{N}$. Therefore,

$$\tilde{c}^T\tilde{n}_t \geq (\tilde{A} + h_{\min}\tilde{b}\tilde{c}^T)\tilde{n}_{t-1}, \tag{3.45}$$

The right hand side of 3.45 is, in vector form,

$$\left[\begin{array}{cccc} c^T(A + h_{\min}bc^T)n_t & p_s c^T b s_{1,t} & \cdots & p_s c^T b s_{N,t} \end{array} \right]^T,$$

which is bounded below by $(2c^T b)\min\{h_{\min}c_{\min}, p_s\}||\tilde{n}_t||$. Since $||\tilde{n}_t||$ is uniformly bounded from below we have that $\tilde{y}_t = \tilde{c}^T\tilde{n}_t$ is uniformly bounded from below for $t \geq 1$. The remainder of the proof of global stability follows, using the methods form [76].

$\square$

3.3 Example

We show how the results in this chapter can be applied to a model for the annual plant *Sesbania vesicaria* with an age-structured seed bank, using data from [46]. *S. vesicaria* is a weedy annual legume found in pastures on damp or low sandy soils of the warm temperate region of the southeastern U.S. ([57]). Both seed production and seedling establishment (which [46] labels as "survivorship") are density dependent (see Fig. 2a and Fig. 2b in [46]). We assume that the plant population is homogenous (and thus can be represented with a scalar) and the seed bank population has three

classes: 0-year-old, 1-year-old and greater than or equal to 2-year-old seeds. Thus $X_1 = \mathbb{R}, X_2 = \mathbb{R}^3$ and $K_1 = \mathbb{R}_+, K_2 = \mathbb{R}^3_+$.

We model seedling-to-plant density dependence by a Michaelis-Menten function

$$\tilde{f}(y) = \frac{\alpha y}{\beta + y},$$

which takes into account that there is a limit on the availability of microsites for seedlings to establish and become adult plants (see Chapter 2 for a discussion of the form of this density dependence). We consider two types of density dependence assumptions for the seed production function h. Contest competition will be modeled with a Michaelis-Menten function

$$h_1(y) = \frac{c_m y}{c_m + y} \tag{3.46}$$

and scramble competition with a Ricker function

$$h_2(y) = y\exp(-y/c_m). \tag{3.47}$$

In [46] the probability of seed dormancy (which is $1-$ the germination probability) was found to vary between 0.5 and 0.9 (see Fig. 5 in [46]). We will assume that the probability of seed dormancy is 0.75, from which it follows that the probability of seed germination is $g_p = 0.25$ and the abundance of adult plants when there are y available seeds is then $f(y) = \tilde{f}(g_p y)$, as a seed must germinate to become a seedling and then establish to become an adult plant.

We denote the probability of an i-year-old seed surviving a given year with s^{i+1}, where s is the probability that a seed survives its initial year in the seed bank and $i = 0, 1, 2$. Note that we are assuming seeds that are older than 2 years old have the

same survival probability. We assume that $s = 0.95$ in our example. The resulting models are

$$
\begin{aligned}
n_{t+1} &= An_t + bf(h_i(cn_t) + s_{1,t} + s_{2,t} + s_{3,t}) \\
s_{1,t+1} &= (1 - g_p)sh_i(cn_t) \\
s_{2,t+1} &= (1 - g_p)s^2 s_{1,t} \\
s_{3,t+1} &= (1 - g_p)(s^3 s_{2,t} + s^4 s_{3,t}), \qquad i = 1, 2.
\end{aligned}
\tag{3.48}
$$

Note that A and c are scalars because the plant population n_t is a scalar. Using the data on Fig. 2a and Fig. 2b in [46] we use the values $\alpha = 72.51$ and $\beta = 89.17$ for both models, $c = 48.64, c_m = 211.9$ in (3.46) and $c = 28.09, c_m = 480.95$ in (3.47). We assume that $A = 0$ because *S. vesicaria* is an annual plant and hence there are no plants remaining from the previous year. Since our model only considerers a single plant stage the juvenile distribution vector becomes the scalar $b = 1$. The parameters for the contest competition and scramble competition models fit the digitized data in [46] for seed production similarly well (AIC 165.53 and 164.78, respectively. See Figure 3.3).

For both models

$$
g_0 = 0.2032915.
$$

In the contest competition model $p_1 = 0.078 \in (0, g_0), p_2 = 0.089 \in (0, 1)$ and $y^* = 577.81 > 0$, which by Theorem 3.2.2 implies the global asymptotic stability of

$$
\begin{aligned}
\tilde{n}^* &= [n^* \ s^*]^T = p_1 y^*[(1 - A)^{-1}b \ \frac{p_2(1 - g_p)s\tilde{M}}{p_e}]^T \\
&= [44.72 \ 137.56 \ 93.09 \ 151.63]^T,
\end{aligned}
$$
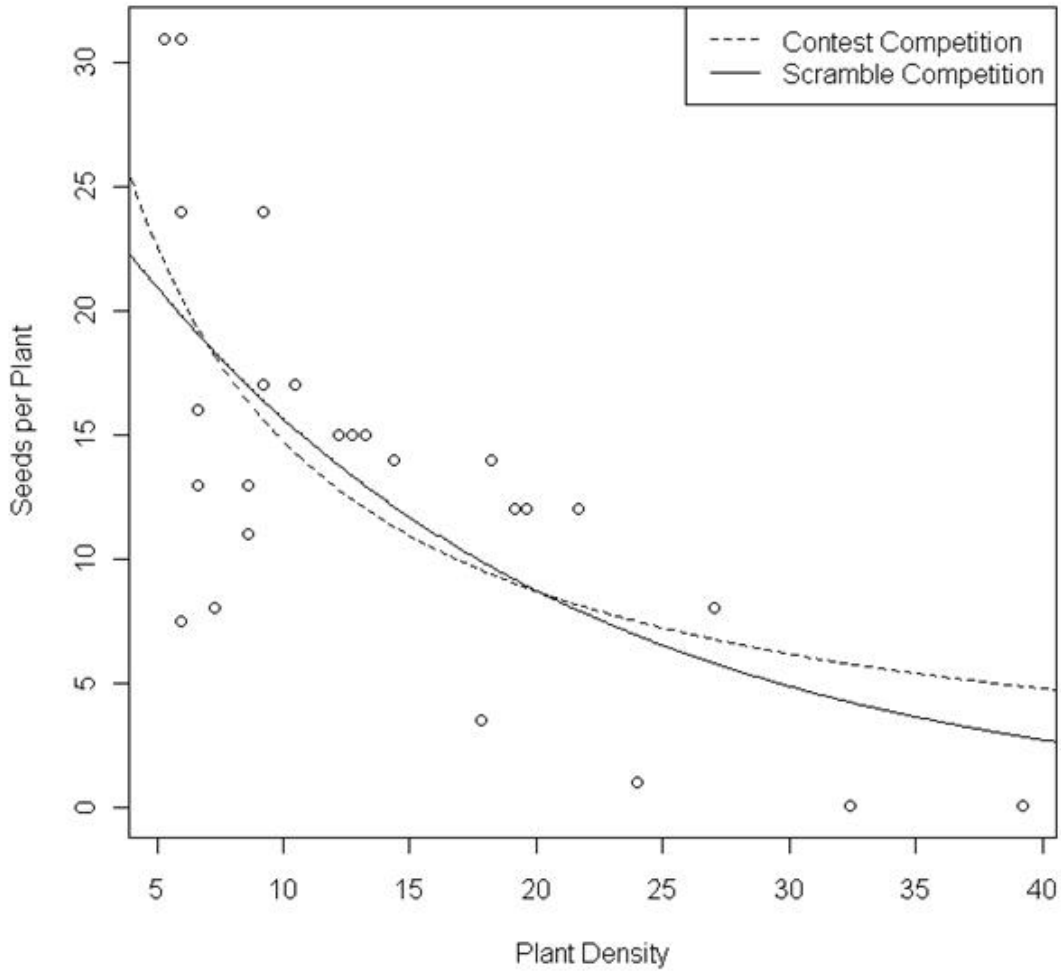
Figure 3.3: The relationship between *per-capita* seed production in year $t + 1$ and plant density in year t. We digitized the data from Fig. 2b in [46]. The dotted line represents the function $\frac{h(y)}{y} = \frac{c_m}{c_m + y}$, which is used to model per-capita seed production in the contest competition case (AIC $= 165.53$). The solid line represents the function $\frac{h_R(y)}{y} = \exp(-y/c_m)$, which is used in the scramble competition case (AIC $= 164.78$).

where $p_e = c(1 - A)^{-1}b = c = 48.64$ is the inverse of the stability radius of the plant-only system and $\tilde{M}$ is the first column of $(I - S)^{-1}$, where

$$S = \begin{bmatrix} 0 & 0 & 0 \\ (1 - g_p)s^2 & 0 & 0 \\ 0 & (1 - g_p)s^3 & (1 - g_p)s^4 \end{bmatrix}.$$

In the scramble competition model $p_1 = 0.101 \in (0, g_0), p_2 = 0.118 < \exp(-2)$ and $y^* = 363.07 > 0$, which by Theorem 3.2.3 implies the asymptotic, but not necessarily global asymptotic stability of

$$\tilde{n}^* = [36.58 \ 86.44 \ 58.50 \ 96.76]^T, \tag{3.49}$$

as the spectral radius of $\tilde{A}_{(1+\ln(p_2))p_2} + f'(y^*)\tilde{b}\tilde{c}_{(1+\ln(p_2))p_2}^T$ is $0.3461 < 1$.

Figure 3.4 shows trajectories of the solutions to the models (3.48) with several initial conditions. Notice that the convergence in the model with the contest competition assumption is rather quick, while the model with scramble competition has more pronounced transient dynamics, as one might expect, as the Ricker function h_2 is not monotone. This example illustrates that with different assumptions for density-dependent seed production one can potentially obtain different stability outcomes even though the two models fit the available data similarly well. However, since the population in the right-hand side of Figure 3.4 converges to the equilibrium under many different initial populations, one may conjecture that there are improvements to be made to Theorem 3.2.3; that the p_2 element of the solution to (3.15) doesn't necessarily need to be $> \exp(-2)$ for there to be global asymptotic stability for (3.7), and thus (3.48) with $i = 2$. However, if the spectral radius of the operator $\tilde{A}_{(1+\ln(p_2))p_2} + f'(y^*)\tilde{b}\tilde{c}_{(1+\ln(p_2))p_2}^T$ is larger than unity, the population does indeed fail
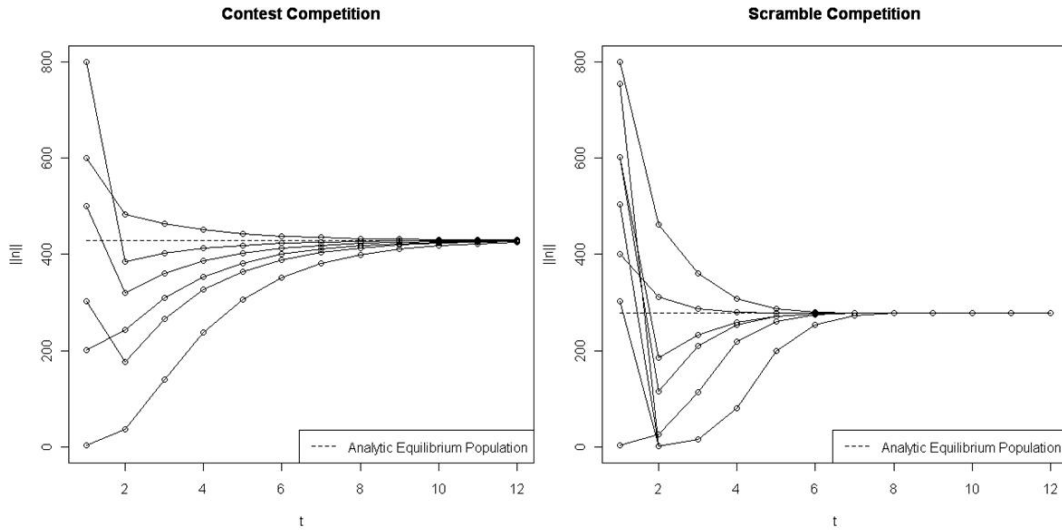
Figure 3.4: Example simulations of the solutions to the models (3.48) for various initial conditions. The graph on the left is in the contest competition (3.46) case and the graph on the right is in the scramble competition (3.47) case. The vertical axis indicates the total population density (*plants + seeds*), and the horizontal axis is *time*. The dashed line is the equilibrium population calculated using (3.10). Note that, although the solution sequences are connected by lines, we are not implying that the solutions behave linearly between (discrete) time-steps.

to achieve a unique, globally stable equilibrium population, which is evident in Figure 3.5, where $c = 1500$.

This example also illustrates the utility of the solution (p_1, p_2, y^*) to the equations in (3.15). This triple reduces the task of obtaining a formula for, and determining the stability of, the equilibrium to the solution of a system of three equations in three unknowns.

3.4 Extensions

So far in this chapter we have proven the global stability of the equilibrium vector $\tilde{n}^*$ for a class of density-dependent structured plant population models with an age-

Scramble Competition - No Global Stability
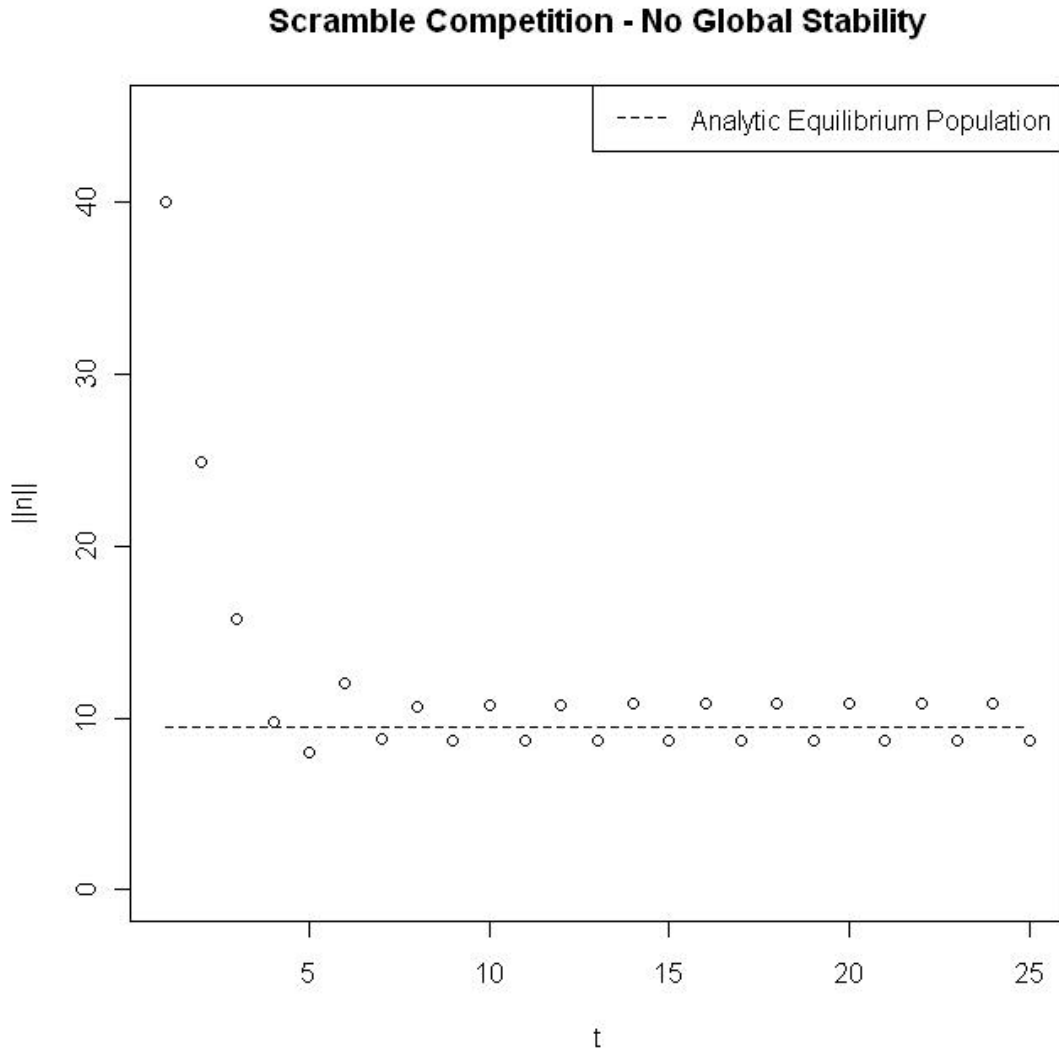
Figure 3.5: The population in (3.48) with $i = 2$ (contest competition) and $c = 1500$. Here, $\tilde{A}_{(1+\ln(p_2))p_2} + f'(y^*)\tilde{b}\tilde{c}^T_{(1+\ln(p_2))p_2} = 1.15 > 1$. Notice that there is no longer a unique, globally stable equilibrium population, but rather a two-cycle.

structured seed bank. We showed how these theoretical results can be applied to a model in the literature. The techniques we used include so-called "small gain" arguments and the use of different stability radii that are common in engineering problems involving feedback systems ([64])

We have, to our advantage, used the fact that the data (A, b, c), and subsequently $(\tilde{A}, \tilde{b}, \tilde{c})$, are *positive*. This may not always be true. An interesting mathematical question arises when one assumes that seed germination (the

$$\text{seeds} \overset{\text{germination}}{\longrightarrow} \text{seedlings}$$

step), is density dependent and determined by the nonlinear function g, which was previously called the establishment function. To see the difficulties that arise in this context assume that the seed population $\{s_t\}_{t=0}^{\infty}$ simply evolves as a scalar in $\mathbb{R}^+$ and that the plant population is as before. In this setting the new model becomes

$$
\begin{aligned}
n_{t+1} &= An_t + bf(c^T n_t + s_t) \\
s_{t+1} &= s_p(1 - g(c^T n_t + s_t))(c^T n_t + s_t),
\end{aligned}
$$

where $0 < s_p < 1$ is the survival probability of a dormant seed in the soil. For this model to make sense biologically we have to assume that $g_0 := \lim_{y \searrow 0} g(y) < 1$. Like (3.7), this system can be written as

$$\tilde{n}_{t+1} = \tilde{A}\tilde{n}_t + \tilde{b}f(\tilde{y}_t), \qquad \tilde{y}_t = \tilde{c}^T \tilde{n}_t, \tag{3.50}$$

where

$$\tilde{A} := \begin{bmatrix} A & 0 \\ s_p c^T & s_p \end{bmatrix}, \qquad \tilde{b} := \begin{bmatrix} b \\ -s_p \end{bmatrix}, \qquad \tilde{c}^T := \begin{bmatrix} c^T & 1 \end{bmatrix}.$$

Note that $\tilde{A}$ and $\tilde{c}$ satisfy (A1) and (A3'), respectively, in [64]. However, $\tilde{b}$ isn't a positive vector in $X_1 \otimes \mathbb{R}^+$, so we cannot use any of the previous results. However, even though $\tilde{b}$ isn't a positive vector we can still use similar techniques to prove the global stability of (3.50) for much of parameter space.

Define

$$p_e^* := (\sum_{k=0}^{\infty} \tilde{c}^T \tilde{A}^k \tilde{b})^{-1} = (\tilde{c}^T (\tilde{I} - \tilde{A})^{-1} \tilde{b})^{-1}.$$

It is simple to show that $p_e^* = \frac{(1-s_p)}{(\frac{1}{p_e} - s_p)}$, where $p_e = (c^T (I - A)^{-1} b)^{-1}$ is again the stability radius from the system without a seed bank. It's clear that, for some (s_p, p_e), p_e^* can be negative and, therefore, while having an analogous equation to the stability radius for the systems in previous sections, the nonpositivity in the system keeps the connection from being a straightforward extension. Be that as it may, p_e^* will still end up serving as the bifurcation point for the global stability of a non-negative vector in $X_1 \otimes \mathbb{R}$ for the system (3.50). The reason we can still achieve a non-negative attractor is that, since $g_0 < 1$, the nonlinear operator

$$\begin{bmatrix} A + g(\tilde{c}^T(\cdot)) & g(\tilde{c}^T(\cdot)) \\ s_p(1 - g(\tilde{c}^T(\cdot)))c^T & s_p(1 - g(\tilde{c}^T(\cdot))) \end{bmatrix}$$

still is a *non-negative* operator: It takes non-negative vectors in $X_1 \otimes \mathbb{R}$ to non-negative vectors in $X_1 \otimes \mathbb{R}$.

We will first prove a lemma about the positivity of the terms $\tilde{c}^T \tilde{A}^k \tilde{b}$ for $k \in \mathbb{N}$.

Lemma 3.4.1 *If there exists a k_0 such that $\tilde{c}^T \tilde{A}^{k_0} \tilde{b} \geq 0$, then $\tilde{c}^T \tilde{A}^k \tilde{b} \geq 0$ for all $k \geq k_0$*

Proof: Assume $\tilde{c}^T \tilde{A}^{k0} \tilde{b} \geq 0$. Then

$$
\begin{aligned}
\tilde{c}^T \tilde{A}^{k_0+1} \tilde{b} &= \sum_{j=0}^{k_0} s_p^{k_0-j+1} c^T A^j b - s_p^{k_0+2} \\
&= s_p \left(\sum_{j=0}^{k_0} s_p^{k_0-j} c^T A^j b - s_p^{k_0+1} \right) \\
&= s_p \left(c^T A^{k_0} b + \sum_{j=0}^{k_0-1} s_p^{k_0-j} c^T A^j b - s_p^{k_0+1} \right) \\
&= s_p \left(c^T A^{k_0} b + \tilde{c}^T \tilde{A}^{k_0} \tilde{b} \right) \geq 0,
\end{aligned}
$$

as sought. $\qquad\qquad\qquad\qquad\qquad\qquad\qquad\qquad\qquad\qquad\qquad\qquad\qquad\qquad$ $\square$

Therefore, even though p_e^* can be negative, we know that if one term of the sequence $\{\tilde{c}^T \tilde{A}^k \tilde{b}\}_{k=0}^{\infty}$ is eventually nonnegative, the remaining terms are nonnegative as well.

We will now prove global stability results of a non-negative vector in $X_1 \otimes \mathbb{R}$ for the system (3.50) analogous that of Sections 3.2.1, 3.2.2 and 3.2.3. We will begin by proving the stability of the zero vector in the case where $\frac{1}{p_e^*} < \frac{1}{g_0}$. This includes the case where $p_e^* \leq 0$, which was not possible for the positive system in Sections 3.2.1, 3.2.2 and 3.2.3. We will then assume that $0 < p_e^* < g_0$ and address the possibility that $\tilde{c}^T \tilde{A}^0 \tilde{b} \geq 0$ (where the stability is a simple Corollary of [64]) and the possibility that $\tilde{c}^T \tilde{A}^0 \tilde{b} < 0$. In the latter case we will assume a particular functional form for f derived in Chapter 2.

Theorem 3.4.1 *Suppose that (D1), (E1), (E2) and (E3) hold, and $s_p, g_0 < 1$. If* $\frac{1}{p_e^*} < \frac{1}{g_0}$, *then the zero vector is a globally stable equilibrium for (3.50) in the sense*

that for every non-negative $\tilde{n}_0 \in X_1 \otimes \mathbb{R}$,

$$\lim_{t \to \infty} \tilde{n}_t = 0.$$

Furthermore, for every $\epsilon > 0$, there exists $\delta > 0$ such that $\|\tilde{n}_t\| < \epsilon$ for all $t \in \mathbb{N}$ whenever $\|\tilde{n}_0\| < \delta$.

Proof: Let $N \in \mathbb{N}$ and $\tilde{n}_0$ be a positive vector in $X_1 \otimes \mathbb{R}$. Note that, since the nonlinear operator for the system (3.50) is non-negative:

$$0 \le \sum_{t=0}^{N} \tilde{c}^T \tilde{n}_t = \sum_{t=0}^{N} \tilde{c}^T \tilde{A}^t \tilde{n}_0 + \sum_{t=0}^{N} \sum_{j=0}^{t-1} \tilde{c}^T \tilde{A}^{t-j-1} \tilde{b} f(\tilde{c}^T \tilde{n}_j).$$

Rearranging the summation, one has

$$= \sum_{t=0}^{N} \tilde{c}^T \tilde{A}^t \tilde{n}_0 + \sum_{j=0}^{N-1} \sum_{t=j+1}^{N} \tilde{c}^T \tilde{A}^{t-j-1} \tilde{b} f(\tilde{c}^T \tilde{n}_j)$$

$$= \sum_{t=0}^{N} \tilde{c}^T \tilde{A}^t \tilde{n}_0 + \sum_{j=0}^{N-1} f(\tilde{c}^T \tilde{n}_j) \sum_{t=j+1}^{N} \tilde{c}^T \tilde{A}^{t-j-1} \tilde{b}. \tag{3.51}$$

The proof now concludes with a sequence of cases.

Case 1: If $p_e^* \le 0$ and $\tilde{c}^T \tilde{A}^k \tilde{b} < 0$ for all $k \in \mathbb{N}$ then one has, using (3.51),

$$0 \le \sum_{t=0}^{N} \tilde{c}^T \tilde{n}_t \le \sum_{t=0}^{N} \tilde{c}^T \tilde{A}^t \tilde{n}_0 \le \tilde{c}^T (\tilde{I} - \tilde{A})^{-1} \tilde{n}_0 < \infty. \tag{3.52}$$

Case 2: If $p_e^* \le 0$ and $\tilde{c}^T \tilde{A}^{k_0} \tilde{b} > 0$ for some $k_0 \in \mathbb{N}$ then one has for $N > k_0$, using Lemma 3.4.1, (3.51) and the fact that $p_e^* = (\sum_{k=0}^{\infty} \tilde{c}^T \tilde{A}^k \tilde{b})^{-1} \le 0$:

$$0 \le \sum_{t=0}^{N} \tilde{c}^T \tilde{n}_t = \sum_{t=0}^{N} \tilde{c}^T \tilde{A}^t \tilde{n}_0 + \sum_{j=0}^{N-1} f(\tilde{c}^T \tilde{n}_j) \sum_{t=j+1}^{N} \tilde{c}^T \tilde{A}^{t-j-1} \tilde{b}$$

$$\leq \sum_{t=0}^{\infty} \tilde{c}^T \tilde{A}^t \tilde{n}_0 + \frac{1}{p_e^*} \sum_{j=0}^{N-1} f(\tilde{c}^T \tilde{n}_j) \leq \sum_{t=0}^{\infty} \tilde{c}^T \tilde{A}^t \tilde{n}_0 \leq \tilde{c}^T (\tilde{I} - \tilde{A})^{-1} \tilde{n}_0 < \infty. \qquad (3.53)$$

Case 3: If $p_e^* > g_0 > 0$ we can find an $m < p_e^*$ such that $g(x) \leq m$ for all $x \geq 0$.
Using (3.51) again we have that

$$0 \leq \sum_{t=0}^{N} \tilde{c}^T \tilde{n}_t = \sum_{t=0}^{N} \tilde{c}^T \tilde{A}^t \tilde{n}_0 + \sum_{j=0}^{N-1} f(\tilde{c}^T \tilde{n}_j) \sum_{t=j+1}^{N} \tilde{c}^T \tilde{A}^{t-j-1} \tilde{b}$$

$$\leq \sum_{t=0}^{\infty} \tilde{c}^T \tilde{A}^t \tilde{n}_0 + \frac{1}{p_e^*} \sum_{j=0}^{N-1} g(\tilde{c}^T \tilde{n}_j) \tilde{c}^T \tilde{n}_j \leq \sum_{t=0}^{\infty} \tilde{c}^T \tilde{A}^t \tilde{n}_0 + \frac{m}{p_e^*} \sum_{j=0}^{N-1} \tilde{c}^T \tilde{n}_j$$

$$\leq \sum_{t=0}^{\infty} \tilde{c}^T \tilde{A}^t \tilde{n}_0 + \frac{m}{p_e^*} \sum_{t=0}^{N} \tilde{c}^T \tilde{n}_t.$$

Since $m < p_e^*$ we have that $(1 - \frac{m}{p_e^*}) > 0$, which implies

$$0 \leq \sum_{t=0}^{N} \tilde{c}^T \tilde{n}_t \leq (1 - \frac{m}{p_e^*})^{-1} \tilde{c}^T (\tilde{I} - \tilde{A})^{-1} \tilde{n}_0 < \infty \qquad (3.54)$$

In (3.52), (3.53), (3.54) we have that the sum $\sum_{t=0}^{N} \tilde{c}^T \tilde{n}_t$ is less than an absolutely convergent series, independent of N. Thus we can conclude that the sequence $\{\tilde{c}^T \tilde{n}_t\}_{t=0}^{\infty} \in \ell_1(\mathbb{N})$, which implies that the terms converge to zero as $t \to \infty$. By supposition (E3) this implies that

$$\lim_{t \to \infty} \tilde{n}_t = 0,$$

as sought. The (ϵ, δ) conclusion follows from the fact that $r(\tilde{A}) < 1$ and Holder's inequality. $\qquad \square$

To determine the global stability of a non-zero vector in positive cone of $X_1 \otimes \mathbb{R}$ we break the problem further into two cases.

Theorem 3.4.2 *Suppose that (D1), (E1), (E2) and (E3) hold, $s_p, g_0 < 1$ and $c^T b \geq s_p$. If $p_e^* < g_0$ then there exists y^* such that $f(y^*) = p_e^* y^*$. The vector $\tilde{n}^*$ given by*

$$\tilde{n}^* = p_e^* y^* (\tilde{I} - \tilde{A})^{-1} \tilde{b}$$

is a strictly positive globally asymptotically stable equilibrium of the system (3.50) in the sense that for every positive $\tilde{n}_0 \in X_1 \otimes \mathbb{R}$

$$\lim_{t \to \infty} \tilde{n}_t = \tilde{n}^*.$$

Furthermore, for every $\epsilon > 0$, there exists $\delta > 0$ such that $\|\tilde{n}_t - \tilde{n}^*\| < \epsilon$ for all $t \in \mathbb{N}$ whenever $\|\tilde{n}_0 - \tilde{n}^*\| < \delta$.

Proof: Since, by assumption, $\tilde{c}^T \tilde{A}^0 \tilde{b} = c^T b - s_p \geq 0$ we have from Lemma 3.4.1 that $\tilde{c}^T \tilde{A}^k \tilde{b} \geq 0$ for all $k \in \mathbb{N}$. The proof now follows directly from [64]. $\square$

To prove the result for when $c^T b - s_p < 0$ we need to compare (3.50) with a model studied abstractly in Section 3.2.1. Consider the model

$$n_{t+1} = An_t + bf(c^T n_t + s_t) \tag{3.55}$$

$$s_{t+1} = s_p(1 - g_0)(c^T n_t + s_t),$$

where $g_0 := \lim_{y \searrow 0} g(y) < 1$. Note that, if we write (3.55) in the form

$$\hat{n}_{t+1} = \hat{A}\hat{n}_t + \hat{b}f(\hat{y}_t), \qquad \hat{y}_t = \hat{c}^T \hat{n}_t, \tag{3.56}$$

with

$$\hat{A} := \begin{bmatrix} A & 0 \\ s_p(1-g_0)c^T & s_p(1-g_0) \end{bmatrix}, \qquad \hat{b} := \begin{bmatrix} b \\ 0 \end{bmatrix}, \qquad \hat{c}^T := \begin{bmatrix} c^T & 1 \end{bmatrix},$$

we have that $\tilde{n}_t \geq \hat{n}_t$ for all $t \in \mathbb{N}$. The global stability of a non-negative vector in $X_1 \otimes \mathbb{R}$ is resolved for (3.56) in Section 3.2.1. If $\hat{p}_e := (\hat{c}^T(\hat{I} - \hat{A})^{-1}\hat{b})^{-1} = (1 - s_p(1-g_0))p_e < g_0$ then this globally stable vector is positive in $X_1 \otimes \mathbb{R}$.

It is useful to note that if $0 < p_e^* < g_0$ then $0 < \hat{p}_e < g_0$. Since we are assuming that $c^T b - s_p < 0$, not all terms $\tilde{c}^T \tilde{A}^k \tilde{b}$ are positive. Our assumptions will therefore be on the summation $\sum_{k=0}^{\infty} |\tilde{c}^T \tilde{A}^k \tilde{b}|$.

Our final assumption is that the nonlinear function f is of the Michaelis-Menten type

$$f(x) = \frac{\alpha x}{\beta + x}. \tag{3.57}$$

The functional form (3.57) is derived in Chapter 2, modeling the effects of density dependence on seeds germinating in an environment with limited microsite availability.

Theorem 3.4.3 *Suppose that (D1), (E1), (E2) and (E3) hold, f is given by (3.57), $s_p, g_0 = \frac{\alpha}{\beta} < 1$ and $c^T b < s_p$. If $0 < p_e^* < g_0$ then there exists y^* such that $f(y^*) = p_e^* y^*$. Assume further that*

$$\sum_{k=0}^{\infty} |\tilde{c}^T \tilde{A}^k \tilde{b}| < \left| \frac{\hat{c}^T \hat{n}^* - y^*}{f(\hat{c}^T \hat{n}^*) - f(y^*)} \right| = \frac{(\beta + \hat{c}^T \hat{n}^*)(\beta + y^*)}{\alpha\beta}, \tag{3.58}$$

where $\hat{n}^*$ is the positive, globally stable vector for (3.56). The vector $\tilde{n}^*$ given by

$$\tilde{n}^* = p_e^* y^* (\tilde{I} - \tilde{A})^{-1} \tilde{b}$$

is a strictly positive globally asymptotically stable equilibrium of the system (3.50) in the sense that for every positive $\tilde{n}_0 \in X_1 \otimes \mathbb{R}$

$$\lim_{t\to\infty} \tilde{n}_t = \tilde{n}^*.$$

Proof: As stated, since $0 < p_e^* < g_0$ it's true that $0 < \hat{p}_e < g_0$. Thus the globally stable equilibrium vector $\hat{n}^*$ of (3.56) is positive in $X_1 \otimes \mathbb{R}$. Assume that $\tilde{n}_0$ is a positive vector in $X_1 \otimes \mathbb{R}$. By (E3) this implies that $\tilde{c}^T \tilde{n}_0 > 0$. Also, since

$$g_0 = \frac{\alpha}{\beta} > \frac{\alpha}{\beta + x} = g(x)$$

for all $x > 0$, if $\tilde{c}^T \tilde{n}_0 > 0$ then $\tilde{n}_t > \hat{n}_t$ for all $t \geq 2$. Therefore, there exists a $k_0 \in \mathbb{N}$ such that

$$\tilde{n}_t > \hat{n}^* \tag{3.59}$$

for all $t \geq k_0$. Finally, since the right-hand side of (3.58) is increasing in $\tilde{c}^T \tilde{n}$, we have that

$$\sum_{k=0}^{\infty} |\tilde{c}^T \tilde{A}^k \tilde{b}| < |\frac{\tilde{c}^T \tilde{n} - y^*}{f(\tilde{c}^T \tilde{n}) - f(y^*)}| \tag{3.60}$$

for all $\tilde{n} \geq \hat{n}^*$.

We can easily verify from (3.50) using [43] that $\tilde{n}^* = \tilde{A}\tilde{n}^* + p_e^* \tilde{b}\tilde{c}^T \tilde{n}^* = \tilde{A}\tilde{n}^* + \tilde{b}f(y^*)$ by construction. Thus,

$$\tilde{n}_{t+1} - \tilde{n}^* = \tilde{A}\tilde{n}_t - \tilde{A}\tilde{n}^* + \tilde{b}f(\tilde{y}_t) - \tilde{b}f(y^*). \tag{3.61}$$

Let k_0 satisfy the condition (3.59). Applying $\tilde{c}^T$ to (3.61) and summing from k_0 to $N > k_0$ we have

$$\sum_{t=k_0}^{N} |\tilde{c}^T \tilde{n}_t - \tilde{c}^T \tilde{n}^*| \leq \sum_{t=k_0}^{N} |\tilde{c}^T \tilde{A}^t (\tilde{n}_0 - \tilde{n}^*)| + \sum_{t=k_0}^{N} \sum_{j=0}^{t-1} |\tilde{c}^T \tilde{A}^{t-j-1} \tilde{b}| |f(\tilde{c}^T \tilde{n}_j) - f(y^*)|.$$

Rearranging the summation we have

$$\leq \sum_{t=k_0}^{N} |\tilde{c}^T \tilde{A}^t (\tilde{n}_0 - \tilde{n}^*)| + \sum_{j=k_0}^{N} \sum_{t=j+1}^{N} |\tilde{c}^T \tilde{A}^{t-j-1} \tilde{b}| |f(\tilde{c}^T \tilde{n}_j) - f(y^*)|$$

$$+ \sum_{j=0}^{k_0-1} \sum_{t=k_0}^{N} |\tilde{c}^T \tilde{A}^{t-j-1} \tilde{b}| |f(\tilde{c}^T \tilde{n}_j) - f(y^*)|$$

$$= \sum_{t=k_0}^{N} |\tilde{c}^T \tilde{A}^t (\tilde{n}_0 - \tilde{n}^*)| + \sum_{j=k_0}^{N} |f(\tilde{c}^T \tilde{n}_j) - f(y^*)| \sum_{t=j+1}^{N} |\tilde{c}^T \tilde{A}^{t-j-1} \tilde{b}|$$

$$+ \sum_{j=0}^{k_0-1} |f(\tilde{c}^T \tilde{n}_j) - f(y^*)| \sum_{t=k_0}^{N} |\tilde{c}^T \tilde{A}^{t-j-1} \tilde{b}|.$$

Adding more terms to the summation we have

$$\leq \sum_{t=0}^{\infty} |\tilde{c}^T \tilde{A}^t (\tilde{n}_0 - \tilde{n}^*)| + \sum_{j=k_0}^{N} |f(\tilde{c}^T \tilde{n}_j) - f(y^*)| \sum_{k=0}^{\infty} |\tilde{c}^T \tilde{A}^k \tilde{b}| + \sum_{j=0}^{k_0-1} |f(\tilde{c}^T \tilde{n}_j) - f(y^*)| \sum_{k=0}^{\infty} |\tilde{c}^T \tilde{A}^k \tilde{b}|.$$

Since the middle summation is from k_0 to $N > k_0$ and the right-hand side of (3.58) is increasing there exists an $m < 1$ such that

$$|f(\tilde{c}^T \tilde{n}_j) - f(y^*)| \leq m \frac{|\tilde{c}^T \tilde{n}_j - y^*|}{\displaystyle\sum_{k=0}^{\infty} |\tilde{c}^T \tilde{A}^k \tilde{b}|} \tag{3.62}$$

for all $j \geq k_0$. Using (3.62) and the fact that f is uniformly bounded above by α one

then has

$$\sum_{t=k_0}^{N} |\tilde{c}^T \tilde{n}_t - \tilde{c}^T \tilde{n}^*| \leq (1-m)^{-1} (\sum_{t=0}^{\infty} |\tilde{c}^T \tilde{A}^t(\tilde{n}_0 - \tilde{n}^*)| + 2\alpha(k_0 - 1) \sum_{k=0}^{\infty} |\tilde{c}^T \tilde{A}^k \tilde{b}|) < \infty,$$

which is independent of $N > k_0$. Therefore the sequence $\{|\tilde{c}^T \tilde{n}_t - y^*|\}_{t=0}^{\infty} \in \ell_1(\mathbb{N})$, which implies that the terms converge to zero as $t \to \infty$. By supposition (E3) this implies that

$$\lim_{t \to \infty} \tilde{n}_t = \tilde{n}^*,$$

as sought. $\qquad\qquad\qquad\qquad\qquad\qquad\qquad\qquad\qquad\qquad\qquad\qquad\qquad\square$

3.4.1 Sensitivity of $\tilde{n}^*$ to Seed Survival

In Chapter 2 we presented a derivation of the sensitivity of a globally stable equilibrium population with respect to arbitrary parameters a model of the form (1.3). We will now present the sensitivity of a positive equilibrium solution $\tilde{n}^*$ in $X_1 \otimes \mathbb{R}$ for (3.50) with respect to the survival probability of a seed in the soil s_p.

To determine the sensitivity of $\tilde{n}^* = p_e^* y^* (\tilde{I} - \tilde{A})^{-1} \tilde{b}$ with respect to s_p it is useful to calculate the terms in $\tilde{n}^*$ explicitly. It's a simple calculation to show that

$$(I - \tilde{A})^{-1}\tilde{b} = \left[\begin{array}{cc} (I - A)^{-1}b & \frac{s_p}{1-s_p}(\frac{1}{p_e} - 1) \end{array} \right]^T. \qquad (3.63)$$

Recall also that

$$p_e^* = \frac{(1 - s_p)}{(\frac{1}{p_e} - s_p)}. \qquad (3.64)$$

From the previous section we need $p_e^* > 0$ to have a $\tilde{n}^*$ be positive, thus $1 > s_p p_e$. However, (3.63) implies also that $p_e < 1$ for $\tilde{n}^*$ to be positive.

Assume for the sake of explanation that f again has the Michaelis-Menten form

$$f(x) = \frac{\alpha x}{\beta + x},\tag{3.65}$$

for which we can easily calculate

$$\psi(p_e^*) = p_e^* y^* = \alpha - \beta p_e^*.\tag{3.66}$$

With (3.63), (3.64) and (3.66) we can calculate $\frac{d\tilde{n}^*}{ds_p}$ using the product rule. By a simple calculation:

$$\frac{d\tilde{n}^*}{ds_p} = \beta \frac{p_e(1 - p_e)}{(p_e s_p - 1)^2} \begin{bmatrix} (I - A)^{-1} b \\ \frac{s_p}{1 - s_p}\left(\frac{1}{p_e} - 1\right) \end{bmatrix} + p_e^* y^* \begin{bmatrix} 0 \\ \frac{1 - p_e}{p_e(1 - s_p)^2} \end{bmatrix}.\tag{3.67}$$

Since $p_e < 1$ all of the terms in the above equation are positive. Therefore, increasing s_p increases the both the likelihood of population persistence (see (3.64)) and the long-term population $\tilde{n}^*$. However, increasing s_p decreases the likelihood that $c^T b - s_p \geq 0$, which increases the difficulty of the proof in Theorem 3.4.3.

As noted in Chapter 2 this sensitivity measurement has the ability to tell us how members of each stage class change in response to changes in specific parameters. To see this note that, biologically, the first term on the right-hand side of 3.67 is a proportional change to the *entire* previous population distribution via an increase in s_p, while the second term is a change in the seed population only. What (3.67) tells us is that an increase in seed survival probability will increase the plant population by a factor of $\beta \frac{p_e(1 - p_e)}{(p_e s_p - 1)^2}$, but will not change the plant population's structure or stage distribution, i.e., the relative frequencies of members of each stage class are not altered.

3.4.2 Toy Example

We will illustrate how to use Theorem (3.4.3) to calculate $\tilde{n}^*$ for a simple example of a plant population with two stages (young and old), with a scalar seed bank. We will then use the derivation of the sensitivity of $\tilde{n}^*$ from Section 3.4.1 to determine the sensitivity of the population to changes in s_p. Assume that young plants stay young with probability $a_{11} < 1$ and graduate to become old with probability $a_{21} < 1$. Assume old plants survive with probability $a_{22} < 1$ and that young plants produce $0 < c_1$ seeds and old plants produce $c_1 < c_2$ seeds. We will continue using the Michaelis-Menten function for f. Our model can be written as in (3.50), where

$$
\tilde{A} := \begin{bmatrix} a_{11} & 0 & 0 \\ a_{21} & a_{22} & 0 \\ s_p c_1 & s_p c_2 & s_p \end{bmatrix}, \qquad \tilde{b} := \begin{bmatrix} 1 \\ 0 \\ -s_p \end{bmatrix}, \qquad \tilde{c}^T := \begin{bmatrix} c_1 & c_2 & 1 \end{bmatrix}.
$$

It's a simple calculation to show that the linear data $(\tilde{A}, \tilde{b}, \tilde{c})$ satisfy the conditions of Theorem (3.4.3) and that $\tilde{c}^T \tilde{A}^0 \tilde{b} = c_1 - s_p$. Because average seed production for young plants can be small (see, for example, [67]), it's possible that $\tilde{c}^T \tilde{A}^0 \tilde{b} < 0$. Therefore, one may need to check the additional condition in Theorem 3.4.3 to determine whether or not the population converges to a globally stable equilibrium population. For example, if $a_{11} = 0.25, a_{21} = 0.6, a_{22} = 0.9, c_1 = 0.1, c_2 = 10, s_p = 0.75, \alpha = 10, \beta = 200$ we have that

$$
\tilde{c}^T \tilde{A}^0 \tilde{b} = c_1 - s_p = -0.65 < 0, \tag{3.68}
$$

while

$$
\tilde{c}^T \tilde{A}^1 \tilde{b} = s_p(c_2 a_{21} - s_p) = 5.5375 > 0, \tag{3.69}
$$

and

$$p_e^* = 0.003149.$$

With (3.68), (3.69) and (3.4.2) and Lemma (3.4.1) one can calculate

$$\sum_{k=0}^{\infty} |\tilde{c}^T \tilde{A}^k \tilde{b}| = 0.65 + \frac{1}{0.003149} + 0.65 = 318.8333.$$

To see if (3.58) is satisfied we use the fact that $\hat{p}_e = (1 - s_p(1 - g_0))p_e = 0.003587713$ to obtain $\hat{c}^T \hat{n}^* = \frac{\alpha}{\hat{p}_e} - \beta = 2587.246$. This, coupled with $y^* = \frac{\alpha}{p_e^*} - \beta = 2975.333$ gives us

$$4425.217 = |\frac{\hat{c}^T \hat{n}^* - y^*}{f(\hat{c}^T \hat{n}^*) - f(y^*)}| > 318.8333 = \sum_{k=0}^{\infty} |\tilde{c}^T \tilde{A}^k \tilde{b}|,$$

which establishes the global asymptotic stability of the vector

$$\tilde{n}^* = p_e^* y^* (I - \tilde{A})^{-1} \tilde{b} = \begin{bmatrix} 12.4935 & 74.96116 & 2224.47239 \end{bmatrix}^T.$$

which is 3-dimensional, as the plant is modeled with a 2-dimensional vector and the seed bank is modeled as a scalar (1-dimensional).

Because we have a simple formula for the sensitivity of the population we can easily calculate how a small increase in seed survival $s_p = 0.75$ will change the equilibrium population of this plant-seed bank model from $\tilde{n}^*$. We know from the previous section that the relative proportion of the young plants n_1^* and old plants n_2^* will not change, they will only increase by a factor of $\beta \frac{p_e(1-p_e)}{(p_e s_p - 1)^2} = 2.511549$. On the other hand, the seed bank population will increase by a factor of 2.511549 *and* by $p_e^* y^* \frac{1-p_e}{p_e(1-s_p)^2} = 11867.03$. Therefore, a small increase in the seed survival probability from $s_p = 0.75$ will increase

the asymptotic seed bank population by

$$2.511549\frac{s_p}{1-s_p}(\frac{1}{p_e}-1)+11867.03=12463.10.$$

What we've shown through the analysis in this section is that once an understanding of the long-term dynamics of a plant-seed bank model is achieved, the biological questions boil down to using the relatively simple formula for sensitivities. Therefore, calculating exactly how the population will react in the long-term to a change in a particular vital rate is relatively clean and simple.

Chapter 4

A Stochastic Integral Projection Model for a Disturbance Specialist Plant: Seed Depth Matters

4.1   Plant-Seed Bank Model

Many annual plants are disturbance specialists, germinating only in freshly disturbed soil. In these species the frequency, intensity, timing, and spatial extent of disturbance can greatly influence the probability of germination and survival of seeds in the seed bank ([20], [61], [59]). Many of these aforementioned characteristics of disturbances happen unpredictably, rendering deterministic models like those studied in Chapter 3 inadequate. Disturbances create a more favorable environment for germination by removing more competitive species ([20], [61], [3], [59]). However, disturbance also alters the depth distribution of seeds in the seed bank: burying some seeds deep in the soil where survival is high (and germination rates are low), and relocating other seeds

closer to the soil surface where germination rates are high (but survival is low) ([61], [60]). Most attempts at understanding the dynamics of plant-seed bank populations, including the modeling in Chapter 3, have ignored the effect of seed depth. Therefore, in this chapter we will develop a stochastic IPM for the population dynamics of a disturbance specialist plant, explicitly modeling the stochasticity of disturbances and the variations in survival and germination probabilities of seeds at different depths.

A stochastic IPM describes how a population structured by a continuous state variable changes in discrete time. We model the following sequence of events: disturbance, redistribution of seeds, seed survival, plant recruitment, and production of new seeds. We consider only disturbances which occur after seeds have been dispersed because disturbances prior to dispersal have a negligible effect on the seed bank ([61]). We model disturbance as a single event in one time-step, which can be thought of as an average of the post dispersal disturbances to the population in a given year.

Disturbance and Redistribution of Seeds

We model disturbances as independent and identically distributed stochastic events influencing the population dynamics each year. The stochastic process ([8]) governing disturbances is denoted $\theta(t, \omega)$, where ω denotes the realization of the sample space Ω of all possible sequences of disturbance outcomes. At each time t we break up $\theta(t, \omega)$ into two random variables $\theta_1(t, \omega)$ and $\theta_2(t, \omega)$. $\theta_1(t, \omega)$ is a Bernoulli random variable determining whether or not the population is disturbed, which is equal to unity with the probability of disturbance h and zero with the probability of no disturbance $1 - h$. Given a disturbance occurs, $\theta_2(t, \omega)$ determines how deep the disturbance affects the seeds in the population at time t. For example, if $\theta_2(t, \omega) = 0.5D$ then the disturbance uniformly redistributes all seeds above one-half of the maximum depth of the seed bank ($[0, \frac{D}{2}]$) and leaves the rest of the seed bank ($[\frac{D}{2}, D]$) undisturbed. The depth of a disturbance is modeled as a truncated exponential distribution with mean depth of

disturbance ρ. Thus,

$$Prob\{\theta_2(t,\omega) \le r|\theta_1(t,\omega) = 1\} := \begin{cases} 1 - \exp(\frac{r}{\rho}) & : r < D \\ 1 & : r = D. \end{cases}$$

Note that we are going to assume that every disturbance depth that would otherwise be greater than D is simply a disturbance of depth D, which contributes to the jump in the above cumulative distribution function.

Using the convention that disturbing the population throughout the interval $[0,0]$ is the same as not disturbing it at all, it follows that one could define $\theta(t,\omega)$ with the following equation

$$\theta(t,\omega) = \theta_1(t,\omega)\theta_2(t,\omega),$$

for every $t = 0, 1, 2, ...$ Using this definition $\theta(t,\omega)$ determines both the occurrence and depth of disturbance for each time t. We define the disturbance kernel $K(\cdot,\cdot,\theta(t,\omega))$ at time t for the stochastic process $\theta(t,\omega)$, acting on the population $u(\cdot)$, as

$$\int_0^D K(x,y,\theta(t,\omega))u(y)\,dy := (\theta(t,\omega))^{-1} \int_0^{\theta(t,\omega)} u(y)\,dy\chi_{[0,\theta(t,\omega)]} + u(x)\chi_{[\theta(t,\omega),D]},$$

$$(4.1)$$

with the convention that the first term in the right hand side of (4.1) is equal to zero when $\theta(t,\omega) = 0$ and $\chi_{[a,b]}$ is the characteristic function of the interval $[a,b]$, which is equal to unity when $x \in [a,b]$ and zero when $x \notin [a,b]$. The first term in the right hand side of (4.1) is modeling the population being uniformly re-distributed within the interval $[0,\theta(t,\omega)]$ and the second term is the population being left alone within the interval $[\theta(t,\omega), D]$. The dimension of $K(\cdot,\cdot,\theta(t,\omega))$ is $depth^{-1}$ for all $\theta(t,\omega) \in \Omega$.

Survival

Only a fraction of the seeds that do not germinate survive to the next time-step. We

make the simplifying assumptions that this fraction only depends on the seed's depth in the seed bank ([60]), that seeds survive at their lowest rates near the surface of the soil (due largely to seed predation) and that the likelihood of survival increases as seed depth increases. The survival function is therefore

$$s(x) := s_0(1 - \exp(-bx)), \tag{4.2}$$

where $s_0 < 1$ is the maximum possible survival probability of a seed and b models the incremental gain in survival probability that occurs through an incremental increase in seed depth. The function $s(\cdot)$ is dimensionless.

Plant Recruitment

We assume that germination only occurs in the presence of a disturbance, thus the germination probability is a function of $\theta(t, \omega)$, i.e.

$$g(x, \theta(t, \omega)) := \begin{cases} g_p(x) & : \theta(t, \omega) \neq 0 \\ 0 & : \theta(t, \omega) = 0, \end{cases}$$

where $g_p(x)$ is the probability of a seed of depth x germinating in a given time-step, given a disturbance. We assume that the probability of a seed germinating is such that seeds germinate at their highest rate near the surface of the soil and the likelihood of germination drops off as seed depth increases ([16]). Thus

$$g_p(x) := g_0 \exp(-ax) \tag{4.3}$$

where $g_0 < 1$ is the probability of a seed on the surface of the soil germinating and a models the loss in germination probability that occurs through an incremental increase in seed depth ([60]). The function $g(\cdot, \cdot)$ is dimensionless.

We assume that recruitment is density-dependent and follows a Holling Type II functional form ([44], we referred to this function as the Michaelis-Menten in Chapters 2 and 3). A derivation of an analogous relationship for a general plant population is available in Chapter 2, which utilizes the idea of competing for a finite number of available microsites. The number of plants that result from x $seeds(area)^{-1}$ is calculated as follows

$$f(x) := \frac{\alpha x}{\beta + x}. \tag{4.4}$$

As summarized in Chapter 2, the parameter α is the maximum number of adult plants that can grow in a given area, with dimension $plants(area)^{-1}$. The parameter β (with dimension $seeds(area)^{-1}$) is the half saturation constant. $f(\cdot)$ is the only term in the model that is density dependent. The dimension of $f(\cdot)$ is $plants(area)^{-1}$.

Seed Production

We do not implement the size structure of the plants explicitly because we envision annual plants and the model uses a time-step of one year. Each plant produces an average number of seeds c which are distributed according to the depth distribution $J(\cdot)$. We assume that $J(\cdot)$ is a truncated exponential distribution with mean $\mu << 1$ ([60]), which ensures that most seeds are set on the surface of the soil. As a consequence most newly created seeds die if there is no disturbance in the following year. The dimension of c is $seeds(plants)^{-1}$ and $J(\cdot)$ has dimension $(depth)^{-1}$.

Integral Projection Model

Our IPM simulates how the distribution of seeds in the seed bank and the plant population density of an annual species changes from one year to the next. We do not present the dynamics of the plant population in our results because the long-term mean and variance is not a very good measurement of the plant population due to the number of time-steps the above ground plant population equals zero.

Let $n(x, t, \omega)$ be the density of seeds in the seed bank at time t between depths x and $x + dx$, and $p(t, \omega)$ be the density of plants in the population at time t, for $t = 0, 1, 2, \ldots$. ω denotes the realization in the sample space Ω, which is the collection of all sequences of possible disturbance outcomes. The dimensions of $n(\cdot, \cdot, \cdot)$ and $p(\cdot, \cdot)$ are $seeds(depth)^{-1}(area)^{-1}$ and $plants(area)^{-1}$, respectively. We assume that all plants in the population behave like the average plant, so $p(t, \cdot)$ is simply a nonnegative number for all t. D is the maximum disturbance depth, thus the function $n(\cdot, t, \cdot)$ has the interval $[0, D]$ as its domain for every t. The model is therefore

$$n(x, t + 1, \omega) = \int_0^D \Delta(x, y, \theta(t, \omega))(n(y, t, \omega) + cJ(y)p(t, \omega)) \, dy \qquad (4.5)$$

$$p(t + 1, \omega) = f\left(\int_0^D \int_0^D \delta(x, y, \theta(t, \omega))u(y) \, dy \, dx \right),$$

for $t = 0, 1, 2, \ldots$ and $n(\cdot, 0, \cdot) > 0$. Here $\Delta(x, y, \theta(t, \omega)) := s(x)(1 - g(x, \theta(t, \omega))K(x, y, \theta(t, \omega))$ and $\delta(x, y, \theta(t, \omega)) := g(x, \theta(t, \omega))K(x, y, \theta(t, \omega))$.

The model in (4.5) is not a traditional stochastic IPM (as seen in [19], [34], [65]) in the sense that the (mathematical) operation (defined by the disturbance kernel above) from one time-step to the next is not necessarily compact for each t. This is because the identity operator modeled by the Dirac kernel (which occurs when there is no disturbance at time t) is never compact in a function space ([5]). Because non-compact operators are often difficult to handle mathematically, the mathematical properties of this model will require further theoretical attention, which we will reserve for another manuscript. In this chapter we use simulations to conjecture that as $t \to \infty$ the population sequence $\{[n(\cdot, t, \omega) \quad p(t, \omega)]\}_{t=0}^{\infty}$ converges to a stationary random population $\{[n^*(\cdot, \omega) \quad p^*(\omega)]\}$, independent of nonzero initial population $\{[n^*(\cdot, 0, \omega) \quad p^*(0, \omega)]\}$. Thus, for large t, the probability distribution of the population converges (and thus the long-term population has a constant mean and variance).

We perform Monte Carlo simulations to analyze how the mean and variance of the populations change with changes in the disturbance parameters h (the probability of disturbance) and ρ (the mean depth of disturbance), as well as the fecundity (seeds per plant) c and the recruitment parameters α and β (from (4.4)).

4.2   Model Analysis

All simulations were done in R ([62]), using numerical integration techniques explained in [34], with parameter values listed in Table 4.1. The main R codes used are in Appendix C. In our simulation studies we set the maximum depth $D = 1$, so that shallower depths are represented as a proportion of the maximum depth. We considered two different scenarios for carrying capacity and four different scenarios for fecundity. The values $\alpha = 40, \beta = 50$ were consistent with Fig. 3 in [2] for Wild sunflower (*Helianthus annuus*).

For each run we simulation population dynamics for 10000 time-steps and recorded the total population density for the seed population $||n(\cdot, 10000, \omega)||_1 = \int_0^D n(x, 10000, \omega)\, dx$. We repeated this process 500 times and calculated the long-term mean

$$Mean = \sum_\omega \frac{||n(\cdot, 10000, \omega)||_1}{500}$$

and variance

$$Variance = \sum_\omega \frac{(||n(\cdot, 10000, \omega)||_1 - Mean)^2}{500}$$

of the total seed bank population. In an IPM population size can asymptote to zero, but never actually reach zero. Thus we defined a quasi-extinction threshold (the minimum viable population density) to be $||n(\cdot, t, \omega)||_1 = 50 \ seed(area)^{-1}$ in the seed bank (personal communication with Diana Pilson), and the quasi-extinction probability as

the proportion of 100 with initial population density $||n(\cdot, 0, \omega)||_1 = 500 \; seed(area)^{-1}$ that dropped below $50 \; seeds(area)^{-1}$ at $t = 1000$. We repeated these calculations for 90 evenly spaced (h, ρ) combinations in $[0, 1] \times [0, 1]$ to explore the effect of the probability of disturbance h and the mean depth of disturbance ρ on the mean and variance of the seed bank size, and the quasi-extinction probability.

4.3   Results

Initial exploratory simulations using various parameter combinations suggested that the probability of disturbance h has a large effect on population dynamics. Figure 4.1 illustrates four typical simulation sample paths: Low fecundity and low disturbance frequency always resulted in extinction within $1000 \; years$ (Figure 4.1(a)). Seeds require a disturbance to germinate, and in the periods between disturbances seed density decreased (due to seed mortality). Thus, if the time between disturbances was too long, and seed production following a disturbance was too low to offset seed losses due to mortality the population eventually went extinct. Increasing fecundity while keeping the frequency of disturbance low produced boom and bust dynamics and delayed population extinction (Figure 4.1(b) and (c)). Plants with high fecundity contribute many new seeds into the seed bank each time there is a disturbance. Thus seed density was generally sufficiently high for populations to persist for quite some time even with long intervals between disturbances. However, when simulating populations over longer time periods the seed density eventually decreased below the quasi-extinction threshold, due to the probability of a prolonged streak of years with no disturbance. High fecundity combined with increased disturbance frequency produced fluctuations well above the quasi extinction threshold, even if we extended the simulation interval past the 1000 time-steps shown (Figure 4.1(d)).

Figure 4.2 illustrates that increasing the probability of disturbance h decreased the quasi-extinction probability, regardless of ρ. The seeds in the seed bank need disturbances to germinate, so increasing the disturbance frequency increased the total seed bank population, which reduced the extinction probability (Figure 4.3). The higher the fecundity c, the lower the required disturbance frequency to prevent extinction. Interestingly, increasing the mean depth of disturbance, ρ, actually *increased* the quasi-extinction probability for all fecundity values c considered, although increasing the fecundity decreased the effect of ρ on the quasi-extinction probability. If fecundity was low the redistribution (which is dependent on ρ) resulted in a smaller number of newly produces seeds being deposited to larger depth than seeds being moved close to the surface where they either germinated or died if there was no disturbance in the following year. How many new seeds that are produced following a disturbance, M, depended on the maximum number of plants that can establish in a time-step, which was less than α, and their fecundity, c, so $M \leq c\alpha$. Thus the net effect of this redistribution on seed bank size can be negative, resulting in decreasing seed bank size with increasing ρ for h values where the quasi-extinction probability is smaller than one and larger than zero (Figures 4.2 and 4.3).

The carrying capacity of the plant population α had a smaller effect on the quasi-extinction probability than fecundity c, the frequency of disturbance h, and the mean depth of disturbance ρ (Figure 4.3 (a) and (c)). This was consistent with the theoretical results of other similar stochastic population models ([41] and [7]), where the behavior of a population when rare (i.e. when density dependence is not a factor) uniquely determined the population's chance of persistence.

The variance of seed bank size was significantly influenced by the disturbance probability h and had a roughly parabolic shape for most mean depths of disturbance ρ (Figure 4.4). The initial increase of the variance with increasing h was consistent

with an increasing mean seed bank size, as variance typically increases with the mean (Figure 4.3). However if h got sufficiently large the carrying capacity of the population imposed an upper bound to the number of seeds that could be produced within one time step. This upper bound reduced the variance in seed production because the population could only have large fluctuations toward the zero function. Thus, for high h the limit imposed by the carrying capacity increasingly restrained upper fluctuations. For small ρ the variance did not display a parabolic shape as a function of h. This is because, for small ρ, the total seed bank populations were small relative to the carrying capacity, and so the population could have large fluctuations in both directions.

The qualitative effect of h and ρ and on the mean and variance of the long-term seed bank size remained roughly similar under a range of different parameter scenarios. Other model parameters basically rescaled the relationships. In general, increasing the fecundity c and/or the carrying capacity α led to larger means and variances of the seed bank size (notice the scales in Figures 4.3 and 4.4). For example, an increase by a factor of ten in α and β led to an increase of almost exactly a factor of ten in the mean and variance of the total seed bank population.

The probability of disturbance h also affected the distribution of population densities for large t: increasing h shifted the distribution from skew right (most populations were very small when disturbance is rare) to skew left (most populations were very close to the carrying capacity when disturbance is common) (Figure 4.5). For small h, the seed bank size rarely reached the carrying capacity, and as $h \to 0$ the proportion of runs where the population drops below the quasi extinction threshold increased and more and more of the frequency is concentrated near very small seed bank sizes. Conversely, when h was larger, the population was almost always being disturbed (and producing new seeds), and as a consequence the total seed bank size fluctuated around the carrying capacity, The skewedness became less profound for

Parameter	Value	Equation	Scenario
Maximum survival s_0	0.95	(4.2)	
Rate of change in survival b	10	(4.2)	
Maximum germination g_0	0.95	(4.3)	
Rate of change in germination a	10	(4.3)	
Mean depth of dispersal μ	0.05	(4.5)	
Holling parameters α, β	40, 50	(4.4)	"low" carrying capacity
Holling parameters α, β	400, 500	(4.4)	"high" carrying capacity
Seed production per plant c	50	(4.5)	"low" fecundity
Seed production per plant c	150	(4.5)	"medium low" fecundity
Seed production per plant c	500	(4.5)	"medium high" fecundity
Seed production per plant c	1000	(4.5)	"high" fecundity

Table 4.1: Parameter values for simulations of the model in (4.5).

large h if the maximum plant population α increased, but the fecundity c remained small, because the seed bank was sufficiently small so that density dependence was rarely limiting plant recruitment.

4.4   Discussion

We developed an integral projection model that mechanistically incorporated the stochastic effect of the disturbances on population dynamics of disturbance specialist plants by explicitly considering the vertical dynamics of seeds in the seed bank. The model suggested that the probability of a disturbance h was important for long-term population dynamics, which is consistent with [20], [61], and [59]. In addition to disturbance frequency, our model illustrated that the mean depth of disturbance ρ was also a critical component determining population persistence.

We have shown that a model which structures a plant population's seed bank with respect to depth can not only provide a mechanistic way of modeling disturbance intensity but also illustrates the tradeoffs experienced by the seed bank population
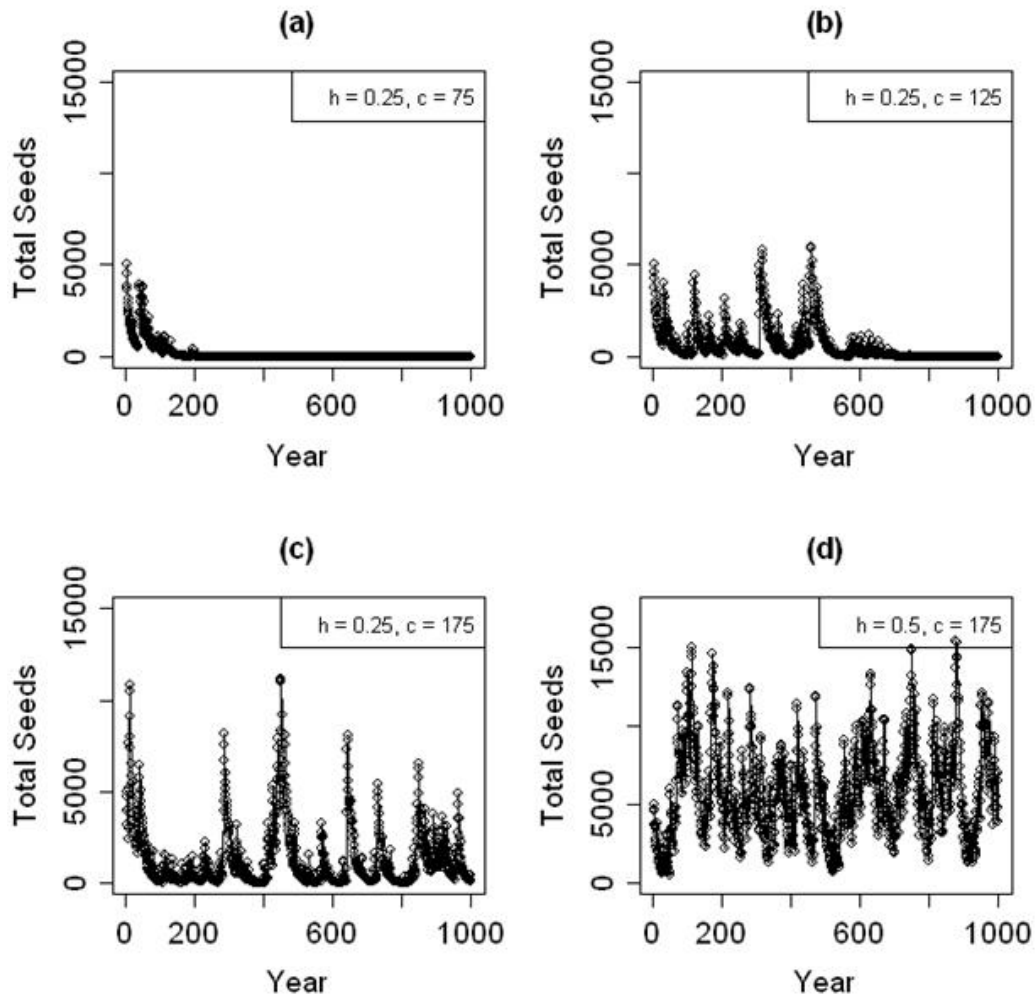
Figure 4.1: Example sample paths of the total seed bank population for four scenarios with different probability of disturbance h and fecundity c. The mean depth of disturbance $\rho = 0.5$ and the Holling parameters $\alpha = 40, \beta = 50$.
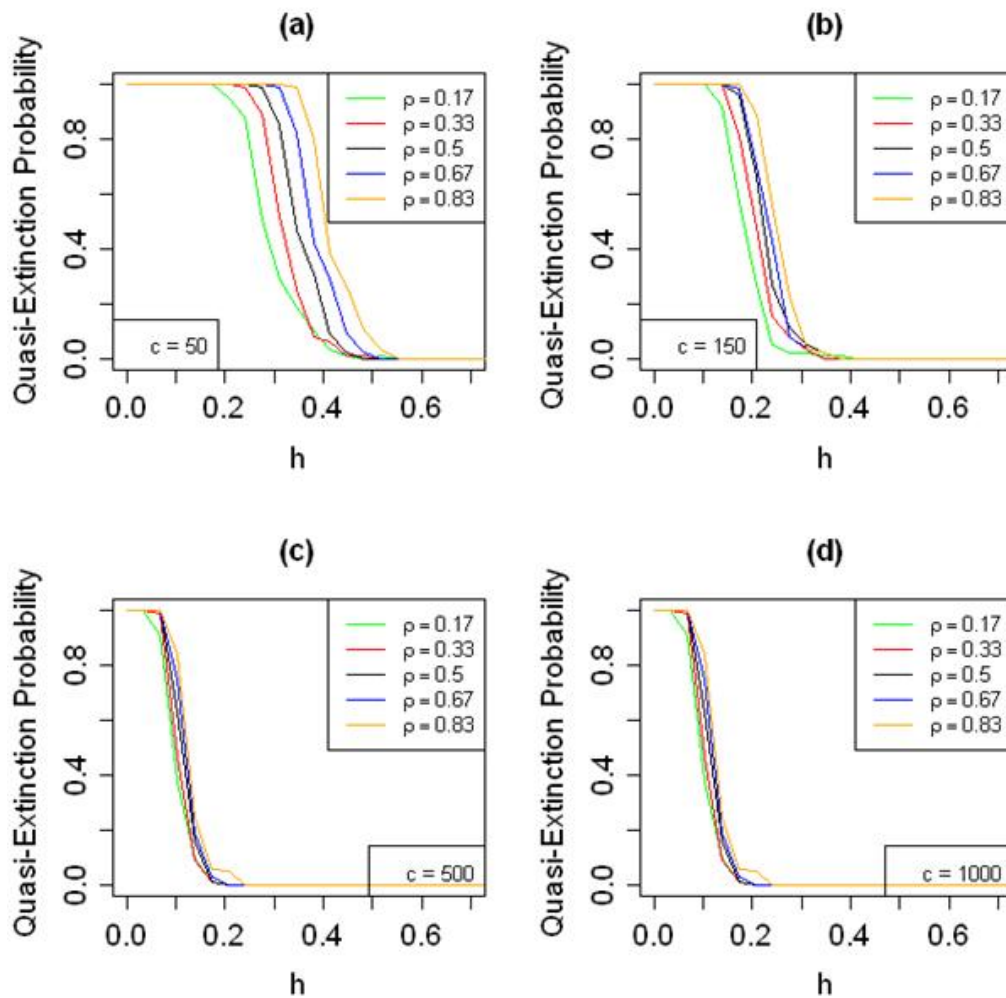
Figure 4.2: Probability of dropping below the quasi-extinction threshold of 50 $seeds(area)^{-1}$ by time $t = 1000$, as a function of the probability of disturbance h with different fecundity c values. The Holling parameters $\alpha = 40, \beta = 50$.
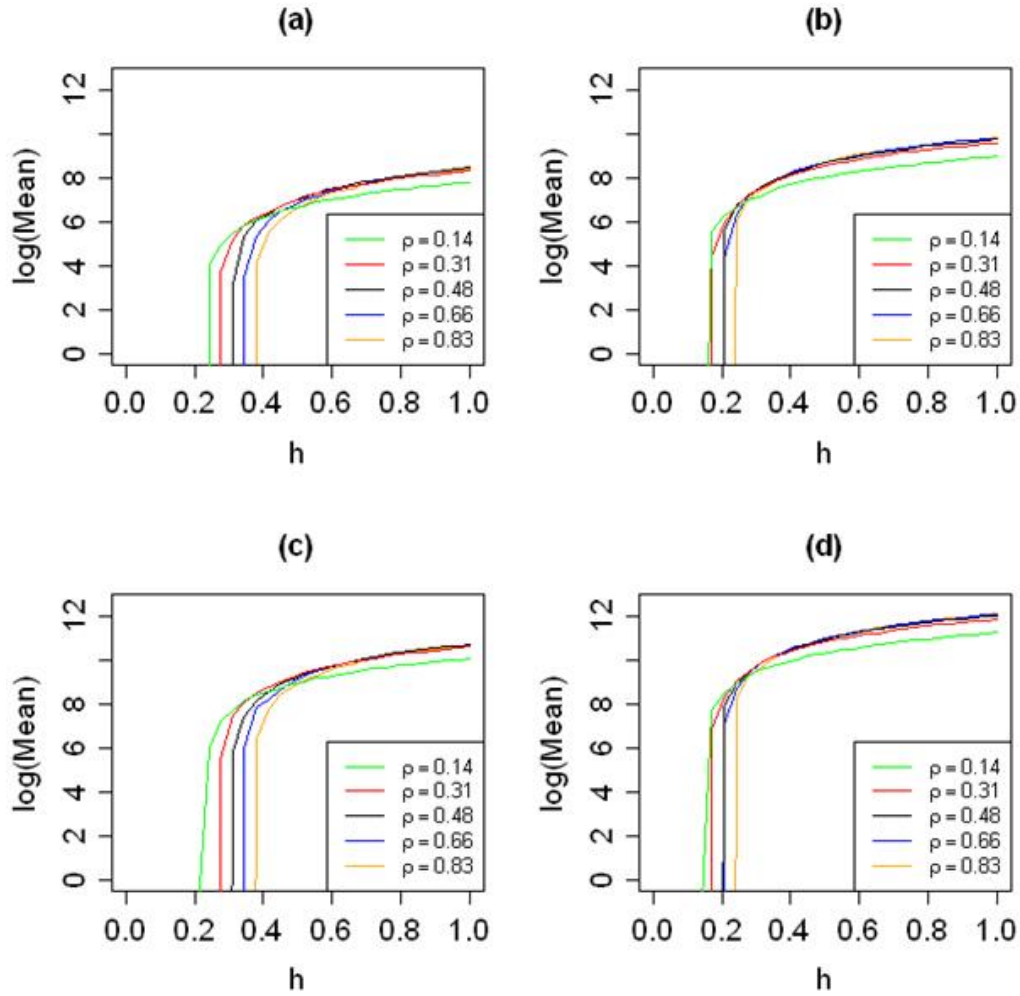
Figure 4.3: The natural logarithm of the mean of the total seed bank population as a function of h, the probability of disturbance, at time $t = 10,000$. Notice for each plot there exists an h value such that total seed bank population goes from being a decreasing function of ρ to an increasing function of ρ (for example, in graph (a) $h \sim 0.5$). The fecundity and Holling parameter combinations in the above plots are (a) $c = 50, \alpha = 40, \beta = 50$(b) $c = 150, \alpha = 40, \beta = 50$ (c) $c = 50, \alpha = 400, \beta = 500$ (d) $c = 150, \alpha = 400, \beta = 500$.
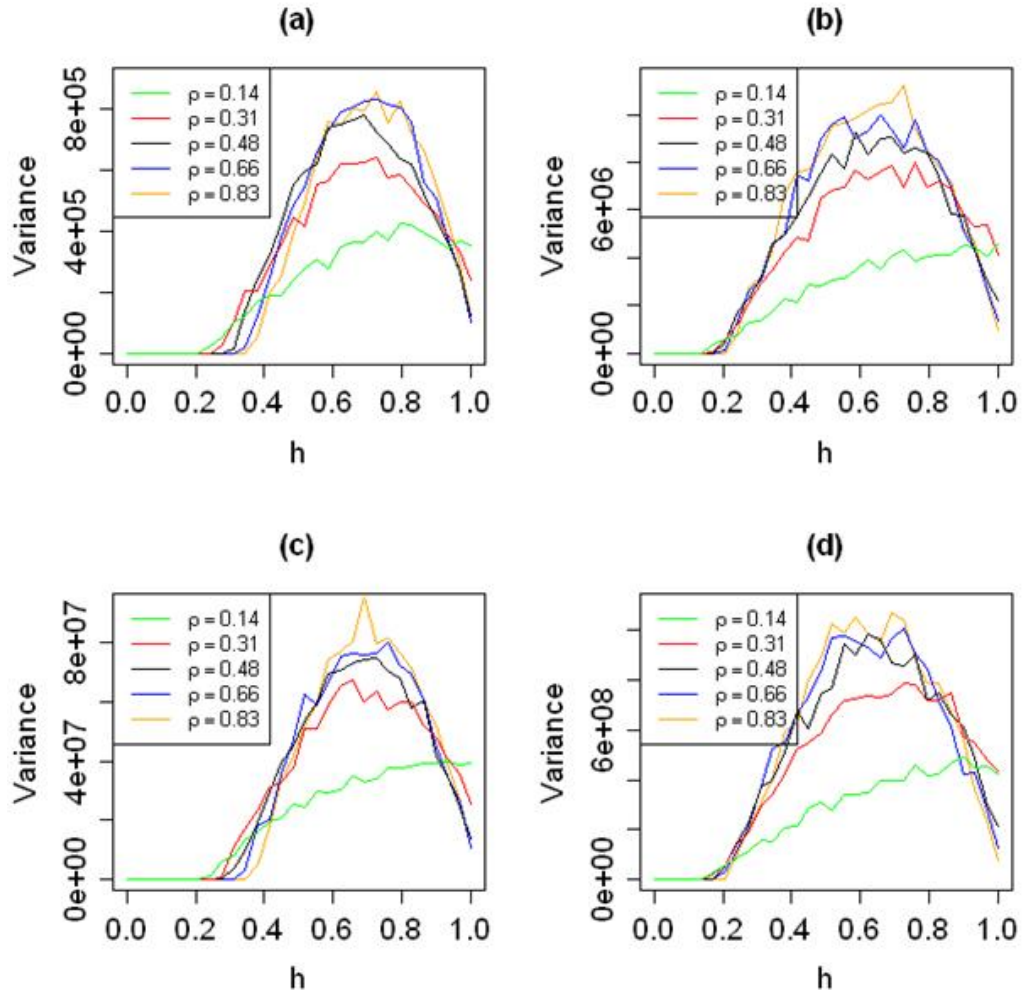
Figure 4.4: The variance of the total seed bank population as a function of h, the probability of disturbance, at time $t = 10,000$. The fecundity and Holling parameter combinations in the above plots are (a) $c = 50, \alpha = 40, \beta = 50$ (b) $c = 150, \alpha = 40, \beta = 50$ (c) $c = 50, \alpha = 400, \beta = 500$ (d) $c = 150, \alpha = 400, \beta = 500$.
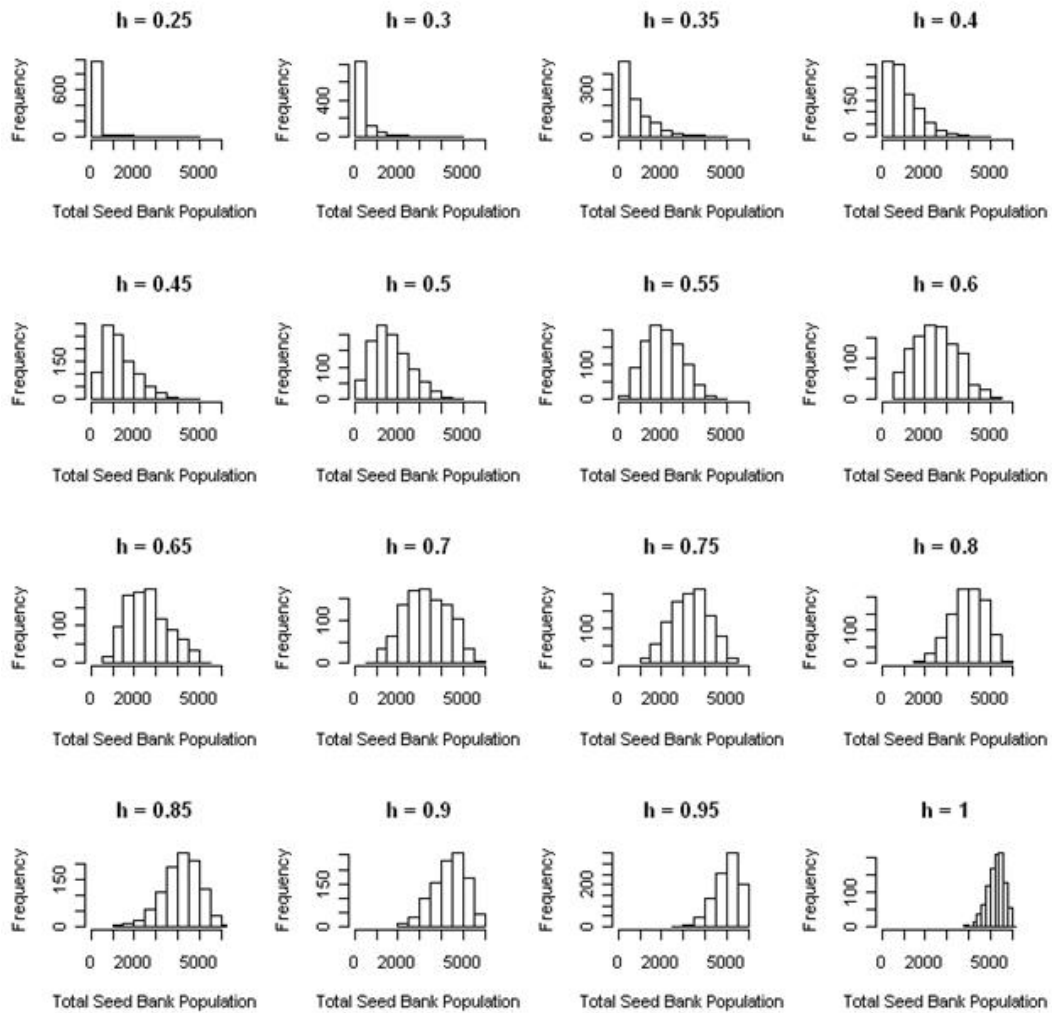
Figure 4.5: Histograms of the total seed bank population at $t = 1000$ of a typical sample path as the probability of disturbance h varies from 0.25 to 1.

when survival and germination depend on how deep the seeds are buried. Previous work has highlighted a lack of knowledge regarding the effect of the vertical distribution of seeds in the soil on plant population dynamics and encouraged integrating seed bank dynamics into mathematical models ([2]). Our model has illustrated that incorporating vertical movement of seeds within the seed bank can affect predicted long-term plant population viability, and motivates further studies of seed depth as a contributor to the stochastic population dynamics of disturbance specialist plants.

Our model has provided a new avenue for studying the seed bank of disturbance specialist plants through representing the seed bank as a function of continuous depth and characterizing disturbances explicitly by their intensity, building on the models by [20] and [60]. The two-depth model in [20] considered only one type of disturbance, thus seedling survival and germination probability is either low in the absence of a disturbance or high in the presence of a disturbance. They also assumed that fecundity was independent of the presence of a disturbance and could be either high in a "good year" or low in a "bad year". In contrast, the goal of our model was to isolate the effects of disturbance for disturbance plant species. In addition to disturbance frequency (as in [20] and [60]), we also examined the effect of different types of disturbances that influence seeds at different depths on plant population dynamics. Incorporating the redistribution of seeds in the seed bank explicitly is important because seed survival and germination are determined by seed depth. We modeled depth as a continuous variable and by varying only two parameters (h, ρ) we could produce a large number of potential disturbance outcomes. Using the long-term behavior of the system we are still able to obtain useful information about the dynamics of the population even with this larger range of disturbance situations and the implementation of stochasticity and density dependence. Our model showed that population persistence is an increasing function of disturbance frequency, which is consistent with the predictions in [20]

(see Fig 2 (b) in [20]). In this chapter we showed that the mean depth (intensity) of disturbance also has an effect on the long-term population dynamics of disturbance specialists, which is not considered in [20].

The model in [60] was concerned with evaluating the short-term outcomes of different tilling regimes as weed management strategies. As a consequence, his model simulated short-term, deterministic sequences of disturbances. In contrast, in our model disturbances were governed by a stochastic process that was roughly mimicking an overall, long-term disturbance regime that may not have been planned at all. The model in [60] predicted that some tilling (disturbance) scenarios can decrease the seedling density of weed species relative to no-tillage scenarios. For example, rotary and plow tillages were shown to produce fewer weed seedlings in initial years than no tillage. In contrast, our model was tailored to disturbance specialist plants in natural systems, whose seeds do not germinate (and thus seedlings do not emerge) in the absence of a disturbance.

There are some potential extensions to our model. First, for some species the maximum germination probability may not be at the surface of the soil ([60]), but rather at a deeper depth $x_{\max}$. For example, for larger seeds the highest germination probability is often at deeper depths in the seed bank. This could be implemented by replacing the exponential function $g_p(\cdot)$ in (4.3) with a Ricker-type function

$$g_R(x) := g_0 x \exp(-ax). \tag{4.6}$$

In (4.6) the maximum germination probability occurs when $x_{\max} = a^{-1}$ instead of $x_{\max} = 0$, as in (4.3). Having (4.6) instead of (4.3) for the germination function may reduce seed bank densities when disturbances are infrequent because newly created seeds near the surface of the soil are less likely to germinate (and thus create no new

seeds) and the remaining seeds suffer high mortality near the surface. However, the effect of replacing (4.3) with (4.6) is likely to be small for small enough $x_{\max} = a^{-1}$, i.e. as long as the maximum germination probability is achieved sufficiently close to the surface of the soil.

Second, we could change the way density dependence is incorporated into our model and assume that seed production is also density dependent, which may be best represented as scramble competition (i.e. Ricker-type function) as opposed to contest competition (Holling Type II form) ([46]). Because nonlinear functions like the Ricker function are not monotone, this extension of our current model may produce more than one stationary distribution of population sizes. It may also lead to a reduced long-term population size, compared to a model with constant seed production. This would occur if the maximum density of plants produced (α) yields a small number of seeds due to a high level of scramble competition. This situation can occur because the Ricker function goes to zero as the input (the density of plants) becomes large. Other possible extensions of our model include keeping track of the age structure of seeds, incorporating environmental stochasticity in seedling survival and germination parameters (e.g. "good" and "bad" years as in [20]) and considering seed dispersal (and thus the lateral position) of the seeds in seed bank.

Appendix A

Calculating Parameters to Ensure Common Equilibrium Values in Chapter 2

This first chapter of the Appendix demonstrates how to find the parameter values for the seedling recruitment function in the mechanistic model that ensures that the power function model and mechanistic model in Chapter 2 have a common equilibrium population. For (2.15), [64] ensures that this equilibrium population exists and is globally stable, independent of non-zero initial population. To find this equilibrium population, recall from Section 2.2 that we can write (2.15) in the abstract form (1.3). Recall also that the stability radius of the data (A, b, c) is

$$p_e = (c^T (I - A)^{-1} b)^{-1},$$

and the equilibrium population is given by

$$n^* = p_e \gamma^* (I - A)^{-1} b,$$

where γ^* is the limiting seed production, which is the solution of the equation $f_i(\gamma) = p_e \gamma$ for $i = 1, 2$. Using the kernel functions in Table 2 of [67], we compute that $p_e = 0.0216$, which is independent of the choice of f_i. To find the limiting seed production γ^* for both models, we simply solve $f_i(\gamma) = 0.0216\gamma$ for both $i = 1, 2$.

For the power function model the equation $f_1(\gamma) = 0.0216\gamma$ becomes

$$5.0899(\gamma)^{1-0.4453} = 0.0216,$$

from which we obtain $\gamma^* = 18,908.01$. To match the mechanistic model we need to choose α and β in the Michaelis-Menten function such that

$$\frac{\alpha}{\beta + 18,908.01} = 0.0216, \tag{A.1}$$

while the model fits the data in Fig. 4 of [67] as well as possible. The Michaelis-Menten function has two parameters, which will allow us to use one parameter to ensure (A.1) is true, with one additional parameter to fit to data. We will allow β to be the free parameter, to be fitted to data, and solve for α in terms of β to obtain the common equilibrium population. In this case $\alpha = 0.0216(18,908.01 + \beta)$. Finally, using nonlinear regression ([62]), we obtain $\beta = 4706$ from the data in [67].

The calculation of p_e and all other simulations of the IPMs in Chapter 2 use the numerical integration techniques described in [33]. All numerical techniques were carried out using the statistical software R ([62]), and codes are available upon request.
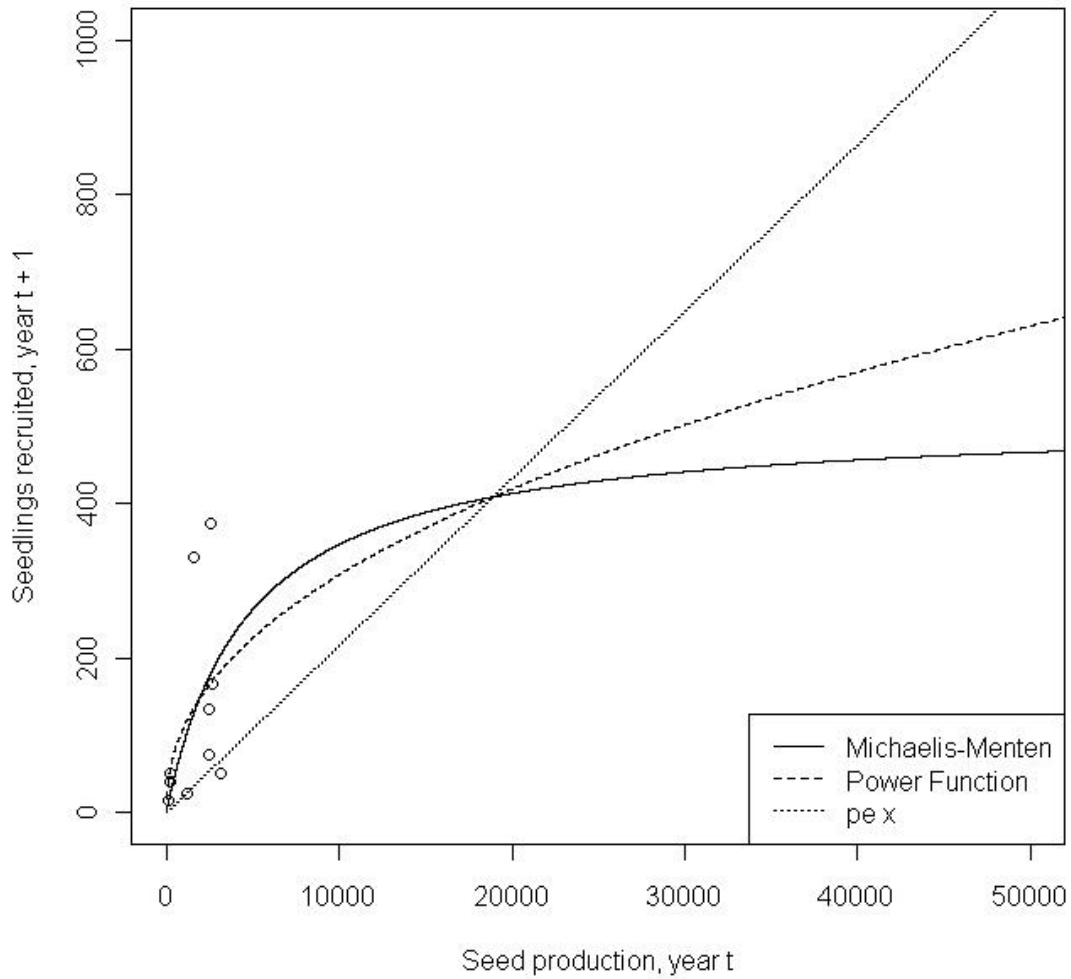
Figure A.1: The relationship between seedling recruitment in year $t+1$ and estimated seed production in year t. The intersection of the two recruitment functions with $h(x) = p_e x$ elicits the equilibrium seed production γ^*. We used this intersection to find the equilibrium population density in Appendix A.

Appendix B

Chapter 2 Computer Programs

B.1   Example - Contest Competition

```
#Program to Simulate the Dyanmics of the Example in Chapter 3

#from Jarry et al. 1995 CONTEST COMPETITION CASE

c0 = 48.64

#This is called "c" in the text

cm = 211.9

alpha = 72.51

beta = 89.17
```

```
A = 0.0

s = 0.95

g_p = 0.25


gam1 = (1 - g_p)*s

gam2 = (1 - g_p)*s^2

gam3 = (1 - g_p)*s^3


gam4 = (1 - g_p)*s^4


alpha = 72.51

beta = 89.17/g_p


#Nonlinear functions

h = function(x){cm*c0*x/(cm + c0*x)}


f = function(x){alpha*x/(beta + x)}


#Number of time-steps


N = 12


#Initializing the population


s1 <- 10
```

```
s2 <- 10

s3 <- 10

p <- 10

#Making vectors to count the total population size

totseeds <- rep(s1 + s2 + s3,N)

totplants <- rep(p,N)

#Simulating the population

for (i in 2:N) {

    s11 <- s1
    s12 <- s2
    s13 <- s3
    p1 <- p

    s1 <- gam1*(h(p1))
    s2 <- gam2*s11
    s3 <- gam3*s12 + gam4*s13
    p <- A*p1 + f(h(p1) + s11 + s12 + s13)
```

```
totseeds[i] <- s1 + s2 + s3


totplants[i] <- p


}


#Calculating the analytic equilibrium population


pe = (1-A)/c0


S <- matrix(0,3,3)


S[2,1] <- gam2


S[3,2] <- gam3


S[3,3] <- gam4


I <- diag(3)


Sinv <- solve(I - S)


#Solving the three equations in three unknowns


gamma = pe/(1 + gam1*sum(Sinv[,1]))
```

```
p2 = (pe*cm + beta*gamma)/(pe*cm + alpha)


p1 = gamma/p2


p1y = alpha - beta*p1


#The equilibrium population


atotplants <- p1y*(1 - A)^-1


atotseeds <- p1y*gam1*(p2/pe)*sum(Sinv[,1])


equil = rep(atotplants + atotseeds,N)


#Graphics


plot(totplants + totseeds, xlab = "", ylab = "", ylim = c(0,1500))

lines(totplants + totseeds) title(main = "Contest Competition")

title(xlab = "t", ylab = "||n||") lines(equil, lty = 2)

legend("bottomright", legend = "Analytic Equilibrium Population",

lty = 2)
```

B.2   Example - Scramble Competition

```
#Program to Simulate the Dyanmics of the Example in Chapter 3
```

```
#from Jarry et al. 1995 SCRAMBLE COMPETITION CASE


c0 = 28.09


#This is called "c" in the text


#For the example where global stability does not hold


c0 = 2000


cm = 480.95


alpha = 72.51
beta = 89.17


A = 0.0


s = 0.95


g_p = 0.25


gam1 = (1 - g_p)*s
gam2 = (1 - g_p)*s^2
gam3 = (1 - g_p)*s^3
```

```
gam4 = (1 - g_p)*s^4


alpha = 72.51


beta = 89.17/g_p


#Nonlinear functions


h = function(x){c0*x*exp(- c0*x/cm)}


f = function(x){alpha*x/(beta + x)}


#Number of time-steps


N = 12


#Initializing the population


s1 <- 10


s2 <- 10


s3 <- 10


p <- 10
```

```
#Making vectors to count the total population size


totseeds <- rep(s1 + s2 + s3,N)


totplants <- rep(p,N)


#Simulating the population


for (i in 2:N) {


    s11 <- s1

    s12 <- s2

    s13 <- s3

    p1 <- p


    s1 <- gam1*(h(p1))

    s2 <- gam2*s11

    s3 <- gam3*s12 + gam4*s13

    p <- A*p1 +  f(h(p1) + s11 + s12 + s13)



totseeds[i] <- s1 + s2 + s3


totplants[i] <- p


}
```

```
#Calculating the analytic equilibrium population

pe = (1-A)/c0

S <- matrix(0,3,3)

S[2,1] <- gam2

S[3,2] <- gam3

S[3,3] <- gam4

I <- diag(3)

Sinv <- solve(I - S)

#Solving the three equations in three unknowns

gamma = pe/(1 + gam1*sum(Sinv[,1]))

Ind = function(x){x*exp((x*beta - alpha)/(cm*pe)) - gamma}

p1 = uniroot(Ind, c(0, 1))$root

p2 = gamma/p1
```

```
p1y = alpha - beta*p1
```

```
#The equilibrium population
```

```
atotplants <- p1y*(1 - A)^-1
```

```
atotseeds <- p1y*gam1*(p2/pe)*sum(Sinv[,1])
```

```
equil = rep(atotplants + atotseeds,N)
```

```
#Graphics
```

```
plot(totplants + totseeds, xlab = "", ylab = "", ylim = c(0,1500))
lines(totplants + totseeds) title(main = "Scramble Competition")
title(xlab = "t", ylab = "||n||") lines(equil, lty = 2)
legend("bottomright", legend = "Analytic Equilibrium Population",
lty = 2)
```

```
#Checking for local stability
```

```
A0 <- matrix(0,4,4)
```

```
A0[1,1] <- A + (beta/alpha)*(p1^2)*p2*(1 + log(p2))*c0
```

```
A0[1,2] <- (beta/alpha)*(p1^2)

A0[1,3] <- (beta/alpha)*(p1^2)

A0[1,4] <- (beta/alpha)*(p1^2)

A0[2,1] <- gam1*p2*(1 + log(p2))*c0

A0[3,2] <- S[2,1]

A0[4,3] <- S[3,2]

A0[4,4] <- S[3,3]




VA = eigen(A0) Stability = VA$values abs(Stability[1])
```

Appendix C

Chapter 3 Computer Programs

C.1   Stochastic IPM Demo Program

```
#Program to Simulate the Dynamics of the Stochastic IPM for

#the Plant-Seed Bank Population of a Disturbance Specialist

#Parameters Displayed are of a current, but not necessarily
#typical, run

#Parameters

#Dimension of approximating matrices

N = 75;

#Number of time-steps
```

```
M = 1000
```

```
# Maximum seed bank depth
```

```
D = 1
```

```
#Mean disturbance depth
```

```
rho = 0.5
```

```
#Probability of disturbance
```

```
h = 0.35
```

```
#Program writting for h as the probability of !no! disturbance, so
```

```
h <- 1 - h
```

```
#Holling parameters
```

```
alpha = 400
```

```
beta = 500
```

```
#Fecundity


c0 = 100


#Functions
survival = function(x){(95/100)*(1 - exp(- 10*x))}


germination = function(x){(95/100)*exp(- 10*x)}


f = function(x){alpha*x/(beta + x)}


dispersal = function(x){c0*50*exp(-50*x)}


#Initializing vectors


#Creating Steps/Midpoints z = rep(0,N + 1); w = rep(0,N);


germ = rep(0,N); surv = rep(0,N); c = rep(0,N); germ1 = rep(0,N)


W = D/N


z[1] = 0 for(i in 1:N){
    z[i+1] = z[i]+W
        }
z[N+1] = D
```

```
for(i in 1:N){

    w[i] = (z[i+1] + z[i])/2

    }




#Discretizing survival and germination functions for (k in 1:N) {

        surv[k] <- survival(w[k])

        germ[k] <- germination(w[k])

        germ1[k] <- (1 - germination(w[k]))

        c[k] <- W*dispersal(w[k])

    }


#Initial Populations


Pop = 5000


initseeds = function(x){(Pop)*(1/D)}


initplants = 15 seeds = rep(0,N)



#Discretizing initial population


for (l in 1:N) {

        seeds[l] <- W*initseeds(w[l])
```

```
    }

plants <- initplants

#Total vectors

totseeds = rep(0,M)

totplants = rep(0,M)

totseeds <- sum(seeds)

totplants <- plants

seeds1 <- rep(0,N)

plants1 <- 0

#Initializing the Stochastic Process

r <- 0

r0 <- 0

#Simulating the population
```

```
for (i in 2:M) {


    Dist <- diag(N)

    r <- runif(2,0,1)



        if (r[1] <= h) {


            seeds1 <- surv*(seeds + c*plants)

            plants1 <- 0

        }



#Creating the Disturbance Kernel


        else {

            q <- (log(1 - r[2])*(- rho))/D

            k <- ceiling(min(c(q*N, N)))


            for (j in 1:k) {
                for (l in 1:k) {
                    Dist[j,l] <- 1/k

                    }

                }


            seeds1 <- surv*germ1*Dist%*%(seeds + c*plants)

            plants1 <- f(sum(germ*Dist%*%(seeds + c*plants)))
```

```
        }



#Plotting the pdf of the seed bank population at each time-step


xx <- seq(0,D, by=1/(N - 1)) plot(xx, seeds1/sum(seeds1), type =
'l', xlab = "Depth", ylab = "PDF of Seeds")



totseeds[i] <- sum(seeds1)


totplants[i] <- plants1


seeds <- seeds1


plants <- plants1


#Asking if the population is extinct or not


        if (totseeds[i] < 1) {
            seeds <- rep(0, N)
            plants <- 0
        }
}


#Plotting the population at the end of the simulation
```

```
plot(totseeds, xlab = " ", ylab = " ", col="black") lines(totseeds)

title(xlab="Year", col.lab="black"); title(ylab="Total Seeds",

col.lab="black"); title(main = "")
```

C.2   Stochatic IPM Quasi-Extinction Code

```
#Program to Determine the Quasi-Extinction Probabilities For Various

#Values of rho, as a function of h


#Parameters Displayed are of a current, but not necessarily

#typical, run



# Number of mesh points


N = 20;


# Number of sample paths


M0 = 100




#Number of probability of NO DISTURBANCE h values sampled
```

```
M1 = 30
```

```
#Number of rhos values sampled
```

```
M2 = 5
```

```
# Number of time-steps
```

```
M = 1000
```

```
#Maximum depth
```

```
D = 1
```

```
#Holling parameters
```

```
alpha = 40
```

```
beta = 50
```

```
#Fecundity
```

```
c0 = 50
```

```
#probabilities of NO disturbance (You have to reverse the vectors
#obtained to get the figures in the paper)
```

```
h0 <- seq(0,1, by = 1/29)


#Extinction threshold


thresh <- 50


#Functions for survival, germination, Holling and dispersal


survival = function(x){(95/100)*(1 - exp(- 10*x))}


germination = function(x){(95/100)*exp(- 10*x)}


f = function(x){alpha*x/(beta + x)}


dispersal = function(x){50*c0*exp(-50*x)}


#Initializing vectors


#Creating Steps/Midpoints


z = rep(0,N + 1); w = rep(0,N); germ = rep(0,N);


surv = matrix(0,N,N)


cT = rep(0,N); germ1 = matrix(0,N,N);
```

```
Dist1a <- matrix(0,N,N); Dist2a <- rep(0,N)


W = D/N


z[1] = 0 for(i in 1:N){

    z[i+1] = z[i]+W

        }
z[N+1] = D


for(i in 1:N){

    w[i] = (z[i+1] + z[i])/2

    }




#Discretizing survival and germination functions for (k in 1:N) {

        surv[k,k] <- survival(w[k])

        germ[k] <- germination(w[k])

        germ1[k] <- (1 - germination(w[k]))

        cT[k] <- W*dispersal(w[k])

    }


#Creating intermediate matrices


csurv <- surv%*%cT
```

```
Dist1 <- surv%*%germ1%*%diag(N)

Dist2 <- germ%*%diag(N)


#Initial Populations


Pop = 500


initseeds = function(x){(Pop)*(1/D)}


initplants = 15


seeds = rep(0,N)



#Discretizing initial population


for (l in 1:N) {

        seeds[l] <- W*initseeds(w[l])

    }


plants <- initplants


#Total vectors


totseeds = rep(0,M)
```

```
totseeds <- sum(seeds)


seeds1 <- rep(0,N)


plants1 <- 0


extinct <- 0


prob <- rep(0,M1)



#Vector of rhos


rhovec = seq(0,1, by = 1/(M2 + 1))


Extinction = matrix(0, M2, M1)



#For the ttt'th particular rho value


for (ttt in 1:M2) {


rho <- rhovec[ttt + 1]


#For the iii'th h value
```

```r
for (iii in 1:M1) {

    h <- h0[iii]

#For the kkk'th sample path for this h and rho

        for (kkk in 1:M0) {

            for (l in 1:N) {
                seeds[l] <- W*initseeds(w[l])
                }

            plants <- initplants

#For the i'th time step for this sample path, h and rho

            for (i in 2:M) {

                Dist1a <- Dist1
                Dist2a <- Dist2

                r <- runif(2,0,1)

                    if (r[1] <= h) {

                        seeds1 <- surv%*%seeds + plants*csurv
```

```
                                   plants1 <- 0

                        }

#Creating the Disturbance Kernel

                  else {

                        q <- (log(1 - r[2])*(- rho))/D

                        k <- ceiling(min(c(q*N, N)))


                        for (j in 1:k) {


                              Dist2a[j] <- germ[j]*(1/k)


                           for (l in 1:k) {

                              Dist1a[j,l] <- surv[j,j]*germ1[j,j]*(1/k)

                              }

                           }


                        seeds1 <- Dist1a%*%(seeds + cT*plants)

                        plants1 <- f(sum(Dist2a%*%(seeds + cT*plants)))

                  }


#Keeping count of the population


            totseeds[i] <- sum(seeds1)

            seeds <- seeds1

            plants <- plants1
```

```
        }


#Determining if the population is extinct or not


        if (totseeds[M] < thresh) {


            extinct <- extinct + 1


            }



        }


#Updated extinction probability


    prob[iii] <- extinct/M0


    extinct <- 0


    }


#Recording extinction probabilities


Extinction[ttt,] <- t(prob)


prob <- rep(0,M1)
```

```
print(ttt)



}




#Outputting data


write(Extinction, "ExtC50.txt", sep = ",")
```

C.3   Stochastic IPM Monte-Carlo Code

```
#Program to Determine the Long-Term Mean and Variance of the

#Seed-Bank Population as a function of h, with rho chosen


#Parameters Displayed are of a current, but not necessarily

#typical, run


# Number of mesh points


N = 20;


# Number of time-steps


M = 10000
```

```
#Maximum depth

D = 1

#Mean disturbance depth for the Kth run

rho = K*(0.033)

#NOTE HERE THAT K NEEDS TO BE CHOSEN BEFORE SIMULATION

#Holling parameters

alpha = 400

beta = 500

#Fecundity

c0 = 1000

#probabilities of NO disturbance (You have to reverse the vectors
obtained to get the figures in the paper)

h0 <- seq(0,1, by = 1/29)
```

```
#Number of sample paths taken


Reps = 500


#Functions for survival, germination, Holling and dispersal


survival = function(x){(95/100)*(1 - exp(- 10*x))}


germination = function(x){(95/100)*exp(- 10*x)}


f = function(x){alpha*x/(beta + x)}


dispersal = function(x){c0*50*exp(-50*x)}


#Initializing vectors


#Creating Steps/Midpoints


z = rep(0,N + 1); w = rep(0,N);


germ = rep(0,N); surv = rep(0,N); c = rep(0,N); germ1 = rep(0,N)


#Discretizing the interval [0,D]


W = D/N
```

```
z[1] = 0 for(i in 1:N){

    z[i+1] = z[i]+W

        }

z[N+1] = D



for(i in 1:N){

    w[i] = (z[i+1] + z[i])/2

    }
```

```
#Discretizing survival and germination functions


for (k in 1:N) {

        surv[k] <- survival(w[k])

        germ[k] <- germination(w[k])

        germ1[k] <- (1 - germination(w[k]))

        c[k] <- W*dispersal(w[k])

    }


#Initial populations


Pop = 5000


initseeds = function(x){(Pop)*(1/D)}
```

```
initplants = 15


seeds = rep(0,N)



#Discretizing initial population


for (l in 1:N) {

        seeds[l] <- W*initseeds(w[l])

    }


plants <- initplants


#Vectors keeping track of population during simulation


totseeds = rep(0,M)


totseeds0 = rep(0, Reps)


meantotseeds = rep(0, length(h0))


vartotseeds = rep(0, length(h0))


#Initializing


totseeds[1] <- sum(seeds)
```

```
seeds1 <- rep(0,N)

plants1 <- 0

#Initializing Stochastic Process

r <- 0

r0 <- 0

#Running the simulation

#Here is the jjth probability of no disturbance

for (jj in 1:length(h0)) {

h <- h0[jj]

#Here is the kkth sample path for this h0

    for (kk in 1:Reps) {

        for (l in 1:N) {

            seeds[l] <- W*initseeds(w[l])
```

```
        }


#Here is the ith time-step for this sample path and h0


        for (i in 2:M) {


                Dist <- diag(N)

                r <- runif(2,0,1)



                if (r[1] <= h) {


                    seeds1 <- surv*(seeds + c*plants)

                    plants1 <- 0

                }



                else {

                    q <- (log(1 - r[2])*(- rho))/D

                    k <- ceiling(min(c(q*N, N)))


#Creating the disturbance kernel


                        for (j in 1:k) {

                            for (l in 1:k) {

                                Dist[j,l] <- 1/k

                                }
```

```
                    }

                    seeds1 <- surv*germ1*Dist%*%(seeds + c*plants)

                    plants1 <- f(sum(germ*Dist%*%(seeds + c*plants)))
                }


        totseeds[i] <- sum(seeds1)

        seeds <- seeds1

        plants <- plants1


        }


#Counting the total number of seeds for this sample path at time M


    totseeds0[kk] <- totseeds[M]


    }


#Taking the mean and variance over all the 500 sample paths


meantotseeds[jj] <- mean(totseeds0)


vartotseeds[jj] <- var(totseeds0)
```

```
#This is letting you know how far you are in the simulation, once
you get to 30 you are done.


print(jj)


}


#Since h0 is the probability of no disturbance we need to reverse
the order of these vectors.


#Outputting data, you can reverse the vectors here if you'd like


write(meantotseeds, "mean(K*(0.033)C1000b.txt", sep = ",")
write(vartotseeds, "var(K*(0.033)C1000b.txt", sep = ",")
```

Bibliography

[1] Adams, V.M., Marsh, D.M., Knox, J.S. Importance of the seed bank for population viability and population monitoring in a threatened wetland herb. *Biological Conservation*, 124: 425-436, 2004.

[2] Alexander, H.M., Schrag, A.M. Role of soil seed banks and newly dispersed seeds in population dynamics of the annual sunflower. *Journal of Ecology*, 91: 987-998, 2003.

[3] Alexander, H.M., Pilson D., Moody-Weis, J. Slade, N.A. Geographic variation in dynamics of an annual plant with a seed bank. *Journal of Ecology,* 97: 1390-1400, 2009.

[4] Anazawa, M. Bottom-up derivation of population models for competition involving multiple resources. *Theoretical Population Biology*, DOI: 10.1016/j.tpb.2011.11.007, 2012.

[5] Aubin J.P. *Applied functional analysis, second edition.* Wiley, New York, 2000.

[6] Bacaer, N. *A short history of mathematical population dynamics.* Springer-Verlag, London, 2011.

[7] Benaim, M., Schreiber, S.J. Persistence of structured populations in random environments. *Theoretical Population Biology*, 76: 19-34, 2009.

[8] Billingsly, P. *Probability and measure. 3rd edn.* Wiley, New York, 1995.

[9] Briggs, J., Dabbs, K., Riser-Espinoza, D., Holm, M., Lubben, J., Rebarber, R., Tenhumberg, B. Structured population dynamics and calculus; an introduction to integral modeling. *Mathematics Magazine*, 83: 243-257, 2010.

[10] Brown, J.S., Venable, D.L. Life history evolution of seed-bank annuals in response to seed predation. *Evolutionary Ecology*, 5: 12-29, 1991.

[11] Caswell, H. A general formula for the sensitivity of population growth rate to changes in life history parameters. *Theoretical Population Biology*, 14:215-230, 1978.

[12] Caswell, H. *Matrix population models: construction, analysis and interpretation. 2nd edn.* Springer, New York, 2001.

[13] Caswell, H., Takada, T., Hunter, C.M. Sensitivity analysis of equilibrium in density-dependent matrix population models. *Ecology Letters*, 7:380-387, 2004.

[14] Caswell, H. Sensitivity analysis of transient population dynamics. *Ecology Letters*, 10:1-15, 2007.

[15] Caswell, H. Perturbation analysis of nonlinear matrix population models. *Demographic Research*, 18:59-116, 2008.

[16] Chancellor, R.J. *Emergence of weed seedlings in the field and the effects of different frequencies of cultivation.* Proceedings of the 7th Brittish Weed Control Conference. Brittish Crop Protection Council, Londom, England. 607-613, 1964.

[17] Charlesworth, B. *Evolution in age-stuctured populations.* Cambridge University Press, Cambridge, 1980.

[18] Childs, D.Z., Rees, M., Rose, K., Grubb, P.J., Ellner, S.P. Evolution of complex flowering strategies: an age- and size-structured integral projection model, *Proceedings of the Royal Society B.*, 270: 1829-1838, 2003.

[19] Childs, D.Z., Rees, M., Rose, K., Grubb, P.J., Ellner, S.P. Evolution of size-dependent flowering in a variable environment: construction and analysis of a stochastic integral projection model, *Proceedings of the Royal Society B.*, 271: 425-434, 2004.

[20] Claessen, D., Gilligan, C.A., Lutman, J.W., van den Bosch, F. Which traits promote persistence of feral GM crops? Part 1: Implications of environmental stochasticity. *OIKOS*, 110: 20-29, 2005.

[21] Claessen, D., Gilligan, C.A., van den Bosch, F. Which traits promote persistence of feral GM crops? Part 2: Implications of metapopulation structure. *OIKOS*, 110:30-42, 2005.

[22] Cousens, R. Aspects of the design and interpretation of competition (inference) experiments. *Weed Technology*, 5:664- 673, 1991.

[23] Crouse, D.T., Crowder, L.B., Caswell, H. A stage-based population model for loggerhead sea turtles and implications for conservation. *Ecology*, 68: 1412-1423, 1987.

[24] Cushing, J.M. *An introduction to structured population dynamics.* SIAM, Philadelphia, 1998.

[25] Damgaard, C. The probability of germination and establishment in discrete density-dependent plant populations with a seed bank: a correction formula. *Population Ecologly*, 47: 277-279, 2005

[26] Diaz, L.G., Leguizamon, E., Forcella, F., Gonzalez-Andujar, J.L. Short communication. Integration of emergence and population dynamic models for long term weed management using wild oat (Avena fatua L.) as an example. *Spanish Journal of Agricultural Research* 5(2): 199-203, 2007

[27] De Kroon, H., Plaisier, A., van Groenendael, J., Caswell, H. Elasticity; the relative contribution of demographic parameters to population growth rate. *Ecology*, 67:1427 - 1431, 1986.

[28] De Kroon, H., van Groenendael, J., Ehrlen, J. Elasticities: a review of methods and model limitations. *Ecology*, 81:607-618, 2000.

[29] Duncan, R.P., Diez, J.M., Sullivan, J.J., Wangen, S., Miller, A.L. Safe sites, seed supply, and the recruitment function in plant populations. *Ecology*, 90:2129-2138, 2009.

[30] Eager, E.A., Rebarber, R., Tenhumberg, B. Choice of density-dependent seedling recruitment function affects predicted transient dynamics: a case study with Platte thistle. *Theoretical Ecology*, DOI 10.1007/s12080-011-0131-3, 2012.

[31] Easterling, M.R., Ellner, S.P., Dixon, P.M. Size-specific sensitivity: applying a new structured population model. *Ecology*, 81:694- 708, 2000.

[32] Edelstein-Keshet, L. *Mathematical models in biology.* SIAM, Philadelphia, 2005.

[33] Ellner, S.P., Rees, M., Integral projection models for species with complex demography. *American Naturalist*, 167: 410-428, 2006.

[34] Ellner, S.P., Rees, M. Stochastic stable population growth in integral projection models: Theory and application. *Journal of Mathematical Biology*, 54(2): 227 - 256, 2007

[35] Fenner, M., Thompson, K. *The ecology of seeds.* Cambridge University Press, Cambridge, 2005.

[36] Folland, G.B. *Real analysis: modern techniques and their applications.* Wiley, New Jersey, 1999.

[37] Freckleton, R.P., Sutherland, W.J., Watkinson, A.R., Stephens, P.A. Modelling the effects of management on population dynamics: some lessons from annual weeds. *Journal of Applied Ecology*, 45:1050-1058, 2008.

[38] Grant, A. Population consequences of chronic toxicity: incorporating density dependence into the analysis of life table response experiments. *Ecological Modelling*, 105:325-335, 1998.

[39] Grant, A., Benton, T.G. Elasticity analysis for density dependent populations in stochastic environments. *Ecology*, 81:680-693, 2000.

[40] Grant, A., Benton, T.G. Density-dependent populations require density-dependent elasticity analysis: an illustration using the LPA model of *Tribolium. Journal of Animal Ecology*, 72:94-105, 2003.

[41] Hardin, D.P., Takac, P., Webb, G.F. Asymptotic properties of a continuous-space discrete-time population model in a random environment. *Journal of Mathematical Biology,* 26: 361-374, 1988.

[42] Hastings, A. Transients: the key to long-term ecological understanding? *Trends in Ecology and Evolution*, 19:39-45, 2004.

[43] Hinrichsen, D., Pritchard, A.J. *Mathematical systems theory I: modeling, state space analysis, stability and robustness.* Springer, New York, 2005.

[44] Holling, C.S. Some characteristics of simple types of predation and parasitism. *Canadian Entomologist* 91:385-398, 1959.

[45] Hunter, C.M., Moller, H., Fletcher, D. Parameter uncertainty and elasticity analyses of a population model: setting research priorities for shearwaters. *Ecological Modelling*, 134:299-323, 2000.

[46] Jarry, M., Khaladi, M., Hossaert-McKey, M., McKey, D. Modeling the population dynamics of annual plants with seed bank and density dependent effects. *Acta Biotheoretica*, 43: 53-65, 1995.

[47] Kalisz, S. Experimental determination of seed bank age structure in the winter annual Collinsia verna. *Ecology*, 72(2): 575-585, 1991.

[48] Kalisz, S., McPeek, M.A. Demography of an age-structured annual: Resampled projection matrices, elasticity analyses and seed bank effects, *Ecology* 73(3): 1082-1093, 1992.

[49] Kalisz, S., McPeek, M.A. Extinction dynamics, population growth and seed banks. *Oecologia*, 95: 314-320, 1993.

[50] Koons, D.N., Grand, J.B., Zinner, B., Rockwell, R.F. Transient population dynamics: relations to life history and initial population state. *Ecological Modelling*, 185:283-297, 2005.

[51] Krasnosel'skij, M.A., Lifshits, J.A., Sobolev, A.V. *Positive linear systems - the method of positive operators.* Heldermann Verlag, Berlin, 1989.

[52] Logan, J.D. *Applied mathematics, 3rd edn.* Wiley, New Jersey, 2006.

[53] Lubben, J. *Modeling and analysis of biological populations.* PhD thesis, University of Nebraska, Lincoln, 2009.

[54] MacDonald, N., Watkinson, A.R. Models of an annual population with a seedbank. *Journal of Theoretical Biology*, 93: 643-653, 1981.

[55] Maki, D., Thompson, M. *Mathematical modeling and computer simulation.* Thomson Brooks/Cole, Belmont, 2006.

[56] Mangel, M. *The theoretical biologist's toolbox: quantitative methods for ecology and evolutionary biology.* Cambridge University Press, Cambridge, 2006.

[57] Marshall, D.L. Effect of seed size on seedling success in three species of Sesbania (Fabaceae). *American Journal of Botany*, 93: 457-464, 1986.

[58] Meyer, S.E., Quinney, D., Weaver, J. A stochastic population model for lepidium papilliferum (Brassicacea), a rare desert ephemeral with a persistent seed bank. *American Journal of Botany,* 93(6): 891-902, 2006.

[59] Miller, A.D., Roxburgh, S.H., Shea, K. Timing of disturbance alters competitive outcomes and mechanisms of coexistence in an annual plant model. *Theoretical Ecology* DOI 10.1007/s12080-011-0133-1, 2011.

[60] Mohler, C.L. A model of the effects of tillage on emergence of weed seedlings. *Ecological Applications* 3(1): 53-73, 1993.

[61] Moody-Weis, J., Alexander, H.M. The mechanisms and consequences of seed bank formation in wild sunflowers (Helianthus annuus). *Journal of Ecology*, 95: 851-864, 2007.

[62] R Development Core Team *R: a language and environment for statistical computing.* Vienna, Austria , 2006.

[63] Ramula, S., Rees, M., Buckley, Y.M. Integral projection models perform better for small demographic data sets than matrix population models: a case study of two perennial herbs. *Journal of Applied Ecology*, 46:1048-1053, 2009.

[64] Rebarber, R., Tenhumberg, B., Townley, S. Global asymptotic stability of density dependent integral population projection models. *Theoretical Population Biology*, 81: 81-87, 2012.

[65] Rees, M.n Ellner, S. Integral projection models for populations in temporally varying environments. *Ecological Monographs*, 79(4): 575 - 594, 2009.

[66] Roff, D.A. *Evolution of Life Histories*. Chapman and Hall, New York, New York, 1986.

[67] Rose, K.E., Louda, S.M., Rees, M. Demographic and evolutionary impacts of native and invasive insect herbivores on Cirsium canescens *Ecology*, 46: 1048-1053, 2005.

[68] Runge, M.C., Johnson, F.A. The importance of functional form in optimal control solutions of problems in population dynamics. *Ecology*, 83:1357-1371, 2002.

[69] Sletvold, N. Effects of plant size on reproductive output and offspring performance in the facultative biennial Digitalis purpurea. *Journal of Ecology*, 90:958-966, 2002.

[70] Snyder, R.E. Transient dynamics in altered disturbance regimes: recovery may start quickly, then slow. *Theoretical Ecology* 2:79-87, 2009.

[71] Stott, I., Franco, M., Carslake, D., Townley, S., Hodgson, D. Boom or bust? A comparative analysis of transient population dynamics in plants. *Journal of Ecology*, 98:302-311, 2010.

[72] Suli, E., Mayers, D. *An introduction to numerical analysis.* Cambridge University Press, Cambridge, 2006.

[73] Tenhumberg, B., Tyre, T.J., Rebarber, R. Model complexity affects transient population dynamics following a dispersal event: a case study with pea aphids. *Ecology* 90:1878-1890, 2009.

[74] Townley, S., Carslake, D., Kellie-Smith, O., McCarthy, D., Hodgson, D. Predicting transient amplification in perturbed ecological systems. *Journal of Applied Ecology* 44:1243-1251, 2007.

[75] Townley, S., Hodgson, D.J. Erratum et addendum: transient amplification and attenuation in stage-structured population dynamics. *Journal of Applied Ecology*, 45:1836-1839, 2008.

[76] Townley, S., Tenhumberg, B., Rebarber, R. Feedback control systems analysis of density dependent population dynamics, *Systems and Control Letters*, 61: 309-315, 2012.

[77] Vandermeer, J.H., Goldberg, D.E. *Population ecology: first principles.* Princeton University Press, Princeton, 2003.

[78] Tuljapurkar, S. *Population dynamics in variable environments (lecture notes in biomathematics).* Springer- Verlag, Germany, 1990.

[79] Uribe, G. *On the relationship between continuous and discrete models for size-structured population dynamics.* PhD thesis, University of Arizona, Tucson, 1993.

[80] Venable, D. L. Modeling the evolutionary ecology of seed banks. *Ecology of Seed Banks,* 67-87. Academic Press, Inc., Waltham, Massachusetts, 1989.

[81] Weiner, J., Martinez, S., Muller-Scharer, H., Stoll, P., Schmid, B. How important are environmental maternal effects in plants? A study with Centaurea maculosa. *Journal of Ecology*, 85:133-142, 1997.

[82] Weller, M., Spratcher, C. *Role of habitat in the distribution and abundance of marsh birds. Special report 43.* Iowa Agriculture and Home Economics Experiment Station, Ames (1965)

[83] Yearsley, J., Fletcher, D., Hunter, C.M. Sensitivity analysis of equilibrium population size in a density-dependent model for Short-Tailed Shearwaters. *Ecological Modelling*, 163:119-129, 2003.